Critical Insight into the Relentless Progression Toward Graphene and Graphene-Containing Materials for Lithium-Ion Battery Anodes

Rinaldo Raccichini, Alberto Varzi, Di Wei,* and Stefano Passerini*

Used as a bare active material or component in hybrids, graphene has been the subject of numerous studies in recent years. Indeed, from the first report that appeared in late July 2008, almost 1600 papers were published as of the end 2015 that investigated the properties of graphene as an anode material for lithium-ion batteries. Although an impressive amount of data has been collected, a real advance in the field still seems to be missing. In this framework, attention is focused on the most prominent research efforts in this field with the aim of identifying the causes of such relentless progression through an insightful and critical evaluation of the lithium-ion storage performances (i.e., 1st cycle irreversible capacity, specific gravimetric and volumetric capacities, average delithiation voltage profile, rate capability and stability upon cycling). The "graphene fever" has certainly provided a number of fundamental studies unveiling the electrochemical properties of this "wonder" material. However, analysis of the published literature also highlights a loss of focus from the final application. Hype-driven claims, not fully appropriate metrics, and negligence of key parameters are probably some of the factors still hindering the application of graphene in commercial batteries.

1. Introduction

First isolated in 2004[1] as a one-atom thick layer of sp^2-bonded carbon, graphene drew worldwide attention after its discoverers won the physics Noble prize in 2010.[2] Since then, the global scientific community invested a huge amount of human and material resources to study this "wonder" material, confident that its extraordinary properties would enable revolutionary new technologies, which gave birth to the "graphene era".[3,4]

Relying on this scenario, in 2013, the European Union launched the €1 billion "Graphene Flagship" project aimed to investigate the properties of this new form of carbon for various applications (e.g., electronics, sensors and energy storage devices), with the ambitious goal of guiding graphene from laboratories to commercial applications within a decade.[5,6] In the same period, the Chinese Government set up a similar investment to mass-produce graphene as thin films (e.g., for touchscreen electrodes) and platelets (e.g., for use in batteries).[6] In the following years, hundreds of patents, mainly focused on manufacturing and application in energy storage, were filed and the worldwide production of graphene and graphene-containing materials rapidly increased. Although a few Chinese industries claimed to already use graphene-containing materials for smartphone production, no revolutionary practical application relying on graphene has been yet developed.[6]

Specifically with respect to the battery field, a close analysis of the scientific literature reveals a struggle to meet the ambitious initial targets. A potential loss of focus from the final application caused by hype and ease of publication on such a novel matter, together with the delivery of very misleading information[7,8] and erroneous statements[7] concerning the use of graphene in batteries are emerging as possible reasons of the ineffective graphene-era outburst. In this progress report, we do not focus on production and classification of graphene and graphene-containing materials, which were already well reported in the past years.[3,9–11] In contrast, due to the lack of an exhaustive analysis of the progression of the use of such materials in lithium-ion battery (LIB) anodes, we report here a critical evaluation of the most prominent research papers published from 2008 until the end of 2015. As shown in **Figure 1**, three different stages of the graphene research in LIB anodes can be distinguished: a first stationary phase between 2008 and 2010 where the lithium-ion storage properties of different graphene and graphene-containing materials were preliminarily explored, a second exponential stage, spanning from 2010 to 2014, where graphene and graphene-containing anode materials were broadly developed and investigated, and finally, a third phase, (i.e., starting from 2015), where the research seems to have approached a plateau. After

Dr. R. Raccichini, Dr. A. Varzi, Prof. S. Passerini
Helmholtz Institute Ulm (HIU)
Helmholtzstrasse 11, 89081 Ulm, Germany
E-mail: stefano.passerini@kit.edu
Dr. R. Raccichini, Dr. A. Varzi, Prof. S. Passerini
Karlsruhe Institute of Technology (KIT)
P.O. Box 3640, 76021 Karlsruhe, Germany
Dr. D. Wei
Nokia Technologies
Broers Building
21 JJ Thomson Av., Madingley Road, CB3 0FA Cambridge, UK
E-mail: dw344@cam.ac.uk

PROGRESS REPORT

a brief description of the state-of-the-art materials for LIB anodes, the performance metrics used to claim the superiority of graphene will be discussed in order to identify the most promising approaches.[12] The analysis is divided into three main topics. Li-ion host anodes based on: i) graphene and ii) graphene-containing materials, tested in half-cell configuration, are discussed. Finally, iii) full-cells employing graphene and/or graphene-containing anodes are covered. Within each subject, we try to follow as much as possible the temporal evolution of research in this field and highlight the most relevant advances. While the pioneering reports of the early years are discussed in detail, starting from 2011 only the most relevant contributions (in terms of novelty and/or improved electrochemical properties) are discussed. For sake of clarity, all discussed data are also summarized in tables.

2. A Brief Excursion into Graphene's Classification and Production

Graphene is the generic name of a large family of 2D carbons comprising materials with very different properties. A Carbon editorial[10] has recently rationalized the graphene nomenclature, putting an end to the initial confusion caused by the use of inappropriate terms. When taking the number of layers into account, graphene can be classified in: i) single-layer (or monolayer) or ii) multilayer (i.e., when their number is comprised between 2 and 10). The prefix "nano-" is used when the lateral dimension is <100 nm, while it is replaced by "micro-" if this ranges between 100 nm and 100 µm. With regard to the aspect ratio (i.e., length:width), when ≤10 suffixes like "-sheet", "-flake", "-plate" or "-platelet" can be used. Differently, "-ribbon" is more appropriate when it exceeds 10.[11] The removal or introduction of carbon atoms from or into graphene sheets gives rise to vacancies, edges and deformations which are identified as "intrinsic defects". When heteroatoms are introduced, e.g., in the case of doping, we are dealing with "extrinsic defects" instead.[11]

It is now well recognized that the graphene properties are highly dependent on the synthetic route employed. Several reviews[3,5,9,11] have described in detail the available methods for the production of graphene-based materials. In general, these can be divided in two main categories which are, namely, top-down and bottom-up approaches. Reduction of graphene oxide (GO) and liquid-phase exfoliation of graphite are the principal examples of top-down synthesis. With regard to bottom-up methods, chemical vapor deposition (CVD) is the mostly used technique.[11,13,14] Although GO's reduction represents the most widely employed approach to obtain graphene as reduced graphene oxide (RGO),[11] both liquid-phase exfoliation and CVD methods are generally interesting for industrial purposes due to their potential to scale up for mass production.[15] However, the properties of graphene obtained from these latter manufacturing methods are very different and they all have advantages and drawbacks.[16] Indeed, the liquid-phase exfoliation is very cost-effective, but the obtained graphene flakes have generally small lateral size (i.e., <100 nm) with higher sheet resistance.[15] The CVD method may also introduce some undesired contaminants, but large size graphene flakes (i.e., >100 nm) can be produced, to the detriment of a moderate affordability of the process.

Di Wei is a senior research scientist at Nokia Technologies. He was one of the initiators of the research in the field of nanocarbon and graphene technologies at Nokia. He participated strongly in the early phase of defining and initiating the European Union Graphene Flagship programme during 2011–2013, and has carried out responsibilities benchmarking and standardizing graphene battery technologies in the flagship activities.

Stefano Passerini is currently Professor at KIT (Karlsruhe Institute of Technology, Germany) and Deputy Director at HIU (Helmholtz Institute Ulm, Germany). Formerly Professor at the University of Münster he co-founded the MEET (Münster Electrochemical Energy Technology, Germany) battery research center. His research activities have been focused on electrochemical energy storage since 1986.

3. The Quest for the Ideal Anode

3.1. State-of-the-Art Materials and Emerging Candidates

The "ideal" active material for a LIB anode should possess some specific properties, as indicated in the review of M. V. Reddy et al.[17] Generally, it should accommodate a large amount of lithium ions per formula unit, with insertion/deinsertion potentials very close to that of Li metal. It must be, furthermore, stable upon cycling, and possess not only excellent gravimetric (mAh g^{-1}) but also volumetric capacity (mAh cm^{-3}) at a sufficiently high mass loading (mg cm^{-2}).[18,19] It should not show large voltage hysteresis between charge and discharge, in order not to sacrifice the battery energy efficiency,[19] and possess a minimal irreversible capacity during the first cycle. Of course, in order to allow good rate capability, it should provide good mixed conduction (high electrical and ionic conductivity) and, preferentially, be cheap and environmentally friendly.

By meeting most of these requirements it is not surprising that graphite is still considered, since 1990, the state-of-the-art material for LIB anodes.[20] The low intercalation/deintercalation potentials (see **Figure 2**, profile a) and the high Coulombic and voltage efficiency (i.e., very small hysteresis) are clearly at the basis of its success. Graphite is, indeed, used in all the commercially available rechargeable hard case LIBs[17,19] although it presents some relevant limitations. It suffers indeed from poor lithium-ion storage capability at low temperatures (e.g., $T < 0\,°C$),
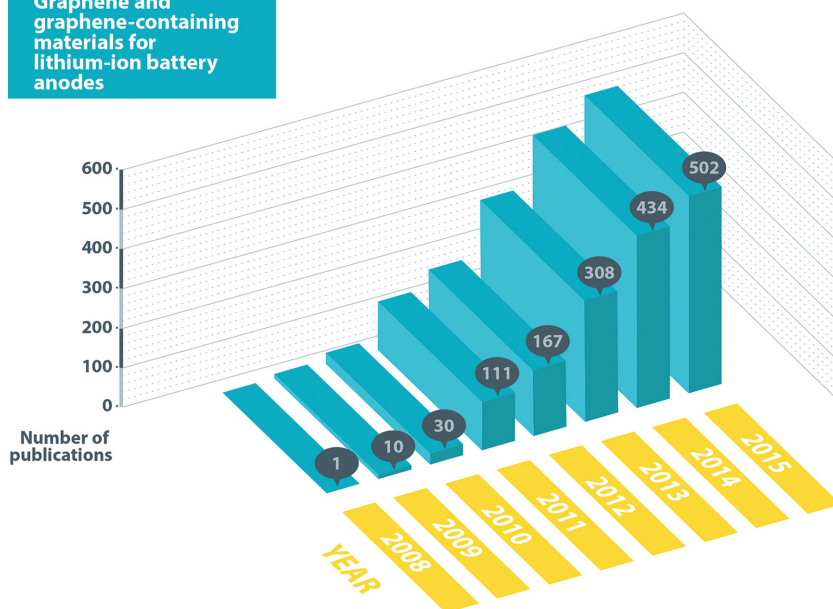
Figure 1. Number of papers related to the use of graphene and graphene-containing materials for lithium-ion battery anodes, published between 2008 and 2015. The data were obtained by applying the following criteria in the search field of Scopus: "graphene lithium", "graphene li-ion", "graphene lithium-ion" and "graphene anode". The document types "article" and "article in press" have been considered for these statistics and all the results were individually selected. It should be pointed out that publications related to theoretical or computational approaches are not considered in these statistics. The last update was done on January 31, 2016.

and its specific capacity rapidly decays when high current loads are applied. Finally, and most importantly, graphite provides a maximum (theoretical) gravimetric capacity of "only"

372 mAh g^{-1}. These limitations motivated the development of different host materials in the past 20 years. Alternative anodes can be classified, as function of their reaction mechanism, in three classes: i) hosts able to insert/deinsert lithium ions (e.g., TiO_2),[17] ii) materials forming alloys with lithium (e.g., Sn, Si, Ge),[19] and iii) materials undergoing a reversibly conversion reaction with lithium (e.g., metal oxides).[21]

Titanium oxides (e.g., TiO_2 and $Li_4Ti_5O_{12}$) are the insertion materials that have received the most attention. Although very stable, cheap, safe and environmentally benign, they provide limited gravimetric capacities (inferior to graphite). Furthermore, their relatively high operative voltage (between 1 and 3 V vs Li/Li$^+$, see Figure 2, profile b) dramatically affects the energy density. The promising rate capability is, however, very appealing for power-oriented LIBs. Alloying materials such as silicon provide substantial advantages, including very high gravimetric and volumetric capacity (i.e., 3579 mAh g^{-1} and 2194 Ah L^{-1}, respectively)[19] and low operating voltage, i.e., below 1 V vs Li/Li$^+$ (see Figure 2, profile c). Unfortunately, the large volume expansion upon lithiation causes poor cycling stability.[22] Metal oxides like MnO_2 and Fe_3O_4 became also appealing for their low cost and environmental friendliness. Nevertheless, as conversion reactions normally occur at high voltage (above 1 V, see Figure 2, profile d), they need to be combined with
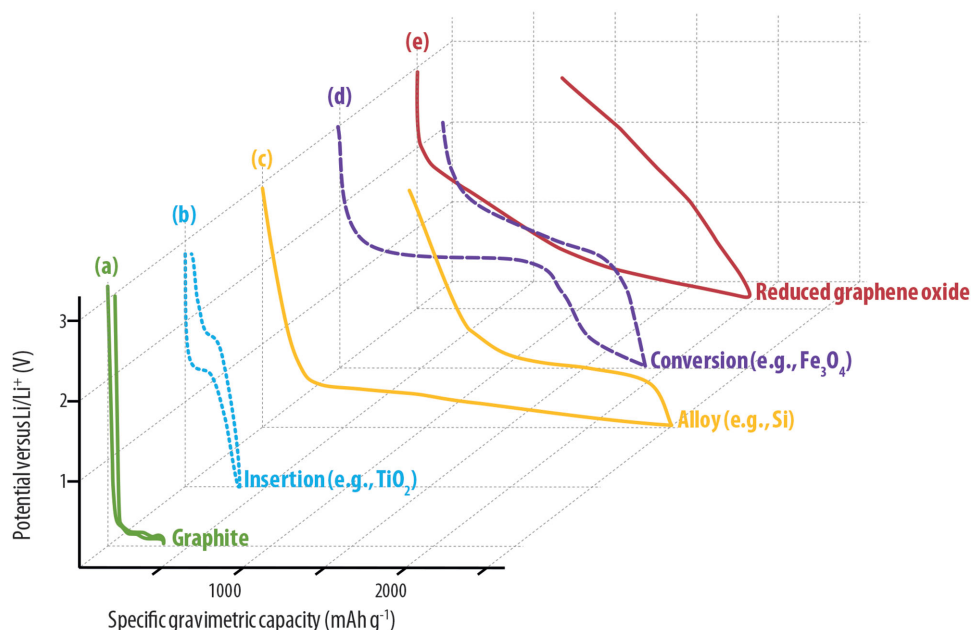

Figure 2. Comparison of typical voltage profiles of lithium-ion battery anode materials: a) Li intercalation into graphite, b) insertion of Li in high voltage oxides (e.g., TiO_2), c) materials forming alloying with Li (e.g., Si), d) materials undergoing conversion reactions with Li (e.g., Fe_3O_4), and e) Li storage in reduced graphene oxide.

high voltage cathodes in order to compete with graphite. The same issue is generally observed for RGO-based anodes which, despite the large specific capacity, often display considerably hysteresis between lithiation and delithiation profile (see Figure 2, profile e).

3.2. Cell Configurations and Canonical Electrochemical Tests of Lithium-Ion Batteries

Electrochemical characterizations of LIB anode active materials could be generally carried out with two different cell configurations. In the first one, called "half-cell" configuration, the anode active material acts as a positive electrode with Li metal as the counter negative electrode.[17] Consequently, the lithiation/delithiation processes of the anode active material are considered as "discharge"/"charge" reactions, respectively. In the second configuration, called "full-cell", the anode active material (in this case the negative electrode) is coupled with a lithium-containing oxide (e.g., $LiFePO_4$) which acts as positive electrode (i.e., cathode). In this second case, the anode "discharge"/"charge" reactions are named in the reverse way. Indeed, the "full-cell" configuration represent the basic unit of a practical battery[23] where, during the "discharge", lithium ions are extracted from the anode and they are inserted into the cathode (i.e., the lithium-containing oxide) while, during the "charge", the lithium ions are extracted from the cathode and inserted into the anode.[17] Although the half-cell configuration is practical to study the intrinsic electrochemical properties of a specific material, it does not enable direct assessment of its applicability in real batteries. As a matter of fact, half-cells employ a large excess of lithium that often buffers charge consumption during cycling. On the other hand, in a full-cell the Li reservoir is limited, and parasitic reactions become of more serious concern. Here, in order to: i) avoid a large first cycle irreversible capacity and ii) extend the cycle life of the battery, a process called "pre-lithiation"[24,25] of the anode can be used prior to assembly of the full-cell. Such approach is nearly always used in literature when testing full-cells. The most common pre-lithiation methods include the use of a sacrificial lithium metal electrode, which could be directly placed in contact with the anode (previously wet by the electrolyte) or, alternatively, cycled in half-cell configuration vs the anode to be activated.

It should be furthermore pointed out that, when a LIB anode is tested in half-cell configuration (i.e., a single electrode against a Li metal electrode), its energy and/or power density cannot be determined. Indeed, as clearly stated by M. N. Obrovac and V. L. Chevrier[19] "One difficulty in choosing proper metrics for anodes stems from basic electrochemistry: it is not possible to calculate the energy of a single electrode". Energy and/or power densities of a full-cell employing a specific anode material could be, however, estimated from preliminary tests in half-cells. For example, by assuming its coupling in full-cell with a defined cathode material, current collector and separator.[19] Such evaluation is rarely found in literature and is also quite difficult "a posteriori" due to the lack of specific information.[19] In general, however, gravimetric and volumetric capacity, together with the average lithiation and delithiation voltages are excellent metrics to properly evaluate an anode active material in half-cell configuration.

In view of the above, we specifically discriminate in our discussion the results obtained in half- and full-cells (to which a separate chapter is fully dedicated).

4. Progress on the use of Graphene for Lithium-Ion Battery Anodes

4.1. Graphene as Li-Ion Host

In 2008, motivated by promising theoretical capacities of 744 mAh g^{-1} and 1157 mAh g^{-1} (corresponding to a Li_2C_6 and Li_3C_6 stoichiometry, respectively),[26,27] predicted more than a decade before, graphene was initially investigated as possible Li$^+$ host by I. Honma et al.[28] In their pioneering work, graphene was prepared by chemical reduction of GO to obtain RGO.[29] Moreover, prior to the reduction step, acid treated carbon nanotubes (CNT) and fullerenes (C_{60}) were mixed with the GO to obtain hybrid carbon nanostructures. The predicted capacity could not be achieved by the bare RGO electrode, but it was exceeded by the RGO/C_{60} composite. The author attributed such extra capacity to different electronic structure of the composite and to the d-spacing enlargement. Nevertheless, after only 20 cycles, the capacity dropped to only 54, 66, and 77% of the initial value for RGO, RGO/CNT, and RGO/C_{60} respectively (**Table 1**). Interestingly, the authors showed that most of the Li ions were inserted at potentials >0.5 V vs Li/Li$^+$ without any distinguishable plateau, similarly to the well-known "hard carbons".[30] However, the deinsertion took place at much higher voltages (with more than 80% of capacity delivered between 1 and 3.5 V vs Li/Li$^+$), resembling the behavior of H-rich carbons[30,31] (similarly to the previously described Figure 2, profile e). Furthermore the authors noticed that, upon manipulations (e.g., electrode manufacture), the layered structure of graphene tended to reassemble and restack, thus, unfavorably affecting the lithium-ion storage properties. This was the first evidence of one of the most serious issues associated with the use of RGO in LIB anodes. It was immediately clear that, if not properly addressed, the layers' restacking would lead to the loss of all the predicted advantages of graphene, thus jeopardizing a possible advent of graphene-based LIBs.[11] Although this was a first proof of concept, the lack of data about 1st cycle Coulombic efficiency, mass loading of the electrodes, as well as density of these materials, made it difficult to properly evaluate the real potential of graphene with respect to the state of the art.

In the following year (2009), few more research efforts focusing on RGO anodes were published.[32–36] In these papers, the rather poor reversibility and the limited number of cycles verified the drawbacks initially observed by I. Honma.[28] Specifically, Z. Jiao et al.[34] correlated the sensitivity of RGO's Li$^+$ storage properties to the method of GO reduction employed (i.e., thermal reduction in N_2 at different temperatures, chemical reduction with hydrazine and electron beam irradiation, see Table 1). They also showed that the high specific surface area (SSA) of RGO, which was generally considered a beneficial property of these classes of materials,[3] in this specific case represented a drawback. As a matter of fact, large SSA

Table 1. Lithium-ion storage performances of different kind of graphene reported between 2008 and 2015 (all the tests refer to half-cell configuration).

Active material	Graphene in the active material [wt%]	Active material in electrode [wt%]	Potential range applied (vs Li+/Li) [V]	Specific current applied [mA g−1]	1st cycle lithiation capacity [mAh g−1]	1st cycle irreversible capacity [%]	No. Cycles	Last specific gravimetric capacity [mAh g−1]	Ref.
2008									
RGO	100	95	0.01–3.5	50	540	–	20	290 (lithiation)	[28]
RGO/CNT	90	95	0.01–3.5	50	510	–	20	480 (lithiation)	[28]
RGO/C$_{60}$	90	95	0.01–3.5	50	760	–	20	600 (lithiation)	[28]
2009									
RGO	100	–	0.05–3.5	50	530	–	30	300 (lithiation)	[32]
RGO	100	90	0.02–3	372	945	31	100	460 (delithiation)	[33]
GO	100	80	0.005–3	50	758	56	15	230 (delithiation)	[34]
RGO (hydrazine)	100	80	0.005–3	50	708	53	15	200 (delithiation)	[34]
RGO (300 °C)	100	80	0.005–3	50	1544	34	15	830 (delithiation)	[34]
RGO (600 °C)	100	80	0.005–3	50	1528	48	15	640 (delithiation)	[34]
RGO (electron beam)	100	80	0.005–3	50	2042	48	15	740 (delithiation)	[34]
RGO paper (hydrazine)	100	100	0–3	50	680	88	50	50 (lithiation)	[35]
RGO paper (800 °C − N$_2$)	100	100	0–2	50	1015	70	50	220 (lithiation)	[35]
RGO	100	80	0.01–3.5	0.2 [mA cm−2]	1233	45	30	502 (delithiation)	[36]
2010									
GO (hollow spheres)	100	80	0.01–2.5	0.2 [mA cm−2]	1065	54	30	420 (delithiation)	[43]
RGO	100	100	0.02–1.5	4	1700	85	100	120 (delithiation)	[37]
RGO (paper)	100	100	0–3	50	314	73	70	65 (delithiation)	[39]
RGO (powder)	100	80	0–2.5	50	691	58	70	170 (delithiation)	[39]
RGO	100	75	0.005–3	200	1472	74	30	250 (delithiation)	[44]
RGO	100	80	0.01–3	74	1210	54	20	390 (lithiation)	[45]
RGO	100	80	0.005–3	89	1740	48	30	582 (delithiation)	[46]
RGO	100	70	0.01–3	50	2179	56	30	638 (delithiation)	[47]
RGO	100	90	0.01–3.5	100	2035	38	5	1144 (delithiation)	[48]
RGO	100	80	0.02–3	264	940	51	50	197 (delithiation)	[49]
RGO	100	80	0.005–2	50	1525	64	50	338 (delithiation)	[50]
Unzipped CNT graphene	100	85	0.0–3.5	0.1 [mA cm−2]	1400	41	14	510 (delithiation)	[51]
bottom-up-synthesized graphene	100	80	0.02–1.2	100	1274	78	30	200 (delithiation)	[52]
CVD-synthesized graphene	100	100	0.02–3.2	5 [μA cm−2]	0.145 (mAh cm−2)	75	50	0.033 (delithiation mAh cm−2)	[40]
CVD-synthesized N-doped graphene	100	100	0.02–3.2	5 [μA cm−2]	0.25 (mAh cm−2)	78	50	0.044 (delithiation mAh cm−2)	[40]

Table 1. Continued.

Active material	Graphene in the active material [wt%]	Active material in electrode [wt%]	Potential range applied (vs Li$^+$/Li) [V]	Specific current applied [mA g^{-1}]	1st cycle lithiation capacity [mAh g^{-1}]	1st cycle irreversible capacity [%]	No. Cycles	Last specific gravimetric capacity [mAh g^{-1}]	Ref.
2011									
N-doped RGO	100	70	0.01–3	50	2127	51	30	872 (delithiation)	[57]
B-doped RGO	100	70	0.01–3	50	2783	43	30	1227 (delithiation)	[57]
Functionalized RGO (honeycomb film)	100	100	0.01–3	50	3025	47	50	1150 (delithiation)	[59]
Functionalized RGO (nonpatterned film)	100	100	0.01–3	50	1957	45	50	678 (delithiation)	[59]
RGO	100	90	0.01–3	100	785	56	100	260 (delithiation)	[61]
N-doped RGO	100	90	0.01–3	100	1325	65	100	440 (delithiation)	[61]
CNT-functionalized RGO paper	35	100	0.001–2.5	30	1090	73	40	290 (lithiation)	[62]
CNT-functionalized RGO	–	80	0.01–3	0.12 [mA cm^{-2}]	1175	43	30	600 (delithiation)	[63]
RGO	100	80	0.01–3	0.12 [mA cm^{-2}]	1560	71	30	280 (delithiation)	[63]
Activated RGO paper	100	100	0.02–2.5	20	609	86	10	80 (delithiation)	[64]
Functionalized activated RGO paper	100	100	0.02–2.5	20	493	70	10	85 (delithiation)	[64]
2012									
Graphene balls	100	40	0–2	30	90	72	5	27 (delithiation)	[69]
RGO/Cellulose	3.2	100	0–2.5	100	1980	80	45	245 (delithiation)	[70]
Aerogel-derived RGO paper	100	100	0.01–1.5	100	1105	75	100	160 (delithiation)	[71]
Functionalized RGO/CNT	50	90	0.05–3	90	1370	34	100	770 (lithiation)	[72]
RGO/sulfur-doped carbon	–	80	0.01–3	1000	1250	51	500	780 (delithiation)	[73]
2013									
P-doped RGO	100	75	0.01–3	100	915	51	80	455 (delithiation)	[83]
N-S-doped RGO	100	80	0.01–3	5000	840	48	3000	500 (delithiation)	[84]
Bottom-up-synthesized graphene	100	85	0.01–3	100	3535	77	10	600 (delithiation)	[85]
Electrochemically exfoliated graphene	100	80	0.01–3	50	527	32	30	390 (delithiation)	[86]
Holey-RGO hydrogel	100	80	0.01–3	19	2207	60	3	895 (delithiation)	[87]
CVD-synthesized graphene paper	100	100	0.01–3	50	2400	66	4	820 (delithiation)	[88]
Polysulfide-functionalized RGO	100	80	0.005–3	250	2440	49	378	1800 (delithiation)	[89]
Catalytically exfoliated graphene	100	80	0.001–3	100	1243	52	23	600 (delithiation)	[90]
2014									
N-S-codoped graphene	100	70	0.01–3	50	6907	49	4	3190 (delithiation)	[91]
RGO paper (300 °C)	100	100	0.01–2.5	100	740	85	40	100 (delithiation)	[92]
RGO paper (500 °C)	100	100	0.01–2.5	100	945	69	40	170 (delithiation)	[92]
RGO paper (700 °C)	100	100	0.01–2.5	100	755	58	40	225 (delithiation)	[92]

Table 1. Continued.

Active material	Graphene in the active material [wt%]	Active material in electrode [wt%]	Potential range applied (vs Li⁺/Li) [V]	Specific current applied [mA g⁻¹]	1st cycle lithiation capacity [mAh g⁻¹]	1st cycle irreversible capacity [%]	No. Cycles	Last specific gravimetric capacity [mAh g⁻¹]	Ref.
RGO paper (900 °C)	100	100	0.01–2.5	100	965	62	40	310 (delithiation)	[92]
				2015					
N-doped RGO	100	80	0.01–3	2000	1500	–	1600	300 (lithiation)	[95]
Porous RGO aerogel	100	80	0.1–3	100	2900	57	100	1100 (delithiation)	[96]
N-doped macroporous RGO	100	80	0.005–3	1000	1170	–	500	691 (lithiation)	[97]
Bottom-up-synthesized N-doped graphene	100	80	0.01–3	1000	1430	65	1500	588 (delithiation)	[98]
N-S-codoped RGO	100	80	0.01–3	1000	1320	51	5000	211 (delithiation)	[99]
N-F-codoped RGO	100	80	0–001–3	100	1894	43	50	762 (lithiation)	[100]
N-doped holey RGO foam	100	80	0.01–3	74.4	2847	58	50	1070 (delithiation)	[101]
Porous graphene	100	80	0–3	2000	650	31	120	450 (delithiation)	[102]

unavoidably lead to huge irreversible capacity and, often, to instability upon cycling.

In this period, the first steps were moved toward the removal of electrode's inert components, like the binder, leading to the first examples of free-standing graphene electrodes. G. G. Wallace et al.[35] observed, however, that RGO-paper had an enormous irreversible capacity in the first lithiation/delithiation cycle (Table 1). Moreover, upon the following lithiation, only 12.4% of the initial capacity was retained. This was the first evidence of the drawbacks of RGO binder-free electrodes. Indeed, it was subsequently found that, in absence of binder, the 1st cycle irreversible specific capacity was always higher than 40%[37–41] and, in some cases, the binder-free electrodes were very fragile and difficult to handle.[41] Despite few research efforts starting the good practice of reporting the electrodes' active material loadings,[35,42] still the focus was only on gravimetric capacity, and no indication on volumetric values was given. Thus, making even harder a fair estimation of RGO potential as LIB anode.

In 2010, the further progression of graphene-based host structures (i.e., hollow GO spheres,[43] RGO,[37,39,44–50] unzipped CNT,[51] bottom-up-synthesized graphene,[52] CVD-synthesized graphene[40] and N-doped graphene[40]) only enabled limited progresses (Table 1). However, some major advances in understanding the Li-ion storage mechanism in different kinds of graphene were reported. The first finding concerned the difference in the Li⁺ storage mechanism in single- and few- layer graphene. Berkeley's researchers[53] showed that few-layer graphene has a behavior resembling that of bulk graphite. Single-layer graphene behaved radically different instead and the intercalation stage "1", corresponding to the LiC_6 stoichiometry for the fully lithiated graphite, could not be reached. Based also on previous models developed few years before,[54,55] the authors proposed that the strong Coulombic repulsion of Li atoms facing opposite sides of the same graphene sheet results on lower binding energies, likely leading to a very low surface coverage equivalent only to a graphitic intercalation "stage 20" (i.e., stoichiometry of LiC_{120}). These findings were further supported, few years later (i.e., in 2013), by a DFT study from B. I. Yakobson et al.[56] showing that, in single-layer graphene, the formation of Li clusters is energetically favored with respect to any stable Li-graphene phase. These reports dispelled the myth of the theoretical Li_2C_6[26] and Li_3C_6[27] stoichiometries, and clearly indicates that single-layer graphene cannot be proficiently used as Li⁺ host in LIB anodes. Interestingly, the same authors[56] proposed that doping the graphene matrix with boron could help to overcome the capacity limitation of pristine graphene. In fact, as Li donates its $2s$ electron to the host, an electron-poor matrix such as C_3B could better accept such extra charge.

Following such theoretical predictions, in 2011, many researchers focused on doping, functionalization and development of complex graphene-based hierarchical architectures. N- and B- doped graphenes showed large reversible capacity (exceeding 1000 mAh g⁻¹) and, most interestingly, an impressive rate capability with capacities of about 200 and 235 mAh g⁻¹ at a massive current of 25 A g⁻¹, for N- and B- doped samples, respectively[57] (Table 1). Despite the promising results, the authors estimated power and energy density on a single electrode basis (in half-cell configuration), hence,

providing meaningless values.[19] Indeed, as previously discussed in Section 3.2, energy and power can be only referred to a full device.[23] Similarly, G. Cui et al.[58] reported the synthesis of a further N-doped RGO, with enhanced performance with respect to the un-doped one. Interestingly, the voltage profiles seemed to be improved by the N-doping, with substantial amount of charge stored/released at relatively low potentials (<1.5 V vs Li/Li$^+$). The presence of the dopant was also beneficial for the rate capability (as demonstrated by the 250 mAh g^{-1} delivered at 2.1 A g^{-1}) and the cycling stability. The authors claimed such improvements to arise from faster Li$^+$ diffusion and decreased electrolyte decomposition, respectively. X. Chen et al.[59] also reported a honeycomb hierarchical (i.e., ordered) film composed of functionalized RGO. The binder-free film showed enhanced lithium-ion storage properties with respect to the non-patterned (i.e., disordered) film, with very large delivered capacity (see Table 1). However, the steep delithiation voltage profiles, together with the high 1st cycle irreversible capacity, left few chances for its practical application. A further approach was reported by H. H. Kung et al.,[60] who introduced in-plane carbon vacancies into the graphene structure, to produce a flexible defect-rich RGO paper named "holey graphene". When used as Li-ion host, the holey graphene could sustain massive current loads (i.e., 10 A g^{-1}) providing reasonable reversible capacity values (i.e., about 75 mAh g^{-1}). However, the low electrode mass loading (i.e., in the 0.2–0.3 mg cm^{-2} range) surely helped to achieve such numbers. Additionally, once again, the authors calculated power and energy densities of a single electrode and improperly compared the obtained values, with other electrochemical energy storage technologies.[60] Despite previous papers claimed a certain fragility of bare RGO paper electrodes,[35] these last two research efforts clearly demonstrated that the introduction of defects, or the direct functionalization of RGO's surface with other electroactive species, could enable flexible graphene-based electrodes. Similarly, other research efforts on N-doped RGO[61] and RGO paper functionalized with CNT[62,63] were reported, but no substantial improvement in terms of electrochemical performance could be observed (Table 1). Moreover, a chemically activated RGO paper was also tested as LIB anode[64] but, unfortunately, it showed very poor performance (i.e., 1st cycle irreversible capacity of about 86% and a lithiation capacity retention of about 16% after 10 cycles at 20 mA g^{-1}) (Table 1).

In the meanwhile, enhanced performances (in terms of 1st cycle irreversible capacity, capacity retention, stability upon cycling and moderate delithiation voltage) were achieved by graphene obtained from liquid-phase exfoliation in cases of the microwave-irradiated graphene[65] and graphene functionalized with 1-pyrene sulfonic acid sodium salt.[66] In few cases, RGO was also investigated as minor component, e.g., as conductive additive, in graphite-based anodes.[67,68] Unfortunately, even if slightly higher gravimetric capacities were obtained, the still higher cost of RGO production does not justify the replacement of conventional carbon additives.

In 2012, the work on graphene as Li-ion host proceeded with the development of a hollow structure (i.e., "graphene balls")[69] and a conductive paper made of RGO-shelled cellulose fibers.[70] However, their lithium-ion storage performances were not very promising (Table 1). Several other structures such as aerogel-derived RGO paper,[71] functionalized-RGO/carbon nanotubes hybrid[72] and RGO/sulfur-doped porous carbons[73] (with carbons derived from the 1-butyl-3-methylimidazolium hydrosulfate ionic liquid) were also reported (Table 1). Nevertheless, despite the enhanced cycling stability of the RGO/sulfur-doped porous carbons,[73] no effective progress could be clearly appreciated in the other cases. Worth to be mentioned is that, in this year, a RGO anode was for the first time tested in combination with an ionic liquid-based electrolyte[74] (i.e., N-methyl-N-propylpyrrolidinium bis(trifluoromethanesulfonyl)-imide). Despite the promising specific capacity obtained, the ionic liquid did not help solving the major issues of RGO, such as 1st cycle irreversibility, poor stability upon cycling and steep delithiation voltage.

Most importantly, in this year some relevant discoveries on the storage properties of lithium ions in graphene were reported. Particularly, the Li$^+$ diffusion mechanism was deeply investigated.[75] It was demonstrated that Li$^+$ diffusion perpendicular to the basal plane of graphene (obtained by CVD) is facilitated by defects, whereas diffusion parallel to the plane is limited by the steric hindrance that originates from aggregated Li ions adsorbed on the abundant defect sites which, also, lead to the previously described drawbacks (i.e., irreversible capacity and voltage hysteresis). Furthermore, the effects on the Li-ion storage properties of different sonication times (for liquid-phase-exfoliated graphene),[76] methods of reduction for graphene oxide[77–81] and electrode preparations[82] were intensely studied, thus demonstrating again how the processing of this class of materials can strongly influence the electrochemical properties of graphene.

Starting from 2013, further doping approaches were reported, for example, P-doped[83] and N-S-codoped[84] graphenes were investigated as lithium-ion host (see Table 1). Particularly, the codoped graphene[84] showed an impressive rate capability and cycling stability but, because of the porous structure, a large 1st cycle irreversibility was also present. Interestingly though, testing the material in a wide temperature range (i.e., from −20 °C to 55 °C), the authors demonstrated how graphene can be a cutting-edge material in the niche of low-temperature LIB applications. Indeed a stable gravimetric capacity of about 220 mAh g^{-1} was obtained for 150 cycles at −20 °C applying a specific current of 1 A g^{-1}. Unfortunately, the authors erroneously calculated the energy and power on a single electrode basis. Other materials such as bottom-up-synthesized graphene,[85] electrochemically exfoliated graphene,[86] holey-RGO hydrogel,[87] CVD-derived flexible graphene paper,[88] polysulfide-functionalized RGO[89] and catalytically exfoliated few-layer graphene[90] were characterized and tested. Unluckily, despite the valuable cycling performances observed in two cases,[89,90] none of them seemed to have the potential of meeting the requirements of practical use.

With the growing progression of highly porous electrode architectures, in 2014, some reports started to recognize the importance of volumetric parameters in the evaluation of anodes having graphene as main active material. J. Gao et al.[91] (Table 1), reported a N-S-codoped graphene (synthesized through CVD) with a compacted density of 0.4 g cm^{-3} which is almost 4 times lighter than compacted graphite (i.e., 1.5 g cm^{-3}).[91] Nevertheless, the authors claimed a volumetric

capacity of about 1410 mAh cm^{-3}, which is more than twice that of graphite ($\approx$560 mAh cm^{-3}) for an applied current of 50 mA g^{-1} in the 0.01–3 V potential range. L. David and G. Singh[92] (Table 1) interestingly found a strong dependence of annealing temperature and gas environment on the lithium storage properties of RGO paper electrodes. Indeed, when reduced at 900 °C, the RGO-paper electrodes delivered an average gravimetric capacity of only about 325 mAh g^{-1} (for an applied current of 100 mA g^{-1} in the 0.01–2.5 V potential range), corresponding to a volumetric capacity of about 100 mAh cm^{-3} (from this data, a density of the graphene paper of about 0.31 g cm^{-3}, more than 7 times lower than the density of graphite,[19] can be calculated). However, if the annealing was performed in a NH$_3$ environment, the graphene-based electrodes showed improved cycling efficiency and rate capability. The authors attributed this behavior to the "increased level of ordering in graphene sheets and decreased interlayer spacing with increasing annealing temperatures in Ar or reduction at moderate temperatures in NH$_3$ atmosphere". Unfortunately, in these latter research investigations, while describing the properties of the materials, the authors did not comment on the steep delithiation voltage profiles which, again, are not very appealing for practical applications.

Interestingly J. B. Baek et al.,[93] with a mechanochemical approach, synthesized different edge-selectively halogenated graphene nanoplatelets (called XGnPs, X = Cl, Br, or I) and probed their electrochemical properties. They found that the IGnP electrode could deliver an initial lithiation gravimetric capacity of 563 mAh g^{-1} (at 250 mA g^{-1} in the voltage range of 0.02–3 V), which is slightly higher than the corresponding value of 511 mAh g^{-1} of the HGnP counterpart. However, after 500 cycles, the IGnP electrode still provided 458 mAh g^{-1} (capacity retention of 81.4%) compared to the 208 mAh g^{-1} of HGnP (corresponding to 40.8%). Unfortunately, apart from the complicated synthetic route employed, all the halogenated graphenes still displayed the usual steep voltage profile with capacity delivered in a very broad voltage range.

In 2015, several hybrid graphene architectures were developed, with particular focus on long term cycling. For example, branched graphene nanocapsules were proposed as enhanced LIB anode material.[94] Indeed, despite the steep delithiation voltage and the considerable 1st cycle irreversible capacity, after 5000 stable cycles, a specific delithiation capacity of about 500 mAh g^{-1} (obtained applying a massive current of 15 A g^{-1} in the 0.01–3 V range) could be still delivered. Other kinds of graphene also proved their strength upon long term cycling. Indeed, N-doped RGO,[95] porous RGO aerogel,[96] N-doped 3D macroporous RGO,[97] N-doped graphene (synthesized by bottom-up procedure),[98] N-S-codoped RGO,[99] N-F-codoped RGO,[100] N-doped holey RGO foam,[101] and porous graphene (obtained by a peculiar top-down process)[102] displayed some of the most promising electrochemical performances among all graphene-based anodes (Table 1). Interestingly, it was also proved that multilayer graphene (obtained by liquid-phase exfoliation in 1-ethyl-3-methylimidazolium acetate ionic liquid) could reversibly store lithium ions down to −30 °C, showing noticeable specific gravimetric capacity even when directly compared to its graphite analogue.[103] Even though the delithiation voltage was not reported, the voltage profile resembling

that of graphite is definitely appealing. K.-B. Kim et al.[104] also showed, through a spray-assisted method for the self-assembly of RGO, how the temperature and type of solvent used during the graphene oxide reduction process directly affected the graphene's SSA.

This year, only few research efforts were focused on the study of volumetric properties of graphene-based electrodes. R. S. Ruoff et al.,[105] reported a compressed graphite foam containing functionalized-RGO with an electrode density of 0.94 g cm^{-3} which shows, for an applied current of about 37 mA g^{-1} in the 0.01–3 V potential range, a specific gravimetric capacity of about 642 mAh g^{-1}, calculated based on the total mass of the electrode (which is comprised of 65 wt% of graphene). The authors reported a volumetric capacity of about 602 mAh cm^{-3} for the whole electrode. X. Duan et al.[106] also reported high volumetric capacities of 753 and 487 mAh cm^{-3} at 0.1 and 1.0 A g^{-1}, respectively, by using solvated graphene framework-based electrodes (obtained by using RGO hydrogel previously prepared by a solvent-exchange approach). The authors claimed that such kind of electrodes exhibit excellent volumetric capacities which approached that of graphite at low currents and considerably exceeded it at high currents.

4.2. Graphene-Containing Materials as a Li-Ion Hosts

Just one year after the first report by I. Honma, RGO already became the "standard graphene" choice for LIB anodes[11] (see **Figure 3**). Although highly defective, the versatility of its oxide precursor (easy to disperse, hydrophilic, etc.)[29] promoted the development of a variety of graphene-containing composite anodes. Indeed, the introduction of additional electroactive species was expected to enable larger storage capability and, at the same time, hinder the layers' restacking.

At the beginning of 2009, I. Honma et al.[32] proposed a hybrid electrode material including RGO and SnO$_2$ nanoparticles. Besides providing additional sites for Li-ion storage, RGO was expected to enhance the cycling stability of tin oxide by containing its volume expansion upon lithiation. They synthesized a composite with a SnO$_2$:RGO molar ratio of 1.5 and, although no details about electrode preparation and electrochemical tests were given, the authors claimed an increase of the specific gravimetric capacity compared to pristine RGO and SnO$_2$. As reported in **Table 2**, although a gravimetric capacity of 810 mAh g^{-1} was reached after 30 cycles, the coexistence of RGO and SnO$_2$ did not lead to a substantially improved cycling stability. Furthermore, the initial conversion of SnO$_2$ to Sn^0 summed up with the solid electrolyte interphase[107] (SEI) formation on graphene, resulting on a massive 1st cycle irreversibility. In the same year, other two reports on graphene with Sn/SnO$_2$ were published.[108,109] In these research efforts, G. Wang et al. synthesized two different graphene-based composites. The first,[108] with a 40 wt% SnO$_2$ content, showed performance comparable with the results previously obtained by I. Honma et al.[32] In the second,[109] aiming to avoid the conversion reaction during the first lithiation, SnO$_2$ was simultaneously reduced with GO to obtain a RGO/Sn composite. Unfortunately, despite a reduction of the 1st cycle irreversible capacity to 35%, this composite showed the same issues
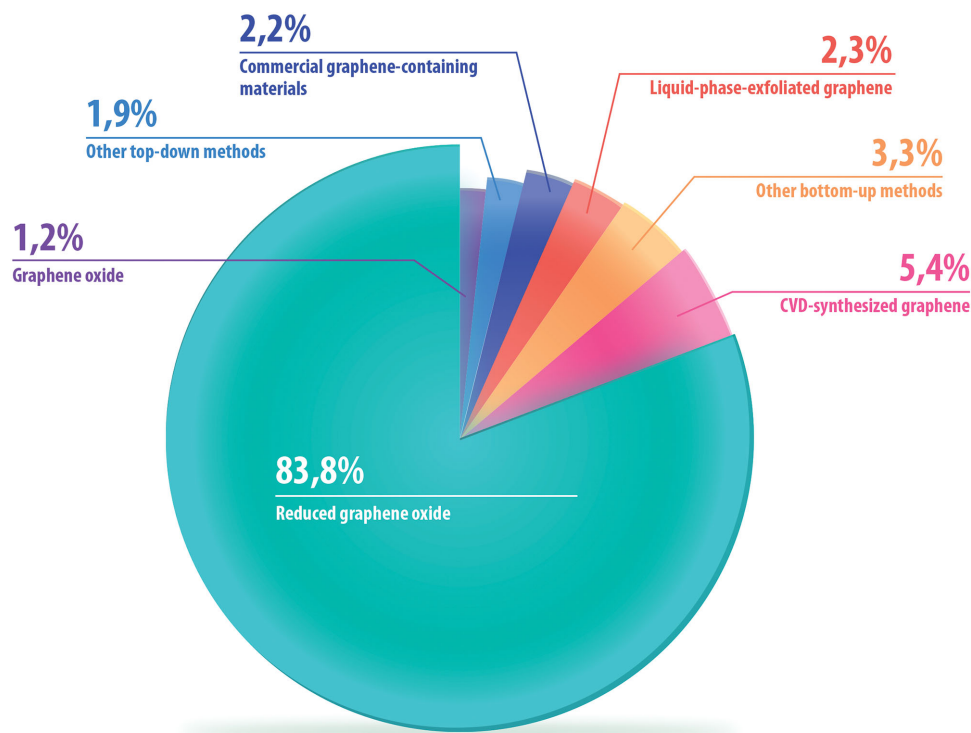
Figure 3. Schematic representation of the different graphene typologies used in LIB anodes between 2008 and 2015 (see Figure 1 caption for the details of the data collection).

of poor cycling stability and poor Coulombic efficiency. Other two kinds of graphene hybrid were also reported in the same year, namely, RGO–cuprous oxide[110] and RGO–silicon oxycarbide.[42] Unluckily, none of these demonstrated substantially enhanced electrochemical properties compared to graphite (see Table 2). In spite of the not exciting performance, in their research effort, F. Hou et al.[42] highlighted the impact of the composite preparation method on its lithium-storage properties. Indeed, two composites featuring the same amount of RGO (25 wt%) were studied. In one of which, the components were simply blended by physical mixing, while in the other, the composite was synthesized via precursor route. It was shown that the chemically synthesized composite improved the electrochemical performance in terms of cycling stability with respect to the physical mixture analogue.

In the same year, the combination of graphene with high voltage anode materials also started to be attractive. The electrochemical properties of a TiO₂–RGO composite were the first to be investigated (Table 2). Through a clever self-assembling method, D. Wang et al.[111] were able to enhance the rate capability of both rutile and anatase TiO₂ by using a small amount (i.e., in the 2.5–10 wt% range) of functionalized RGO as substrate for the growth of the titanium oxide crystals. In this case, graphene was only meant to act as enhanced conductive carbonaceous matrix. However, a large portion of storage sites of RGO were accessible in the potential window comprised between 1 and 3 V vs Li/Li⁺, thus, leading to an additional capacity that the authors claimed to rapidly fade to 25 mAh g⁻¹ within the first 10 cycles (observed at low currents, while at higher currents it could be neglected). In spite

of that, this research effort demonstrated, for the first time, the beneficial effect of graphene on the anode's rate performance, even compared to commercially available carbon black.

In 2010, the same Pacific Northwest's research team (i.e., D. Wang et al.), by using the developed synthetic pathway already applied for producing the aforementioned TiO₂-based hybrids,[111] successfully prepared different metal oxide (MO)-graphene composites with high SnO₂ and NiO content (i.e., about 70 wt%) and tested them as LIB anode active materials[37] (see Table 2). Other graphene-based composites, containing metal-oxides (such as Co₃O₄,[45–47,112] Fe₃O₄,[113–115] Mn₃O₄[116] and CuO[117]) or metal hydroxide (i.e., Co(OH)₂[44]), emerged this year but, unfortunately, even though large specific gravimetric capacities were achieved, they all showed a generally limited cycle life and, in some cases, an unsatisfactory electrochemical reversibility (see Table 2).

Alongside with the first examples of Si-containing graphene composites,[38,41,52,118] few other electrochemical studies on graphene/Li₄Ti₅O₁₂ (i.e., RGO/LTO) hybrid[119] (where graphene was only used as conductive matrix, similarly to the graphene/TiO₂ composites previously mentioned), and graphene-containing composites (i.e., RGO/nitridated-TiO₂,[120] RGO/SnO₂,[49,50,121,122] arc-discharged graphene/SnO₂[123] and RGO/SnSb,[124] hybrids) were performed in this period (Table 2). Unfortunately, except for the RGO/LTO hybrid[119] which showed an excellent stability at high current for more than 1300 cycles (maybe also due to the minimal RGO content, i.e., 1 wt%), none of the proposed systems overcame the previously mentioned drawbacks of graphene. Interestingly though, crucial advances in the synthesis of the metal particles

Table 2. Lithium-ion storage performances of different graphene-containing hybrids reported between 2008 and 2015 (all the tests refer to half-cell configuration).

Active material	Graphene in the active material [wt%]	Active material in electrode [wt%]	Potential range applied (vs Li+/Li) [V]	Specific current applied [mA g⁻¹]	1st cycle lithiation capacity [mA g⁻¹]	1st cycle irreversible capacity [%]	No. cycles	Last specific gravimetric capacity [mAh g⁻¹]	Ref.
2009									
RGO/SnO$_2$	75	–	0.05–2	50	1860	57	30	810 (delithiation)	[32]
RGO/SnO$_2$	60	90	0.01–3	55	1420	46	100	520 (delithiation)	[108]
RGO/Sn	65	90	0.01–3	55	1250	35	100	508 (delithiation)	[109]
RGO/Cu$_2$O	80	85	0–3	0.1 [mA cm⁻²]	1090	55	29	280 (delithiation)	[110]
RGO/SiOC	25	85	0–3.5	40	1141	50	20	357 (delithiation)	[42]
RGO/TiO$_2$ [rutile]	10	90	1–3	34	280	27	3	198 (delithiation)	[111]
RGO/TiO$_2$ [anatase]	2.5	80	1–3	34	263	23	5	181 (delithiation)	[111]
2010									
RGO/SnO$_2$	28	28	0.02–1.5	10	1470	88	120	680 (delithiation)	[37]
RGO/NiO	30	30	0.02–3	0.012 [mA cm⁻²]	1350	74	120	350 (delithiation)	[37]
RGO/Co$_3$O$_4$	34	80	0.01–3	74	1270	53	20	760 (lithiation)	[45]
RGO/Co$_3$O$_4$	46.2	80	0.005–3	89	2310	46	30	1065 (delithiation)	[46]
RGO/Co$_3$O$_4$	25	80	0.01–3	50	1097	31	30	935 (delithiation)	[47]
RGO/Co$_3$O$_4$	8.5	80	0.01–3	74	1680	32	130	1000 (lithiation)	[112]
RGO/Fe$_3$O$_4$	13.3	80	0.01–3	35	1385	35	30	1025 (delithiation)	[113]
RGO/Fe$_3$O$_4$	22.7	75	0.01–3	100	1370	22	40	1050 (delithiation)	[114]
RGO/Fe$_3$O$_4$	12.4	75	0.01–3	100	1280	22	40	540 (delithiation)	[114]
RGO/Fe$_3$O$_4$	3	80	0–3	92.4	1320	34	50	680 (delithiation)	[115]
RGO/Mn$_3$O$_4$	10	80	0.1–3	40	1325	32	5	890 (delithiation)	[116]
RGO/Cuo	26	80	0.01–3	65	890	30	100	650 (delithiation)	[117]
RGO/Co[OH]$_2$	25	75	0.005–3	200	1599	30	30	920 (delithiation)	[44]
RGO/Si	73.6	100	0.02–1.2	50	2170	63	100	708 (lithiation)	[38]
RGO/Si	97.4	100	0.02–1.5	1000	4510	41	80	1960 (delithiation)	[41]
Bottom-up-synthesized graphene/Si	50	80	0.02–1.2	100	2158	27	30	1178 (lithiation)	[52]
Liquid-phase-exfoliated graphene/Si	50	90	0.005–0.8	105	3646	36	20	2041 (delithiation)	[118]
RGO/LTO	1	70	1–3	3850	110	–	1300	101 (lithiation)	[119]
RGO/nitridated-TiO$_2$ [anatase]	10	85	1–3	34	314	25	10	182 (delithiation)	[120]
RGO/SnO$_2$	40	80	0.02–3	264	1280	38	50	558 (delithiation)	[49]
RGO/SnO$_2$	22	80	0.005–2	50	1775	51	50	665 (lithiation)	[50]
RGO/SnO$_2$	38	90	0.001–3	100	1719	50	50	634 (lithiation)	[121]
RGO/SnO$_2$	37	80	0.01–1.5	200	1415	–	35	377 (lithiation)	[122]
Arc-discharge-synthesized graphene/SnO$_2$	33	90	0.05–3	130	673	–	10	513 (lithiation)	[123]
RGO/SnSb	29.9	80	0.005–3	80	1908	41	30	714 (lithiation)	[124]
RGO/SnSb-C coated	29.9	80	0.005–3	80	1498	35	30	896 (lithiation)	[124]

Table 2. Continued.

Active material	Graphene in the active material [wt%]	Active material in electrode [wt%]	Potential range applied (vs Li+/Li) [V]	Specific current applied [mA g−1]	1st cycle lithiation capacity [mA g−1]	1st cycle irreversible capacity [%]	No. cycles	Last specific gravimetric capacity [mAh g−1]	Ref.
					2011				
RGO/Fe$_2$O$_3$	20	95	0.005–3	100	1693	27	50	1027 (lithiation)	[125]
RGO/Fe$_2$O$_3$	21	80	0.01–3	2014	1085	–	350	600 (lithiation)	[126]
RGO/Fe$_2$O$_3$	2.8	80	0.005–3	200	1338	–	100	776 (lithiation)	[127]
RGO/MoS$_2$	33 [mol%]	80	0.01–3	100	2225	41	50	1290 (lithiation)	[129]
RGO/MoS$_2$-C	50 [mol%]	80	0.01–3	100	1760	36	100	1130 (lithiation)	[130]
RGO/MoS$_2$	33 [mol%]	80	0.01–3	100	1570	34	100	1187 (lithiation)	[131]
RGO/MoS$_2$/PEO	2	–	0.01–3	50	1130	26	180	970 (delithiation)	[132]
RGO/CdS	99.5	80	0–3.5	50	1265	44	20	889 (lithiation)	[133]
RGO/NiO	77	80	0.005–3	50	1640	36	40	1031 (delithiation)	[134]
RGO/MoO$_2$	11.2	80	0.01–3	2000	520	–	70	408 (lithiation)	[135]
RGO/Mn$_2$Mo$_3$O$_8$	10.3	80	0.01–3	200	920	28	40	945 (lithiation)	[136]
RGO/MnO$_2$	50	100	0.01–3	100	1250	46	10	610 (lithiation)	[137]
Polymer-functionalized RGO/MnO$_2$	55	90	0.2–3	50	1835	40	15	948 (lithiation)	[138]
Bottom-up-synthesized graphene/MnO$_2$	–	85	0.01–3	–	1235	42	20	585 (lithiation)	[139]
N-doped RGO/VN	50	85	0.01–3	21	590	52	10	340 (lithiation)	[140]
RGO/CeO$_2$	30	80	0.005–3	50	1450	31	100	600 (delithiation)	[141]
RGO/SnSe$_2$	50	80	0.001–3	40	1730	54	30	640 (lithiation)	[142]
RGO/NiSb	7	75	0.05–1.5	40	855	52	30	280 (delithiation)	[143]
RGO/FeSb$_2$	8	75	0.05–1.5	40	1170	62	30	240 (delithiation)	[143]
					2012				
RGO/Ge-C	–	85	0–1	50	1803	48	50	940 (lithiation)	[181]
RGO/Ge-C	15	50	0.01–1.5	160	2300	47	50	1090 (lithiation)	[182]
RGO/Ge	70	78	0.01–3	200	1410	54	15	540 (lithiation)	[183]
RGO/Ge	25	100	0.01–3	65	1050	18	20	620 (delithiation)	[184]
RGO/CoFe$_2$O$_4$	17	80	0.01–3	100	1388	35	50	910 (lithiation)	[185]
RGO/NiFe$_2$O$_4$	20	80	0.01–3	100	1363	30	50	812 (lithiation)	[186]
RGO/CuFe$_2$O$_4$	25	80	0.01–3	100	2000	42	50	1031 (lithiation)	[187]
RGO/ZnFe$_2$O$_4$	36.3	75	0.005–3	50	1185	36	30	620 (delithiation)	[188]
RGO/SnS$_2$	5	80	0.005–1.3	50	1900	63	30	650 (delithiation)	[189]
RGO/SnS$_2$	15	85	0.01–1.5	100	1675	57	50	920 (delithiation)	[190]
RGO/SnS$_2$	68	85	0.001–3	59	1145	13	50	575 (delithiation)	[191]
RGO/Sb$_2$S$_3$	16.5	60	0–2.5	100	1211	28	5	800 (delithiation)	[192]

Table 2. Continued.

Active material	Graphene in the active material [wt%]	Active material in electrode [wt%]	Potential range applied (vs Li+/Li) [V]	Specific current applied [mA g−1]	1st cycle lithiation capacity [mA g−1]	1st cycle irreversible capacity [%]	No. cycles	Last specific gravimetric capacity [mAh g−1]	Ref.
RGO/In$_2$S$_3$	7.1	70	0.005–3	100	1327	35	100	1015 (delithiation)	[193]
RGO/SnO$_2$-SiC	10	70	0.01–1.5	100	2200	34	40	1315 (lithiation)	[194]
RGO/SnO$_x$Fe$_y$S$_z$	–	80	0.001–3	50	1610	55	30	727 (lithiation)	[195]
RGO/FeSn$_2$	5.8	75	0.05–2	50	755	24	25	510 (delithiation)	[196]
RGO/CoSb$_3$	5.8	75	0.05–1.5	40	1128	54	30	320 (delithiation)	[197]
RGO/Bi$_2$Te$_3$	11.5	75	0.005–2.5	50	731	34	50	150 (delithiation)	[198]
RGO/ZnO	14.6	75	0.05–2	50	1235	66	25	295 (delithiation)	[199]
RGO/Ni$_2$P	13	85	0.02–3	54.2	974	41	50	450 (lithiation)	[200]
RGO/TiP$_2$O$_7$	10	30	0.2–2.5	0.1 [mA cm−2]	795	58	15	249 (lithiation)	[201]
RGO/Cr$_2$O$_3$	–	70	0.01–3	100	970	41	30	530 (lithiation)	[202]
RGO/Ag	65	100	0–3	50	975	53	100	350 (delithiation)	[203]
RGO/SiO	43	80	0.01–2.5	100	2285	40	100	890 (delithiation)	[204]
RGO/LiF	88.4	70	0.01–3	500	1360	52	150	545 (lithiation)	[205]
2013									
N-doped RGO/Ni$_3$S$_4$	14.3	80	0–3	140	1660	20	100	1323 (lithiation)	[229]
N-doped RGO/WS$_2$	19.2	90	0.01–3	100	1135	32	100	820	[230]
RGO/CoS	23.5	80	0.005–3	1250	1700	56	100	385 (lithiation)	[231]
RGO/Co$_3$S$_4$	21	75	0–3	140	2151	33	100	720 (lithiation)	[232]
RGO/WS$_2$	20	85	0.01–3	100	1034	52	50	451 (lithiation)	[233]
RGO/FeS	12	70	0.005–3	100	1355	18	30	978 (lithiation)	[234]
RGO/NiS	31.8	75	0.05–3	50	1186	39	100	481 (lithiation)	[235]
RGO/Bi$_2$S$_3$	17.9	80	0.01–3	100	1073	26	50	400 (lithiation)	[236]
N-doped RGO/Co-Co$_3$Sn$_2$	14.1	80	0.01–3	250	1903	18	100	1615 (lithiation)	[237]
RGO/Cu$_6$Sn$_5$	69	80	0.01–2.5	500	1277	30	3000	187 (lithiation)	[238]
RGO/SnCo	82.2	80	0.005–3	720	1755	47	60	475 (lithiation)	[239]
RGO/Zn$_2$SnO$_4$	17.4	75	0.005–3	50	1685	46	25	860 (delithiation)	[240]
RGO/C-Li$_2$SnO$_3$	18	65	0–2	60	2171	51	50	763 (lithiation)	[241]
N-doped RGO/Zn$_2$GeO$_4$	27.8	70	0.001–3	100	1463	40	100	1044 (lithiation)	[242]
RGO/CuGeO$_3$	14.2	70	0.02–3	100	2544	54	130	780 (lithiation)	[243]
RGO/ZnWO$_4$	7	85	0.01–3	50	1016	32	20	585 (lithiation)	[244]
RGO/SnWO$_4$	6	80	0.01–3	50	1517	45	20	500 (lithiation)	[245]
RGO/WO$_3$	7.9	75	0.01–3	100	923	33	100	610 (lithiation)	[246]
RGO/VO$_2$	11	80	0–3	0.1 [mA cm−2]	380	18	50	370 (lithiation)	[247]

Table 2. Continued.

Active material	Graphene in the active material [wt%]	Active material in electrode [wt%]	Potential range applied (vs Li⁺/Li) [V]	Specific current applied [mA g⁻¹]	1st cycle lithiation capacity [mA g⁻¹]	1st cycle irreversible capacity [%]	No. cycles	Last specific gravimetric capacity [mAh g⁻¹]	Ref.
CVD-synthesized graphene/GeO$_x$	30	100	0.01–1.2	320	2049	49	100	1008 (lithiation)	[248]
RGO/Li$_3$VO$_4$	10.5	75	0.2–3	20	410	–	49	370 (delithiation)	[249]
RGO/MnFe$_2$O$_4$	10	80	0.01–3	1000	1530	31	90	767 (lithiation)	[250]
RGO/CoCO$_3$	10	75	0.01–3	50	1980	34	40	930 (lithiation)	[251]
2014									
RGO/NiCo$_2$O$_4$	–	100	0.01–3.0	100	1552	13	10	1267 (lithiation)	[291]
RGO/CuCo$_2$O$_4$	3	70	0.01–3.0	1000	800	34	350	572 (lithiation)	[292]
RGO/ZnCo$_2$O$_4$	10	70	0.01–3.0	90	1211	29	70	756 (delithiation)	[293]
RGO/MnCO$_3$	32	75	0.001–3.0	120	1450	50	100	857 (delithiation)	[294]
RGO/FeCO$_3$	32	70	0.01–3.0	100	1935	45	20	885 (delithiation)	[295]
RGO/CuS	41	70	0.001–3.0	112	851	34	100	711 (lithiation)	[296]
RGO/MnS	25	80	0.005–3.0	50	1512	34	30	976 (lithiation)	[297]
RGO/C$_3$N$_4$	50	80	0.01–3.0	100	3002	43	50	1525 (lithiation)	[298]
RGO/FeN	87.5	80	0.01–3.0	100	750	32	100	555 (lithiation)	[299]
N-doped RGO/MoN	30	80	0.01–3.0	100	545	–	100	518 (lithiation)	[300]
RGO/SiN$_x$	50	100	0.01–1.5	500	1870	–	200	1400 (lithiation)	[301]
RGO/Fe$_3$O$_4$·VO$_x$	–	70	0.1–3.0	2000	735	27	100	730 (lithiation)	[302]
RGO/FeWO$_4$	3	90	0.01–3.0	100	867	16	100	597 (lithiation)	[303]
RGO/ZnMn$_2$O$_4$	25	90	0.01–3.0	2000	1125	22	1500	650 (delithiation)	[304]
RGO/CoSnO$_3$	19	75	0.005–3.0	50	1721	39	5	1095 (lithiation)	[305]
RGO/CoMoO$_4$	26	80	0.01–3.0	74	1250	30	50	915 (lithiation)	[306]
RGO/CuFeO$_2$	–	70	0.005–3.0	708	1110	35	100	450 (lithiation)	[307]
RGO/MgFe$_2$O$_4$	10	70	0.005–3.5	42	1050	32	60	765 (delithiation)	[308]
RGO/Na$_2$Li$_2$Ti$_6$O$_{14}$	3.5	85	1–3	100	205	51	50	104 (delithiation)	[309]
RGO/Sb	16	75	0.005–1.5	50	1034	43	10	515 (delithiation)	[310]
RGO/Sn–In	10	80	0.01–2.0	100	1180	27	50	726 (delithiation)	[311]
RGO/In$_2$O$_3$	20	70	0.01–3.0	58	1322	39	100	480 (lithiation)	[312]
RGO/Co$_2$(OH)$_3$Cl	13.6	75	0.005–3.0	50	1645	34	10	840 (delithiation)	[313]
RGO/LiVPO$_4$F	6.4	80	0.01–3.0	31	385	26	100	303 (delithiation)	[314]
RGO/V$_2$O$_3$	40	80	0.01–3.0	500	870	65	250	270 (lithiation)	[315]
RGO/V$_2$O$_5$	41	75	0.01–3.0	200	1370	40	100	892 (lithiation)	[316]

Table 2. Continued.

Active material	Graphene in the active material [wt%]	Active material in electrode [wt%]	Potential range applied (vs Li$^+$/Li) [V]	Specific current applied [mA g^{-1}]	1st cycle lithiation capacity [mA g^{-1}]	1st cycle irreversible capacity [%]	No. cycles	Last specific gravimetric capacity [mAh g^{-1}]	Ref.
2015									
RGO/Si$_{60}$Sn$_{12}$Ce$_{18}$Fe$_5$Al$_3$Ti$_2$	4	75	0.01–2.5	500	719	21	2000	570 (delithiation)	[327]
RGO/MoSe$_2$	22.5	80	0.005–3	100	1309	27	100	1102 (lithiation)	[328]
RGO/VSe$_2$	–	70	0.01–3	100	775	17	60	630 (lithiation)	[329]
RGO/ZnSe	20	60	0.01–3	1000	1190	48	400	770 (lithiation)	[330]
Commercial graphene/In$_4$Se$_{2.85}$	30	80	0.01–3	100	760	19	50	590 (delithiation)	[331]
RGO/CoSe$_2$	11	70	0.01–3	200	1311	45	200	1577 (lithiation)	[332]
RGO/Ni-NiSiO	–	80	0.1–3	20	1532	54	60	478 (lithiation)	[333]
RGO/CuSiO$_3$	5	70	0.01–3	1000	1360	45	800	747 (delithiation)	[334]
CVD-synthesized graphene/NiMoO$_4$	–	80	0.005–3	200	1385	17	120	1028 (lithiation)	[335]
RGO/Co$_2$Mo$_3$O$_8$	17	70	0.005–3	180	895	33	50	607 (delithiation)	[336]
RGO/Mn$_2$Mo$_3$O$_8$	8	70	0.005–3	180	1368	34	50	518 (delithiation)	[336]
RGO/Zn$_2$Mo$_3$O$_8$	7	70	0.005–3	180	738	52	50	579 (delithiation)	[336]
RGO/Cr$_2$Mo$_3$O$_{12}$	24	80	0.005–3	100	1965	38	50	1000 (delithiation)	[337]
Bottom-up synthesized graphene/MgO	70	70	0.005–3	372	3261	73	60	703 (delithiation)	[338]
RGO/Nb$_2$O$_5$	4.5	80	1–3	20	193	2	50	192 (lithiation)	[339]
RGO/Ga$_2$O$_3$	10	75	0.01–2.5	50	–	39	40	770 (lithiation)	[340]
Commercial graphene/Ca$_2$Ge$_7$O$_{16}$	14	70	0–3	100	2225	55	100	930 (lithiation)	[341]
RGO/Fe$_{0.74}$Sn$_5$	30	80	0.005–2	50	1554	57	100	675 (lithiation)	[342]
RGO/Cu$_3$Ge-Ge	60	80	0.005–3	138	1655	29	100	966 (lithiation)	[343]
RGO/Ni$_x$Zn$_y$Co$_{3-x-y}$O$_4$	5	80	0.01–3	100	1429	25	50	1015 (lithiation)	[344]
Bottom-up synthesized graphene/Bi$_2$WO$_6$	–	85	0.01–3	50	1120	38	50	480 (delithiation)	[345]
RGO/Cu$_{1/3}$Co$_{2/3}$C$_2$O$_4$·xH$_2$O	18	70	0.01–3	1000	1449	47	5000	389 (lithiation)	[346]
RGO/ZnIn$_2$S$_4$	1	75	0.01–3	75	1100	42	25	603 (delithiation)	[347]
RGO/BN	98	100	0–3	200	490	43	200	165 (delithiation)	[348]
RGO/Mo$_2$C	47.4	80	0.005–3	100	1718	47	100	813 (delithiation)	[349]
RGO/Co$_2$P	28	80	0.01–3	100	1090	46	250	870 (delithiation)	[350]

for graphene composites were achieved. It was demonstrated that, by proper nanoscale engineering of the electroactive metal species upon synthesis (i.e., coating the metal particles with a conductive carbon layer), the composite showed substantially enhanced stability upon cycling.[124] Moreover, it was confirmed that for a composite chemically synthesized using RGO, its Li^+ storage ability resulted to be superior to its analogues prepared by simple mechanical mixing.[37,112,117] It was furthermore proven that, if unoxidized graphene (e.g., obtained by liquid-phase exfoliation method) was used to produce a composite with Si,[118] by means of physical mixing, a more stable electrochemical behavior upon cycling was achieved if compared to the analog carbon-black-containing hybrids. The authors believed that, the improved electrochemical performances, could originate from the favorable charge-transport characteristics of the combination of graphene with the porous Si nanostructure.[118] These valuable findings indicated how the synthetic process, and thus the graphene quality (absence of defects,[11] etc.), plays a crucial role in the battery performance of graphene-based composites.

While few research efforts were published in the early years (i.e., between 2008 and 2010), the growing interest on graphene-containing composites resulted in a huge number of publications starting from 2011. After the quite encouraging results obtained with graphene-Fe_3O_4 hybrids in 2010[113–115] (Table 2), R. S. Ruoff et al. reported the synthesis and the electrochemical properties of a RGO-Fe_2O_3 composite.[125] The use of urea to form and anchor $Fe(OH)_3$ on the surface of the GO platelets was an innovative approach. However, it only enabled slight improvements in terms of cycling stability with respect to previous graphene/iron oxide composites (Table 2). Further examples of Fe_2O_3-graphene composites were also reported in the same year.[126,127] In particular, in the work of T. Yu et al.,[127] a first attempt to design a general strategy for preparation and testing of graphene/metal oxide hybrids was proposed. One of the main innovations in 2011 may be the combination of graphene with another 2D material such as MoS_2, belonging to the family of transition metal dichalcogenides.[128] Through the clever use of sulfocarbamide[129,130] or L-cysteine,[131] W. Chen and K. Chang obtained several graphene/MoS_2 hybrids with enhanced cycling stability and larger specific gravimetric capacity than bare MoS_2, even at high specific currents (e.g., 1 A g^{-1}). Particularly, the biomolecular-assisted synthetic approach (i.e., L-cysteine-assisted solution-phase method)[131] enabled, for the composites with a Mo:C molar ratio of 1:2, a specific gravimetric capacity of ca. 1190 mAh g^{-1} after 100 cycles for an applied current of 100 mA g^{-1} (see Table 2). Another MoS_2-graphene hybrid was also reported by J. P. Lemmon et al.[132] In their work, RGO (2 wt%) was incorporated into a MoS_2/polyethylene oxide (PEO) composite but, even if properly engineered, no real progresses in terms of cycling stability or gravimetric capacity were achieved with respect to the previous MoS_2 research efforts (see Table 2). A further graphene/metal sulfide hybrid (i.e., RGO/CdS[133]), alongside with several conversion- (i.e., RGO/NiO,[134] RGO/MoO_2,[135] RGO/$Mn_2Mo_3O_8$,[136] RGO/MnO_2,[137] polymer-functionalized RGO/MnO_2,[138] solvothermally produced graphene/MnO_2,[139] N-doped RGO/VN[140] and RGO/CeO_2[141]), and alloying- (RGO/$SnSe_2$,[142] RGO/NiSb[143] and RGO/$FeSb_2$[143]) based composites were also proposed for the

first time. Unfortunately, none of these enabled satisfactory long term stability (maximum 100 cycles), and most of them showed a high 1st cycle irreversible capacity (see Table 2). At the same time, previously reported graphene-containing alloy (e.g., Sn,[144] SnO_2[145–149] or Si[150–153]), conversion (e.g., Fe_3O_4,[154–157] Co_3O_4[158–161] or CuO[162–164]) and insertion (e.g., TiO_2[165–168] or LTO[169–171]) hybrids were further improved. Interestingly, some appealing approaches, such as the use of ternary hybrids (e.g., RGO/SnO_2/Fe_3O_4[172] or RGO/CNT/Sn[173]), porous 3D (e.g., RGO/Fe_3O_4[174,175]) and hollow architectures (e.g., RGO/Fe_3O_4[176] and RGO/TiO_2[168]), were introduced. In all these cases, however, only modest improvements (especially in terms of cycling stability) were observed with respect to the reports published few years before. Although several publications reported the active material mass loadings,[58,60,65,129,130,132,138,142,147,168,172,177–180] as well as the tap density of the active material[57] and the density of the electrode,[63] no considerations about volumetric capacity were made.

Some progression on composite anodes based on graphene and germanium (i.e., alloy material), MFe_2O_4 (M = Co, Ni, Cu) and M_xS_y (M = Sn, Sb, In) were reported in 2012. Different amounts of RGO were combined with carbon-coated[181,182] or uncoated[183,184] Ge nanoparticles and tested as anode material. Although a large 1st cycle irreversibility was present in most of the cases, the quite stable cycling behavior and the reasonably low delithiation voltage, with a plateau at about 0.5 V, made it a viable candidate for possible use in the LIB field. Interestingly, X. Wang et al., obtained three different RGO/MFe_2O_4 materials (i.e., $CoFe_2O_4$,[185] $NiFe_2O_4$,[186] $CuFe_2O_4$[187]) by applying the same synthetic procedure, but using different MFe_2O_4 precursors. In these research efforts, the graphene components enabled good cycling stability even though the high delithiation voltage (mainly associated to the conversion reaction) made this class of materials poorly suitable for practical battery applications. Such kinds of consideration should be applied to the RGO/$ZnFe_2O_4$ hybrid synthesized by X. Zhao et al.[188] Regarding the RGO/metal sulfide hybrids, the main attention was focused on different high-gravimetric-capacity RGO/SnS_2 composites.[189–191] Particularly, in the work of I. Honma et al.,[191] a low 1st cycle irreversible capacity, alongside with a moderate delithiation voltage, were obtained using a composite with high RGO content (i.e., 68 wt%) (Table 2). Unfortunately though, the cycling stability for this hybrid was quite poor. Other sulfide compounds were tested in combination with graphene, such as RGO/Sb_2S_3[192] and RGO/In_2S_3,[193] but the quite sloping voltage profiles (if compared to the RGO/SnS_2 hybrids) upon delithiation were definitely a drawback. J. Liu et al.,[194] through a uniform dispersion of SnO_2 nanoparticles on a SiC matrix and their encapsulation in the RGO structure, enabled high gravimetric capacity and stable cycling performance at low current (Table 2), although the large 1st cycle irreversibility and high delithiation voltage issues were not overcome. S. U. Son et al.,[195] through a clever organometallic approach, synthesized a RGO/$SnO_xFe_yS_x$, hybrid which, however, showed similar drawbacks as the previous RGO/SnO_2-SiC composite. X.-B. Zhao et al., applying an analogous synthetic procedure, developed and tested different RGO-based composites featuring $FeSn_2$,[196] $CoSb_3$,[197] Bi_2Te_3[198] and ZnO.[199] Unfortunately, none of them were able

to overcome the aforementioned drawbacks of graphene for LIB anodes.

Other phosphides- (i.e., Ni_2P[200] and TiP_2O_7[201]), Cr_2O_3-,[202] Ag-,[203] SiO-,[204] and LiF-[205] containing graphene hybrids were developed but only in the case of RGO/LiF, an enhancement in terms of gravimetric capacity at high current rate (i.e., 181 mAh g⁻¹ for a specific current of 25 A g⁻¹) and stability upon cycling (see Table 2) were achieved (even if the drawback of the steep delithiation voltage was not circumvented and an erroneous calculation of half-cell power and energy densities were reported). The authors claimed that "The discrete crystalline LiF nanoparticles on the graphene surface effectively suppress electrolyte side reactions, affect the formation of both inorganic and organic SEI components, and consequently reduce the thickness of the SEI film formed, enabling fast Li ion transport at the interface between electrode and electrolyte".

Regarding previously developed graphene-containing composites, many different semimetal- (e.g., Si[206–209]), metal- (e.g., Sn[210–213]) and metal-oxide- (e.g., NiO,[214–216] SnO_2,[217–220] Fe_3O_4,[219,221,222] Fe_2O_3,[223] TiO_2,[224] Co_3O_4[225,226] or CoO[227,228]) based graphene hybrids were further reported. However, despite some clever approaches to stabilize the structure of the active material (e.g., freeze-drying,[206] crumpling,[207] spin coating[209] or nanocabling[211]), only few cases reported a successful minimization of the 1st cycle irreversible capacity and improved delithiation voltage.[220,226]

In 2013, new types of hybrids, such as graphene-containing metal sulfides,[229–236] intermetallic compounds,[237–239] metallic stannate,[240,241] -germanate,[242,243] -tungstate,[244,245] -oxides,[246,247] germanium oxide,[248] lithium vanadate,[249] manganese ferrite[250] and cobalt carbonate[251] were introduced. They generally showed an increased specific gravimetric capacity but, except for a few cases,[229,234,237,247] the 1st cycle irreversibility was always higher than 30%. Moreover, a capacity fading was also observed and, unfortunately, the everlasting drawback of the high delithiation voltage, due to the conversion reaction with lithium, was always observable in all the composites.

Regarding the progression of the previously developed hybrids, improved specific capacity values were reported through the exploitation of 3D graphene matrixes incorporating, for example, SnO_2,[252–254] Fe_3O_4,[255,256] MoS_2,[257,258] SnS_2,[259] MnO,[260] TiO_2[261] or Si[262] particles. Indeed, the graphene network appeared to be beneficial for reducing the material resistance and to improve the mechanical stability of the electrode. Moreover, the 3D graphene matrix provided faster ion diffusion which seemed beneficial for achieving improved rate capability. On the other hand, though, porous materials notoriously possess rather low densities, which unavoidably sacrifices the volumetric capacity of the material. Nevertheless, in none of these manuscripts such drawback was mentioned, thus, weakening the strength of the research work for a possible fruition at large scale. Ternary hybrids including species electrochemically active at different potentials (e.g., $RGO/TiO_2/SnO_2$,[263] $RGO/TiO_2/Co_3O_4$[264] or $RGO/Fe_2O_3/SnO_2$[265]) were also proposed to enable larger storage capability. Furthermore, an RGO/SnO_2 composite (containing 42 wt% or graphene) with an excellent low 1st cycle irreversible capacity of only 3.6% was reported for the first time. However, the authors did not investigate this aspect in detail and did not propose any possible explanation.

X. B. Zhang et al.[266] also reported stable cycling behavior (i.e., 500 cycles at 1 A g⁻¹ with a gravimetric capacity of about 400 mAh g⁻¹) for a RGO/CoO hybrid at 0 °C.

Due to the high theoretical specific gravimetric capacity and the promising delithiation voltage, Si-based graphene hybrids started to attract more and more interest. Among the Si-containing hybrids, J.-S. Chen et al.[267] reported a stable gravimetric capacity of about 1240 mAh g⁻¹ for 50 cycles (with a high 1st cycle irreversible capacity) at the massive current of 32 A g⁻¹ (for a composite containing 90 wt% of Si nanoparticles, 5 wt% of Ag and 5 wt% RGO). Moreover, considerations about volumetric capacity were finally taken into account. Making use of an ultrathin graphite foam (UGF) as substrate for the dropcasting deposition of Si nanoparticles encapsulated in a RGO matrix, R. S. Ruoff et al.[268] reported a 1st cycle gravimetric lithiation capacity of 983 mAh g⁻¹ (with respect to the total mass of the active material) and, for the first time, a 1st cycle volumetric lithiation capacity of 1016 mAh cm⁻³ (with respect to the total volume of the electrode) for the Si/RGO/UGF binder-free electrode (in the 0.01–2.2 V range with an applied current of 400 mA g⁻¹). However, the content of RGO in the overall active material was only ca. 4.5 wt% (while the overall Si and UGF contents were 25.2 wt% and 70.3 wt%, respectively). The authors claimed that the specific volumetric capacity obtained is 93% higher than that for a graphite anode used in commercial 18650 cells. However, the authors did not mention that, besides having a 1st cycle irreversible capacity of about 33%, after 100 cycles the electrode exhibited a gravimetric capacity of about 370 mAh g⁻¹, thus, retaining only 38% of the initial gravimetric capacity. Nevertheless, the authors claimed that the easy process of electrode preparation using the graphite foam, could be used at industrial scale for a possible replacement of "traditional flat electrode for commercial LIBs". Alternatively, L. Zhi et al.,[269] proposed a binder-free electrode consisting of Si nanowires coated with graphene (obtained by means of CVD), in order to enhance the volumetric capacity. Indeed, they stated that, despite having only 10 wt% of graphene and a 1st cycle irreversible capacity of about 22%, when the electrode was cycled in the 0.02–2 V range at a current of 840 mA g⁻¹, a stable volumetric capacity of ca. 1500 mAh cm⁻³ over 200 cycles was obtained.

Given the large number of material combinations already reported in the previous years, in 2014, the research efforts were focused on alternative synthetic approaches. In particular, this year was characterized by an intense use of gel-based techniques (e.g., freeze-drying) and Ni foam substrates (subsequently removed by HCl etching) for the preparation of different electroactive hybrids.

RGO aerogels/TiO_2 nanocrystals,[270] CVD-synthesized porous graphene with anchored Sn nanoparticles,[271] Si nanoparticle/RGO hybrid on porous Ni foam,[272] 3D MoS_2/RGO composite,[273] metal-oxide-coated 3D CVD-synthesized graphene hybrid[274] Ni_3S_2 particles encapsulated with crumpled RGO[275] and 3D RGO network/porous Si spheres represent some of the most relevant examples. The electrochemical performances of those hybrids clearly demonstrates how the composite architecture influences the lithium-ion storage properties. Enhanced gravimetric capacities and cycling stabilities were achieved in all the aforementioned research

efforts. However, the general low density of such materials might strongly influence the volumetric performances of the electrode. This could be the reason why almost none of the papers published in 2014 mentioned performances per unit of volume. Only in few cases, the volumetric capacity has been reported. J. M. Tour et al.,[276] for example, proposed a Fe_2O_3/Fe_3C-graphene heterogeneous thin film anode (fabricated by CVD growth with a 9 wt% content of graphene) delivering, for an applied current of 50 μA cm^{-2}, a volumetric capacity of 3560 mAh cm^{-3} (corresponding to a gravimetric capacity of 1118 mAh g^{-1}). Taking into account the geometrical area of the electrode (i.e., 0.785 cm^2), the mass of the electrode (i.e., 0.3 mg) and the electrode thickness (i.e., 1.2 μm), it is possible to calculate an electrode density of about 31.85 μg cm^{-3} which is estimated to be at least four orders of magnitude lower than the density of graphite.[19] Nevertheless, this kind of graphene-containing active material could be beneficial for the progress in the field of micro-batteries.[277] Moreover, only in one case the evaluation of the average lithium-ion insertion voltage was performed. I.-D. Kim et al.[278] described the evolution of a high voltage hybrid anode (i.e., graphene/LTO/nanotube ternary composite) claiming that "the lower average voltage (high polarization) of the slurry-cast $Li_4Ti_5O_{12}$ electrode will reduce the energy density of an electrochemical full-cell".

Growing interest in the failure and aging mechanisms of graphene-containing materials also started to emerge. C. Wang et al.[279] reported a study on the effect of the electrode pulverization upon cycling. They demonstrated that Ni/bottom-up-synthesized graphene yolk–shell[280] nanohybrids (i.e., composites constituted by Ni core particles which behave like a movable yolk inside the graphene hollow shell) exhibited enhanced capacity and rate capability compared to their core–shell[281] counterparts (i.e., composites constructed with a fixed Ni core and an outer shell of graphene). The authors claimed that the improvements arose from lowered activation barriers for lithiation/delithiation and improved availability of ions at the interface, leading to a stable long-term cycling (i.e., more than 1700 cycles for an applied current of 5 A g^{-1} in the potential range 0.005–3 V) with a reversible capacity of about 490 mAh g^{-1}. Although no description of the material density was reported, this study proved the extremely promising properties of graphene as enhanced carbon matrix in composites. Besides the advances in 3D architectures, investigations on different metal-oxide-[282–285] and semimetal-[286–289] containing graphene hybrids proceeded. Generally, an enhancement of the stability upon cycling could be always noticed with respect to the composites developed in the previous years. Interestingly, J.-K. Park et al.[290] evidenced how the temperature (in the 5–50 °C range) at which the liquid-phase exfoliation is performed affects the quality of the produced graphene composite (obtained from a graphite intercalation compound such as KC_8 by mild sonication in water). Employing the graphene with the smaller amount of defects, they obtained a Co_3O_4-containing composite (with a 20 wt% of graphene) capable of capacities (in the 0.01–3 V potential range) as high as 1050 mAh g^{-1} at 0.5 A g^{-1} and 900 mAh g^{-1} at 1 A g^{-1}, even after 200 cycles. Unfortunately, the typical drawbacks of a conversion material are always present (hysteresis, high operative voltage, etc.) and no indications about the density of the materials were reported.

A large number of new graphene-containing hybrids was also tested for the first time (see Table 2) as LIB anode active materials (e.g., graphene-containing cobaltites,[291–293] carbonates,[294,295] sulfides,[296,297] nitrides,[298–301] Fe_3O_4-VO_x,[302] $FeWO_4$,[303] $ZnMn_2O_4$,[304] $CoSnO_3$,[305] $CoMoO_4$,[306] $CuFeO_2$,[307] $MgFe_2O_4$,[308] $Na_2Li_2Ti_6O_{14}$,[309] Sb,[310] Sn-In,[311] In_2O_3,[312] $Co_2(OH)_3Cl$,[313] $LiVPO_4F$,[314] V_2O_3[315] and V_2O_5[316] hybrids) but, unfortunately, none could entirely fulfil the requirements of the ideal anode material for LIBs, although two hybrids[291,303] displayed a promisingly low 1st cycle irreversible capacity (i.e., <20%).

In 2015, the number of publications on graphene-based composite anodes slowed down considerably. This occurrence may be associated to the intensification of graphene exploitation in other electrochemical energy storage devices such as supercapacitors,[317] Li–S,[318,319] Li–air,[320] Li-metal batteries[321] as well as in LIB cathodes,[322] Li-ion capacitors,[323] Na-ion anodes,[324] Na-ion cathodes[325] and Na–air batteries.[326] Nevertheless, some new hybrids were introduced in the LIB anode field too. Indeed, graphene-containing glassy metal alloy nanofiber,[327] selenides,[328–332] silicates,[333,334] molybdates,[335–337] oxides,[338–341] intermetallic compounds,[342,343] intermetallic oxides,[344,345] oxalate,[346] sulfide,[347] nitride,[348] carbide[349] and phosphide[350] hybrids were reported (see Table 2). Despite the usual sloping delithiation voltage and the generally low content of graphene (i.e., ≤30 wt%), few of these hybrids[329,331,335] showed a low 1st cycle irreversible capacity (i.e., <20%). Interestingly, the RGO/Nb_2O_5 hybrid,[339] displayed one of the lowest 1st cycle irreversible capacities (i.e., about 2%) and one of the best capacity retentions in the category of high-voltage anodes (i.e., approaching 100% after 50 cycles). Following the trend begun in 2014, this year was mainly characterized by a large number of works focused on long-term cyclability tests (e.g., ≥1000 cycles), generally performed at medium/high currents (e.g., ≥1 A g^{-1}). Indeed, graphene-containing insertion (e.g., Li_3VO_4,[351–353] TiO_2[354,355] and LTO[356]), conversion (e.g., $CoFe_2O_4$,[357] Co_3O_4[358] FeS_2,[359]) and alloying (e.g., Si[360–362] and SnO_2[363]) binary hybrids, as well as ternary analogues,[364–367] showed remarkable results in terms of specific gravimetric capacity retained after long cycling. Moreover, other intermetallic compounds (e.g., SnSb[368,369]) and metal oxides (e.g., Fe_3O_4[370,371] and MnO[372]), when combined with graphene, showed improved cycling stability with respect to their bare analogues. Interestingly, L. Zhi et al.,[373] reported a self-supporting Si/RGO composite assembly (with a graphene content of about 38 wt%) with high gravimetric capacity (1390 mAh g^{-1} at 2 A g^{-1} with respect to the total electrode weight), high volumetric capacity (1807 mAh cm^{-3}, with an active material packing density of about 1.3 g cm^{-3}), enhanced rate capability (900 mAh g^{-1} applying a massive current of 8 A g^{-1}), excellent cycling stability (0.025% decay per cycle over 200 cycles), and promising areal capacity (as high as 4 and 6 mAh cm^{-2} at 15 and 3 mA cm^{-2}, respectively).

J. K. Lee et al.,[374] synthesizing Si/RGO composites with a variable content of graphene (in the 1–10 wt% range), showed how the graphene matrix effectively stabilizes the electrode upon cycling. Moreover, using strategic material design, one of the composites exhibited a high volumetric capacity of about 141% higher than commercial graphite, even if the material's density was only 0.55 g cm^{-3}. In this case, the high gravimetric

**ADVANCED
SCIENCE NEWS**
www.advancedsciencenews.com

**ADVANCED
MATERIALS**
www.advmat.de

PROGRESS REPORT

capacity of the composite played a key role for enhancing the volumetric capacity with respect to graphite.

4.3. Full-Cells Employing Graphene and Graphene-Containing Anodes

In 2010, a full-cell having a graphene-containing material as the anode was reported for the first time by T. Duong et al.[375] (Table 3). By using a graphene/TiO_2 composite[111] coupled with a $LiFePO_4$ cathode, the full-cell exhibited negligible performance degradation after 700 cycles at 1 C rate (i.e., 170 mA g^{-1}) in the potential range 2.5–1 V, reaching a maximum power density of 4.5 kW kg^{-1} (limited by the cathode) and energy density of 263 Wh kg^{-1} (limited by the anode).

A second example of a full-cell was reported in 2011 by Y. Zhang et al.,[376] who coupled a RGO/Fe_3O_4 anode with a commercially available $LiNi_{1/3}Mn_{1/3}Co_{1/3}O_2$ (NMC) cathode. The cell, tested in the 1.2–3.2 V range, showed a large 1st cycle irreversible capacity (i.e., in the 36–38% range) but, unfortunately, no analyses about the power and energy were given (Table 3). In the same year, K. Kang et al.[377] reported a full-cell comprising a freestanding RGO paper anode and a flexible V_2O_5/RGO cathode, which was directly grown on the graphene surface by means of pulsed laser deposition. The cell was cycled only 20 times in the voltage range 1.7–3.8 V (at a constant current of 10 μA cm^{-2}) reaching a final capacity value of about 5 μAh cm^{-2}. Although the initial irreversible capacity was mitigated by electrochemical pre-lithiation of the RGO paper (before full-cell assembly), the cell showed very poor capacity retention (only ca. 33%) (Table 3). Moreover, no indication about power and energy output was reported.

In 2012, three different graphene-based composites were investigated in full-cell configuration. H.-M. Cheng et al.[378] produced a flexible battery using graphene foam (obtained by CVD) in both the anode (containing LTO) and the cathode (containing $LiFePO_4$) enabling an energy density of ≈110 Wh kg^{-1} (based on the total mass of the anode and cathode active material) and showing a stable cycling behavior (even under bending) for more than 40 cycles at 0.2 C rate. It also showed a rather low 1st cycle irreversible capacity (Table 3). A RGO/TiO_2 hybrid anode was also coupled with a $LiMn_2O_4$ cathode in the research effort of Z. Liu et al.[379] Here, in a cylindrical 18650-type cell, reasonable rate capability and stability upon cycling were obtained, albeit the cell showed a 1st cycle irreversible capacity of about 30% at 0.2 C rate (Table 3). Combining a liquid-phase-exfoliated graphene/Si composite and a commercial NMC cathode, Y. Zhang et al.[380] reported for the first time a battery employing a graphene/alloy hybrid. Unfortunately, the unsatisfactory 1st cycle irreversible capacity (i.e., 28%) and the strong capacity fading upon cycling urged for improvements (Table 3).

In 2013, the importance of tests in full-cell configuration started to be recognized, as testified by the growing number of reports. S.-T. Lee et al.,[381] for example, used CVD to deposit crystalline Si particles (14 wt%) onto RGO sheets (86 wt%), and reported a reversible volumetric capacity of 668 mAh cm^{-3} (calculated based on the electrode density of 0.75 g cm^{-3}) in the 0.01–1 V range for an applied current of 400 mA g^{-1} (in half-cell configuration). Despite having a 1st cycle irreversible capacity of about 35%, the active material was also characterized in full-cell configuration using $Li_{1.2}Ni_{0.2}Mn_{0.6}O_2$ as cathode. Cycled in the 2.0–4.5 V potential range, the full-cell enabled an initial discharge capacity of about 2.5 mAh (for a current of 0.1 mA) with an irreversibility in the 22% range (Table 3). However, after 100 cycles at a current of 0.4 mA, a final discharge capacity of only 1.1 mAh was obtained. This year various graphene/metal oxide hybrids were also tested in full-cell configuration. Y. Shi et al.,[382] coupled their RGO/iron oxide hybrid (with an iron oxide content of about 67 wt%) with commercial $LiMn_2O_4$ and $LiCoO_2$ cathodes. Despite having 1st cycle irreversible capacities in the order of 30%, both full-cells showed a stable behavior for 20–25 cycles exhibiting final discharge capacities (based on the mass of the graphene-containing anode only) in the 780–890 mAh g^{-1} range (Table 3). Unfortunately, poor Coulombic efficiencies and capacity retentions were also observed. A further hybrid with a high MO content (i.e., RGO/NiO with 26.9 wt% of graphene) was tested in full-cell configuration by G. Du et al.,[383] employing a commercially available NMC cathode. In the 1.2–3.2 V potential range (at a current of 100 mA g^{-1}) the full-cell exhibited charge/discharge capacities of 1311/617 mAh g^{-1} in the first cycle (according to the mass of the graphene-containing composite), respectively. After 28 cycles, a discharge capacity of 370 mAh g^{-1}, with a Coulombic efficiency of only 93%, was obtained (Table 3). However, even at higher currents, the Coulombic efficiency of the full-cell did not exceed 98%. Y. Lin et al.[384] also investigated the behavior of a hybrid constituted of NiO and RGO aerogel, in a full-cell featuring a $LiCoO_2$ cathode. In the same study, a bare RGO aerogel was also investigated in the same full-cell configuration for comparison. However, even if the hybrid showed higher capacity compared to the bare graphene, after only 20 cycles (performed in the 0.01–3.7 V vs Li/Li$^+$), the discharge capacities for both materials reached similar values (Table 3). Another full-cell using bare RGO as anode and $LiNi_{0.5}Mn_{1.5}O_4$ as cathode was also reported[385] (Table 3). Unfortunately, even if the anode was pre-cycled against a lithium metal electrode before full-cell assembly, really poor electrochemical performance was reported (i.e., only 8 cycles with a capacity of about 100 mAh g^{-1} and a mean value of Coulombic efficiency of about 80% for an applied current of 29 mA g^{-1} in the voltage range 2.0–4.9 V).

Interestingly, despite the initial interest on graphene was motivated by its theoretical enhanced lithium-ion storage ability, the initial tests in full-cells mainly involved graphene composites featuring other electroactive materials as the main component. Only in 2014, graphene-rich anodes started to be deeply investigated in full-cells. Indeed, this year, four different graphene-based anodes (having graphene as main Li-ion host) were tested in full-cell configuration (Table 3). J. Gao et al.,[91] after an initial pre-lithiation, coupled the N-S-codoped graphene anode with a $LiCoO_2$ cathode (Table 3). In the voltage range 1.5–4.6 V, the full-cell delivered an average reversible capacity of 120 mAh g^{-1} at 0.5 C (i.e., 70 mA g^{-1} related to the cathode mass) with a capacity retention of about 83% after 50 cycles (i.e., about 100 mAh g^{-1}). At 1 C (i.e., 140 mA g^{-1} related to the cathode mass), the full-cell reached an average reversible capacity of 104 mAh g^{-1} after 50 cycles. Unfortunately, the

Table 3. Full-cell performances for different graphene and graphene-containing hybrids reported between 2008 and 2015.

Anode	Cathode	Pre-lithiation (Y/N)	Potential range applied (vs Li$^+$/Li) [V]	Applied current	1st cycle charge capacity [mAh g^{-1}]	1st cycle irreversible capacity [%]	No. Cycles	Last discharge capacity [mAh g^{-1}]	Notes	Ref.
2010										
TiO$_2$/functionalized-RGO	LiFePO$_4$	N	1.0–2.5	1 C	330 (anode weight)	42	700	115 (anode weight)	2.5 wt% graphene in the anode	[375]
2011										
Fe$_3$O$_4$/RGO	NMC	N	1.2–3.2	0.1 C	811 (anode weight) / 134 (cathode weight)	38 / 36	10	454 (anode weight) / 80 (cathode weight)	5.5 wt% graphene in the anode	[376]
				0.2 C	767 (anode weight) / 125 (cathode weight)	36 / 36		486 (anode weight) / 79 (cathode weight)		
RGO	V$_2$O$_5$/RGO	Y (anode)	1.7–3.8	10 (μA cm^{-2})	15.1 (μA cm^{-2})	2	20	5.3 (μA cm^{-2})	80 wt% graphene in the cathode	[377]
2012										
LTO/CVD-synthesized graphene	LiFePO$_4$/CVD-synthesized graphene	N	1.0–2.5	0.2 C	146 (cathode + anode weights)	2	41	138 (cathode + anode weights)	12 wt% graphene in both anode and cathode	[378]
TiO$_2$/functionalized-RGO	LiMnO$_2$	N	1.25–3	0.2 C	993 (mAh)	30	2	685 (mAh)	8 wt% graphene in the anode	[379]
Si/liquid-phase-exfoliated graphene	NMC	N	3–4.3	C/15	189 (cathode weight)	28	6	76 (cathode weight)	34 wt% graphene in the anode	[380]
2013										
Si/RGO	Li$_{1.2}$Ni$_{0.2}$Mn$_{0.6}$O$_2$	N	2.0–4.5	C/20	2.47 (mAh)	22	2	1.60 (mAh)	86 wt% graphene in the anode	[381]
Iron oxide/RGO	LiMn$_2$O$_4$	N	0.9–4.1	C/3	1271 (anode weight)	34	25	885 (anode weight)	33 wt% graphene in the anode	[382]
	LiCoO$_2$				1300 (anode weight)	31	20	787 (anode weight)		
NiO/RGO	NMC	N	1.2–3.2	100 mA g^{-1} (anode weight)	1311 (anode weight)	53	28	370 (anode weight)	73 wt% graphene in the anode	[383]
NiO/RGO aerogel	LiCoO$_2$	N	0.01–3.7	100 mA g^{-1} (anode weight)	249 (anode weight)	–	20	298 (anode weight)	–	[384]
RGO aerogel		N			690 (anode weight)	–	20	245 (anode weight)	–	
2014										
RGO	LiNi$_{0.5}$Mn$_{1.5}$O$_4$	Y (anode)	2.0–4.9	29 mA g^{-1} (cathode weight)	124 (cathode weight)	27	8	87 (cathode weight)	–	[385]
N-S-codoped CVD-synthesized graphene	LiCoO$_2$	Y (anode)	1.5–4.6	0.5 C	–	–	50	107 (cathode weight)	–	[91]
				1 C	–	–	50	92 (cathode weight)	–	[91]

Table 3. Continued.

Anode	Cathode	Pre-lithiation (Y/N)	Potential range applied (vs Li^+/Li) [V]	Applied current	1st cycle charge capacity [$mAh\ g^{-1}$]	1st cycle irreversible capacity [%]	No. Cycles	Last discharge capacity [$mAh\ g^{-1}$]	Notes	Ref.
Liquid-phase-exfoliated graphene	$LiFePO_4$	Y (anode)	0.9–3.9	170 $mA\ g^{-1}$ (cathode weight)	185 (cathode weight)	11	80	136 (cathode weight)	–	[386]
RGO	$LiFePO_4$	N	1.5–3.9	34 $mA\ g^{-1}$ (cathode weight)	149 (cathode weight)	82	50	10 (cathode weight)	–	[387]
		Y (anode)			142 (cathode weight)	13		40 (cathode weight)		
RGO	functionalized-RGO	Y (anode)	0.01–4.3	50 $mA\ g^{-1}$ (anode+cathode weight)	190 (cathode weight)	15	10	157 (cathode weight)	–	[388]
Si/RGO	$LiCoO_2$	N	2.5–4.3	7 C	103 (not specified)	1	100	75 (not specified)	18 wt% graphene in the anode	[390]
Commercially available Si/graphene	NCA	N	2.75–4.2	C/15	195 (cathode weight)	31	5	140 (cathode weight)	10 wt% FEC electrolyte additive	[391]
				C/2	19 (mAh)	33	50	15.7 (mAh)	5 wt% FEC electrolyte additive	[392]
Si/RGO	$Li[Ni_{0.75}Co_{0.1}Mn_{0.15}]O_2$	Y (anode)	2.7–4.2	0.1 C	206 (cathode weight)	5	748 (at 1 C)	150 (cathode weight - at 1 C)	6 wt% graphene in the anode	[393]
Si/top-down-synthesized graphene	$LiMn_2O_4$	N	2.5–4.5	400 $mA\ g^{-1}$ (anode weight)	1280 (anode weight)	46	30	570 (anode weight)	40 wt% graphene in the anode	[394]
Si-WC/top-down-synthesized graphene				0.4 (mA)	–	–	30	0.47 (mAh)	50 wt% graphene in the anode	[395]
Ge/RGO	$LiCoO_2$	N	2.5–4.2	1 C	–	–	100	900 $mA\ g^{-1}$ (anode weight)	20 wt% graphene in the anode	[396]
GeO_x/RGO	$LiNi_{0.5}Mn_{1.5}O_4$	Y (anode)	3.5–4.9	70 $mA\ g^{-1}$ (cathode weight)	130 (cathode weight)	8	55	112 (cathode weight)	8.5 wt% graphene in the anode	[397]
Fe_2O_3/RGO	$LiFePO_4$	N	1.5–3.9	34 $mA\ g^{-1}$ (cathode weight)	142 (cathode weight)	98	50	5 (cathode weight)	18 wt% graphene in the anode	[398]
		Y (anode)			137 (cathode weight)	12		109 (cathode weight)		
$ZnFe_2O_4$/RGO	$LiFePO_4$	N	1.0–3.5	100 $mA\ g^{-1}$ (anode weight)	2000 (anode weight)	60	10	450 (anode weight)	12.4 wt% graphene in the anode	[399]
VS_4/RGO	$LiMn_2O_4$	N	1.0–4.3	0.5 C	72 (not specified – at 0.1 C)	–	30	53 (not specified)	3 wt% graphene in the anode	[400]
2015										
RGO	$LiFePO_4$	N	1.5–3.9	34 $mA\ g^{-1}$ (cathode weight)	134 (cathode weight)	78	40	10 (cathode weight)	Not pre-lithiated	[405]
		Y (anode)			140 (cathode weight)	39		20 (cathode weight)	Electrochemical pre-lithiation (2 cycles)	

Table 3. Continued.

Anode	Cathode	Pre-lithiation (Y/N)	Potential range applied (vs Li^+/Li) [V]	Applied current	1st cycle charge capacity [mAh g^{-1}]	1st cycle irreversible capacity [%]	No. Cycles	Last discharge capacity [mAh g^{-1}]	Notes	Ref.
CVD-synthesized graphene	$LiCoO_2$	N	3.0–4.2	100 µA	90 (cathode weight)	−28	—	38 (cathode weight)	Contact pre-lithiation (120 minutes)	[406]
CVD-synthesized graphene	$LiFePO_4$	Y (anode)	—	310 µA cm^{-2}	72 (not specified)	18	1000	60 µAh cm^{-2}	Cathode delithiated by charging it against Li metal-foil	[407]
Commercial graphene	$LiFePO_4$	Y (anode)	1.5–3.9	C/10	163 (cathode weight)	8	5	146 (cathode weight)	PYR_{14} TFSI–LiTFSI, EC–DMC-added electrolyte	[408]
$ZnMn_2O_4$/RGO	$LiFePO_4$	Y (anode)	0.9–3.9	0.2 C	138 (cathode weight)	4	100	124 (cathode weight)	33 wt% graphene in the anode	[409]
LTO/commercial graphene	$LiFePO_4$/commercial graphene	N	1.0–2.5	0.5 C	—	—	100	150 (cathode weight)	45 wt% graphene in both anode and cathode	[410]
Fe_2O_3/RGO	$LiFePO_4$	N	0.4–3.4	50 mA g^{-1} (anode weight)	2090 (anode weight)	34	35 (at 1600 mA g^{-1})	2090 (anode weight – at 1600 mA g^{-1})	15 wt% graphene in the anode	[411]
SnO_2-Fe_2O_3/RGO	$LiCoO_2$	N	1.2–3.8	50 mA g^{-1} (anode weight)	710 (anode weight)	20	30	340 (anode weight)	wt% graphene in the anode not reported	[412]
SnS_2/RGO	$LiCoO_2$	N	2.0–3.9	200 mA g^{-1} (anode weight)	1465 (anode weight)	77	50	85 (anode weight)	10 wt% graphene in the anode	[413]
		Y (anode)			685 (anode weight)	9	150 (at 500 mA g^{-1})	380 (anode weight – at 500 mA g^{-1})		
$CoFe_2O_4$/RGO	$LiCoO_2$	Y (anode)	1.0–3.8	100 mA g^{-1} (anode weight)	1197 (anode weight)	7	50	800 (anode weight)	32 wt% graphene in the anode	[414]
Fe_3O_4/RGO	NMC	N	1.0–3.8	0.2 C	0.292 (mAh)	39	5	0.158 (mAh)	4.6 wt% graphene in the anode	[415]
$TiNB_2O_7$/RGO	$LiNi_{1/3}Mn_{1/3}Co_{1/3}O_2$: $LiNi_{0.5}Mn_{0.5}O_2$ (wt% ratio 75:25)	N	2.5–4.6	0.1 C	282 (anode weight)	25	25	120 (anode weight)	4 wt% graphene in the anode	[416]
Si/Unzipped CNT graphene	NMC	N	2.5 V (discharge cut-off voltage) 1 mAh (charge cut-off capacity)	0.3 C	1440 (anode weight)	21	25	1385 (anode weight)	5 wt% graphene in the anode	[417]
Sn/RGO	$LiNi_{0.5}Mn_{1.5}O_4$	N	2.0–4.95	0.2 (mA)	1.0 (mAh)	66	15	0.53 (mAh)	92 wt% graphene in the anode	[418]
Si/RGO	$LiFePO_4$	N	2.0 V (discharge cut-off voltage) 0.8 mAh (charge cut-off capacity)	0.08 (mA)	230 (anode weight)	45	33	200 (anode weight)	69 wt% graphene in the anode	[419]

ADVANCED
SCIENCE NEWS
www.advancedsciencenews.com

ADVANCED
MATERIALS
www.advmat.de

PROGRESS REPORT

specific energy as well as the average working potential of the cell were not reported. In another case, size-selected graphene flakes, obtained by liquid-phase exfoliation, were tested as binder-free electrode in a full-cell prior to a mechanical pre-lithiation (i.e., obtained by direct contact with metallic lithium).[386] When coupled with an LiFePO$_4$ cathode, an initial discharge capacity of about 165 mAh g^{-1} (for an applied current of 170 mA g^{-1}, related to the cathode mass, in the 0.9–3.9 V potential range) and a 1st cycle irreversible capacity of about 11% were reported (Table 3). After 80 cycles, a discharge capacity of 136 mAh g^{-1} (i.e., a capacity retention of about 84%) was obtained. Unfortunately, even if the authors claimed that "The use of ultralight high-capacity graphene nanoflakes anode estimates a practical energy density of about 190 Wh kg^{-1}, that is, a value exceeding (≈25–60%) that of current lithium ion battery technology", no calculations about the average working potential and energy density were reported to verify this statement. Moreover, it should be pointed out that, when the binder-free graphene-based electrode was tested in half-cell configuration (without applying any pre-lithiation process), a huge 1st cycle irreversible capacity loss of about 86% and a capacity retention of only about 8% (after 150 cycles and respect to the 1st lithiation cycle at 700 mA g^{-1} in the voltage range 0.01–2 V) can be calculated. Thus, confirming how binder-free graphene-based electrodes, without the help of any "activation" process such as pre-lithiation, seems to have no future in practical applications. To confirm the unfeasibility of batteries containing bare graphene as anode active material (regardless of the method used for the graphene production), E. Rodríguez-Castellón et al.,[387] reported the performances of a RGO anode coupled with a LiFePO$_4$ cathode (Table 3). They evidenced the impossibility of using RGO in a full-cell and, despite the mitigation effect of the pre-lithiation, used to facilitate the SEI formation and to reduce the irreversible Li$^+$ consumption, they found that, upon cycling, the cell with the RGO-based electrode exhibited poorer performance and faster capacity fading with respect to its graphite-based analogue. Interestingly, through XPS studies, they also demonstrated that the poorer performance of the graphene-containing battery was due to the thinness and deficiency in Li inorganic salts of the SEI formed on the RGO-based electrode.

In the same year, an "all-graphene-battery" featuring a pre-lithiated (at the anode) and a functionalized (at the cathode) RGO electrode was also proposed (Table 3). Indeed, K. Kang et al.[388] reported, for an applied current of 500 mA g^{-1} (related to the total masses of anode and cathode active materials) in the 0.01–4.3 V voltage range, a stable cycling behavior for 2000 cycles retaining approximately 56% of the initial specific capacity. The authors reported power and energy densities of 2150 W kg^{-1} and 130 Wh kg^{-1} (related to the total mass of both electrodes), respectively. Although the voltage profile of such all-graphene-batteries resembles that of a supercapacitor, it should be mentioned that using the geometric mean value of the cut-off potential as average working potential is not fully appropriate. On the contrary, as also reported by Goodenough,[389] the proper way to calculate the average working potential for a full-cell consists of dividing the integral of the voltage upon battery discharge by the final value of the capacity. This kind of mistake should be avoided and properly addressed by all researchers;

otherwise, misleading results can be legitimated, thus altering the real progress of the field.

On the side of graphene-containing composites, different Si-based anodes materials were tested in full-cell configuration (Table 3). J. Cho et al.,[390] reported a full-cell made of a RGO-Si hybrid (with a graphene content of 18 wt%) anode coupled with a LiCoO$_2$ cathode, which was tested in the 2.5–4.3 V voltage range between 0.05 and 20 C discharge rates. Although the value of 1 C was not clearly defined, the authors described capacity retentions of 83, 71, 68, and 60% for the applied discharge rates of 5, 10, 15, and 20 C, respectively. Moreover, for a current rate of 7 C, a very low 1st cycle irreversible capacity was reported (i.e., about 1%) (Table 3). Values of energy and power densities were also reported but no explanations on the calculation of the average working potential were provided. T. F. Fuller et al.,[391] by means of commercial graphene-containing Si hybrid anode material and a nickel cobalt aluminum oxide (NCA) cathode, assembled different full-cells and investigated the influence of the fluoro-ethylene carbonate (FEC) additive content on the SEI formation and capacity fading[392] of the batteries (Table 3). The authors found that, when the FEC additive is used (i.e., 10 wt% of the electrolyte mass) an improvement of the cyclability is obtained compared to the additive-free electrolyte, although a constant capacity decrease due to the continuous SEI formation and pulverization of Si on the anode was still noticeable. Interestingly, they proved that using a lower amount of FEC (i.e., 5 wt%), a more stable cycling behavior could be achieved, as a result of the formation of a thinner, more uniform and stable SEI layer containing less CH$_2$OCO$_2$Li, Li$_2$CO$_3$ and LiF compounds, which irreversibly consume lithium upon cycling.

Y. K. Sun et al.[393] also reported a full-cell comprising a Ni-rich Li[Ni$_{0.75}$Co$_{0.1}$Mn$_{0.15}$]O$_2$ cathode and a pre-lithiated RGO/Si hybrid anode (with a graphene content of about 6 wt%) (Table 3). The cell, operating in the potential range 2.7–4.2 V, exhibited first charge and discharge capacities of 206 and 196 mAh g^{-1} (at a current of 20 mA g^{-1}, based on the weight of cathode active material), respectively, yielding a Coulombic efficiency of 95%. The authors claimed that, a practical energy density of 240 Wh kg^{-1} could be obtained (considering 1/3 reduction factor to account for the weight of the electrolyte, current collector, aluminum case, etc.).

M. Zhu et al.,[394,395] by means of high-efficiency discharge-plasma-assisted milling, synthesized a graphene/Si and a graphene/Si-WC hybrid with 40 and 50 wt% graphene, respectively (Table 3). Both anode materials were coupled with a LiMn$_2$O$_4$ cathode and cycled between 2.5 and 4.5 V. Despite the presence of tungsten carbide and the different amount of graphene in the anode, both materials showed a stable cycling behavior for only 30 cycles with a reversible capacity of about 570 mAh g^{-1} (referred to the anode weight) and 0.57 mAh for graphene/Si and graphene/Si-WC, respectively. Unfortunately, no evaluations in terms of average working potential or energy density were reported.

H.-Y. Tuan et al.[396] also tested a RGO/Ge hybrid (with a graphene content of about 20 wt%) versus a LiCoO$_2$ cathode (Table 3). When charge/discharge cycles were performed in the 2.5–4.2 V voltage range at 1 C current rate (1 C corresponding to 1 A g^{-1} of anode active material), the full-cell exhibited a discharge capacity of 1234 mAh g^{-1} (referred to the weight of the

anode active material) in the first cycle. After 100 cycles the cell delivered a reversible capacity of about 900 mAh g^{-1}. Interestingly, through half-cell tests, the authors calculated a volumetric capacity of the RGO/Ge hybrid of about 700 mAh cm^{-3} considering a reversible capacity of 1166 mAh g^{-1}, at a rate of 0.2 C, and an electrode weight, area and thickness of 0.6 mg, 1 cm^2 and 10 μm, respectively. Although this value could be considered promising, the quite large first cycle irreversible capacity loss of the hybrid still represents a major drawback.

In the work of D. Wang et al.,[397] after being pre-lithiated, a GeO$_x$-based anode with a RGO content of 8.5 wt%, was coupled with a high voltage LiNi$_{0.5}$Mn$_{1.5}$O$_4$ cathode. When cycled in the 3.5–4.9 V potential range and applying currents ranging from 70 to 1120 mA g^{-1} (based on the cathode mass), discharge capacities in the order of 120 and 60 mAh g^{-1} could be obtained for the lower and the higher currents, respectively. As stated by the authors, this work clearly indicated that the use of a conductive RGO network in electrode active materials, especially in low contents, is an effective approach to enhance both the rate capability and cycling stability of germanium-based anode materials (Table 3).

Two iron oxide-based anode materials were also tested in full-cell configuration. In the first one, J. Morales et al.,[398] reported a Fe$_2$O$_3$/RGO composite (with a graphene content of about 18 wt%) coupled with a LiFePO$_4$ cathode, which was cycled at a specific current of 34 mA g^{-1} (referred to the cathode active material weight) from 1.5 to 3.9 V over 50 cycles. The rate capability of the full-cell was also evaluated over 10 cycles each at 1 C, 2 C and 5 C, and 20 cycles at 2C (1 C = 170 mAh g^{-1} of cathode active material). Interestingly, the authors made a comparison between the pre-lithiated and the non-pre-lithiated anode material showing how this treatment strongly influences the electrochemical properties of the battery (Table 3). Although a 1st cycle irreversible capacity was always present, the battery exploiting the pre-lithiated graphene-containing anode could sustain 50 cycles at 34 mA g^{-1} showing a reversible capacity of about 110 mAh g^{-1} (despite a slight capacity fading upon cycling). Moreover, during the rate capability test, at a specific current of 850 mA g^{-1} it delivered a capacity of about 50 mAh g^{-1}. In the second one, S. Zhang et al.,[399] used a ZnFe$_2$O$_4$-based hybrid, with a graphene content of 12.4 wt%, coupled with a LiFePO$_4$ cathode and tested it in the 1.0–3.5 V potential range, under a current load of 100 mA g^{-1} (referred to the anode active material weight). Unfortunately, only 10 cycles with a poor capacity retention were reported (Table 3), and no information about the average working potential, energy and/or power of the cell were given. Interestingly, a full-cell comprising a RGO/VS$_4$ hybrid anode (with a graphene content of only 3 wt%) coupled with a LiMn$_2$O$_4$ cathode was also reported by J. Cho et al.[400] Unfortunately, a 1st discharge capacity of only 72 mAh g^{-1} and a capacity retention of 74% after 30 cycles were achieved (Table 3) in the potential range of 4.3–1.0 V and applying a current rate of 0.5 C (after a first formation cycle at 0.1 C).

It should be noticed that few papers[271,276,401–404] have reported the evaluation of the energy and power for a single electrode in half-cell configuration. As previously explained in Section 3.2, we want to stress that this kind of calculation is not appropriate to assess the properties of electroactive materials,

since no coupling with a cathode material was neither performed nor simulated.

In 2015, the progress of the use of graphene as main Li-ion host were minimal. Different kinds of graphene (i.e., pre-lithiated RGO,[405] CVD-synthesized graphene[406,407] and pre-lithiated commercial graphene[408]) were used as active material and coupled with LiFePO$_4$ or LiCoO$_2$ cathodes (Table 3). Particularly, in the work of J. Morales et al.,[405] two pre-lithiation methods were used and compared (i.e., electrochemical lithiation and Li-foil contact lithiation in the presence of an electrolyte). Interestingly, they were able to demonstrate that, although the contact treatment slightly improved the performance of the full-cell with respect to the electrochemical lithiation, the capacity retention upon cycling was poor in both cases (Table 3). Except for the work of C. Gerbaldi et al.,[407] where, after anode lithiation and cathode delithiation (i.e., the full-cell started in "charged" state), a stable cycling behavior for 1000 cycles was reported (although the electrochemical characterization not properly described), none of the other research efforts proved enhanced electrochemical performances (e.g., cycling stability) compared to previously reported full-cells (Table 3). On the other side, many graphene-containing hybrids were tested in full-cell configuration. G. Yu et al.,[409] reported a battery (with flexible properties) using ZnMn$_2$O$_4$–RGO composite (graphene content of 33 wt%) and LiFePO$_4$ as anode and cathode active material, respectively (Table 3). The authors claimed that, although ZnMn$_2$O$_4$ works at high potentials, thus limiting the general output voltage and energy density of the full battery, the larger specific gravimetric capacity and the pre-lithiation treatment may compensate these drawbacks aiming to achieve high energy density in full-cell configuration. Indeed, even if the average working potential was not reported, the authors claimed to obtain an energy density of about 231 Wh kg^{-1} at low current rate (and a power density of ca. 1060 W kg^{-1} at high current rate), in the 0.9–3.9 V potential range. Moreover, rate capability and cycling stability superior to those of the graphite-containing analogue were reported. Another flexible battery, comprising commercial graphene both in the anode (i.e., LTO) and in the cathode (i.e., LiFePO$_4$) and showing a stable capacity of about 150 mAh g^{-1} for 100 cycles at a current rate of 0.5 C (in the voltage range 1.0–2.5 V) was also reported by F. Li et al.[410] (Table 3). Stable cycling performances (even at high current of 1.6 A g^{-1}, related to the anode mass) of a full-cell made of RGO/Fe$_2$O$_3$ anode (graphene content of 15 wt%) and LiFePO$_4$ cathode were reported in the work of Z. F. Ma et al.[411] (Table 3). Despite the good cycling stability of the full-cell for 40 cycles, unfortunately, a noticeable 1st cycle irreversible capacity (i.e., about 34%) was observed.

Other full-cells comprising non-pre-lithiated RGO/SnO$_2$-Fe$_3$O$_4$,[412] RGO/SnS$_2$,[413] pre-lithiated RGO/SnS$_2$[413] and RGO/CoFe$_2$O$_4$[414] composite anodes coupled with LiCoO$_2$ cathodes were also tested (Table 3). However, only the full-cells using the pre-lithiated anodes showed acceptable performance in terms of low 1st cycle irreversible capacity and rate capability. NMC-based cathode materials were also investigated with different graphene-containing (i.e., with a graphene content in the 4–5 wt% range) anodes such RGO/Fe$_3$O$_4$,[415] RGO/TiNb$_2$O$_7$[416] and unzipped-CNT graphene/Si[417] (Table 3). For all the three different studies, no pre-lithiation process was applied. Besides

**ADVANCED
SCIENCE NEWS**
www.advancedsciencenews.com

**ADVANCED
MATERIALS**
www.advmat.de

PROGRESS REPORT

the noticeable 1st cycle irreversible capacities (in the 20–40% range), electrochemical performances similar to the ones of the full-cells previously described should be noticed. A RGO/Sn hybrid was also coupled with a $LiNi_{0.5}Mn_{1.5}O_4$ cathode without applying any pre-lithiation treatment. Unfortunately, only 15 cycles were reported always showing low Coulombic efficiencies and poor capacity retention[418] (Table 3). Similarly, a RGO/Si composite (also non-pre-lithiated) was coupled with a $LiFePO_4$ cathode.[419] Here, only 33 cycles were reported, all showing unsatisfactory electrochemical behavior in terms Coulombic efficiency (always lower than 90%) (Table 3).

H. Chang et al.,[420] by means of CVD, anchored multilayer graphene onto the surface of Si nanoparticles (the graphene content was 5 wt%), with the aim of accommodating the volume expansion of silicon via a sliding process between adjacent graphene layers. When such anode material was paired (without any prior pre-lithiation step) with a commercial $LiCoO_2$ cathode, energy densities of 972 and 700 Wh L^{-1} at the 1st and 200th cycle were achieved, respectively (i.e., 1.8 and 1.5 times higher than those of current commercial lithium-ion batteries calculated based on the same metric). Indeed, the use of such peculiar synthetic approach led the authors to claim that: "The layered structure of graphene allows interlayer sliding upon the volume expansion of Si as well as a highly conductive percolating network, resulting in an unprecedented volumetric energy density of an LIB full-cell with decent cycle life. Overall, the unique 2D character of graphene and the atom-level engineering of its

interface with Si to avoid unwanted SiC formation will allow Si anode technology to make a meaningful step toward its wide commercialization".

Two other research efforts reported the use of two different graphene-containing hybrids in a full-cell configuration.[421,422] Surprisingly, in both of them, only photographic pictures of the battery are shown and no other kind of scientific characterization was provided for the full-cell tests. As for 2014, a few reports[416,423–425] erroneously evaluated energy and power for a single electrode in half-cell configuration also in 2015.

5. Conclusions

Except in a few cases, the graphene era has not yet substantially met the promised expectations of triggering a revolution in the lithium-ion battery field. Even if the enormous efforts in research laboratories led to some encouraging advances (see **Figure 4**) and development of novel materials (see **Figure 5**), the absence of a clear focus for the use in a practical application still mainly relegates graphene to an academic matter. The choice of inappropriate metrics and unfair performance comparisons with the state of the art surely can account among the causes of this failure. Volumetric capacity is rarely reported, despite being much more important than the gravimetric capacity for applications. This is true in general, but it is particularly relevant for graphene-based materials which are often
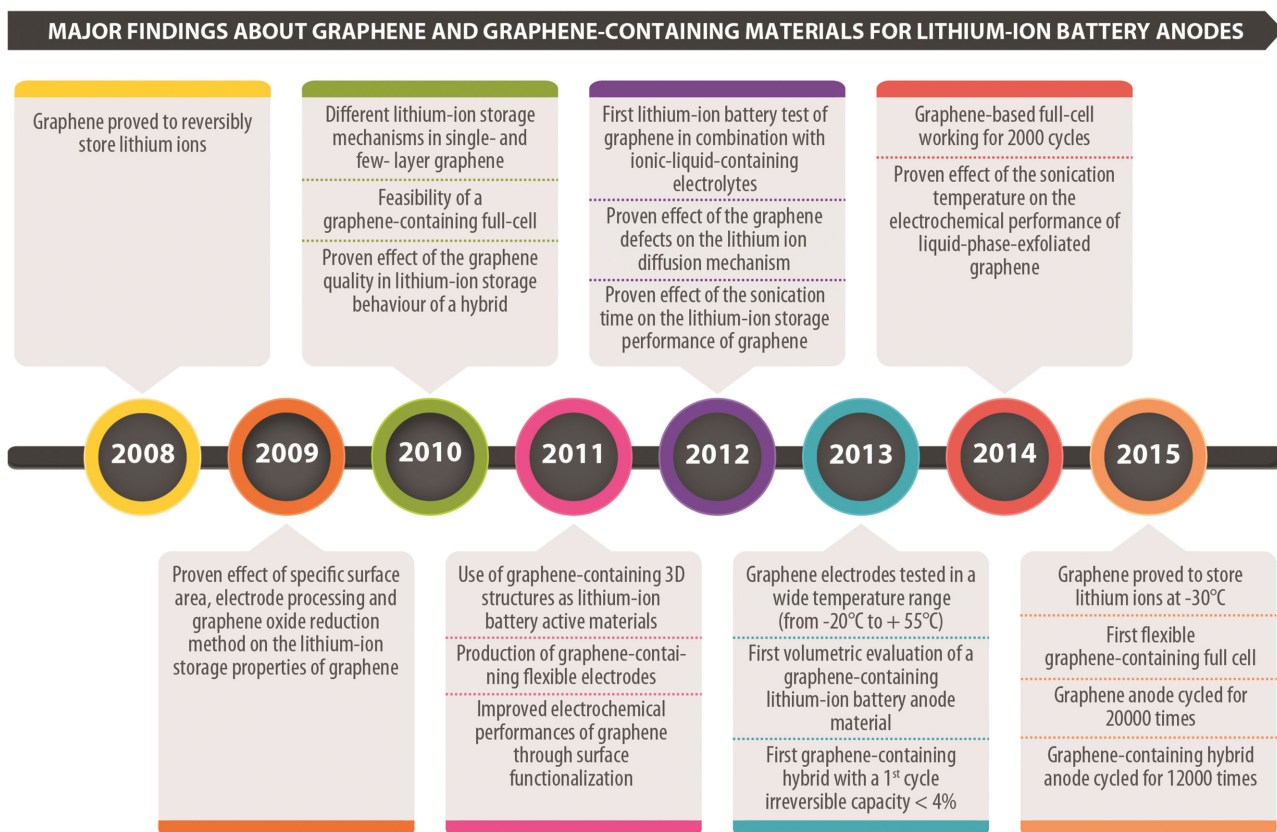

MAJOR FINDINGS ABOUT GRAPHENE AND GRAPHENE-CONTAINING MATERIALS FOR LITHIUM-ION BATTERY ANODES

2008 — Graphene proved to reversibly store lithium ions

2009 — Proven effect of specific surface area, electrode processing and graphene oxide reduction method on the lithium-ion storage properties of graphene

2010 — Different lithium-ion storage mechanisms in single- and few-layer graphene / Feasibility of a graphene-containing full-cell / Proven effect of the graphene quality in lithium-ion storage behaviour of a hybrid

2011 — Use of graphene-containing 3D structures as lithium-ion battery active materials / Production of graphene-containing flexible electrodes / Improved electrochemical performances of graphene through surface functionalization

2012 — First lithium-ion battery test of graphene in combination with ionic-liquid-containing electrolytes / Proven effect of the graphene defects on the lithium ion diffusion mechanism / Proven effect of the sonication time on the lithium-ion storage performance of graphene

2013 — Graphene electrodes tested in a wide temperature range (from -20°C to + 55°C) / First volumetric evaluation of a graphene-containing lithium-ion battery anode material / First graphene-containing hybrid with a 1st cycle irreversible capacity < 4%

2014 — Graphene-based full-cell working for 2000 cycles / Proven effect of the sonication temperature on the electrochemical performance of liquid-phase-exfoliated graphene

2015 — Graphene proved to store lithium ions at -30°C / First flexible graphene-containing full cell / Graphene anode cycled for 20000 times / Graphene-containing hybrid anode cycled for 12000 times

Figure 4. Schematic summary of the major findings reported about graphene and graphene-containing materials as lithium-ion battery anodes between 2008 and 2015.
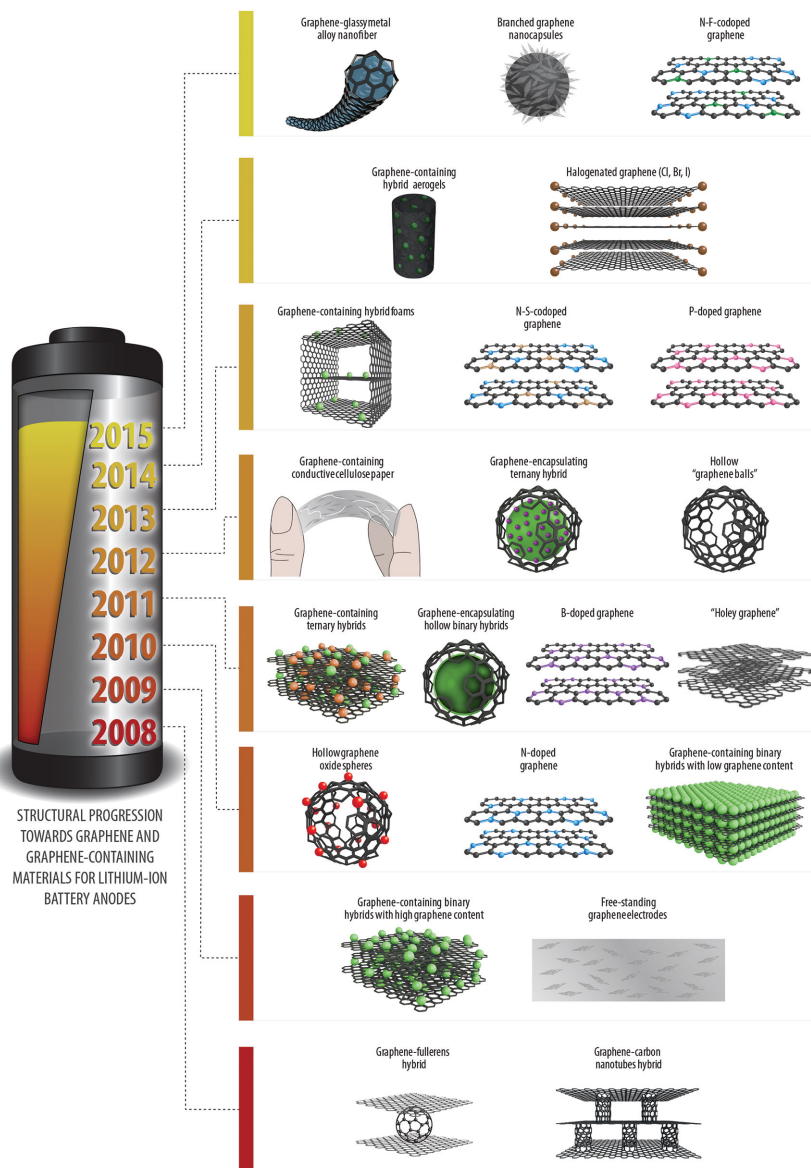
Figure 5. Schematic representation of the structural progression toward graphene and graphene-containing materials as lithium-ion battery anodes developed between 2008 and 2015.

reliable picture of the potential applicability of a specific material. Energy and power of full-cells are, however, often calculated considering only one of the two electrodes (generally the limiting one) leading to highly overestimated numbers. Additionally, nobody considers the weight of the electrolyte, which in the case of graphene-based electrodes is expected to be considerable, in order to fully wet the highly porous electrodes. We suggest extreme caution on this matter, as the risk of "comparing oranges and apples" is high.

The deep and broad analysis of the published data that we have performed here has demonstrated that, at this stage, graphene may be most effective when used as an enhanced electron-conductive carbon matrix in composites containing additional electroactive materials. The best performances were observed with high voltage insertion materials (e.g., TiO_2 or LTO) or with alloying anodes with a low average delithiation voltage (e.g., Si or Ge). In contrast, the properties of graphene could not be fully exploited in combination with conversion anodes, except in a few cases where peculiar hybrids were designed, because of the intrinsic limitations of conversion-type materials. In all cases, the method used to obtain the composite plays a crucial role. One-pot synthesis, decoration and/or anchoring are generally preferred over simple physical/mechanical mixing due to the better electrochemical performance of the former.

When used as a bare active material (i.e., the main lithium host), graphene can only compete with the state-of-the-art graphite in few cases (e.g., where the delithiation voltage resembles that of graphite) and in particular conditions (e.g., low temperatures and high power). It should be pointed out that multilayer graphene is the material of choice in this case. Indeed, pristine mono- and bi- layer graphene cannot be efficiently used as LIB anode active materials. Main reasons for this are the high delithiation voltage, the poor energy-storage efficiency, and the massive irreversible capacity associated with the SEI formation. Due to the latter, when graphene is used in full-cell configuration, a prior pre-lithiation step is always necessary to obtain decent electrochemical performances, which increases the difficulty in battery manufacturing and thus drastically reduces the possibility for practical application. In fact, although several companies employ pre-lithiated anodes in lithium-ion capacitors,[426] we were not able to determine if there are any commercially available lithium-ion batteries that make use of pre-lithiated anodes.

Regarding the different kinds of graphene, the ones obtained through liquid-phase exfoliation and CVD in most cases show better results than their RGO analogues, although the latter were the most used in research studies. Moreover,

very porous and, thus, have low density. The high porosity has certainly a beneficial effect on the ion conduction. Nevertheless, the superior performance of graphene and graphene-containing materials is most commonly attributed to their enhanced electronic conductivity. Interestingly though, such parameter was rarely reported and never adopted as standard metric for a fair comparison with an equal amount of state-of-the-art material.

Half-cells with Li metal are perfectly suited for studying the electrochemical behavior of newly synthesized materials. However, values of energy and power density calculated on a single electrode basis should not be reported because they are meaningless and misleading. With this cell configuration, parameters such as the average lithiation/delithiation voltage, the voltage and the Coulombic efficiency are more appropriate metrics. Tests performed in full-cells provide a fairer and more

the introduction of heteroatoms through doping seems to be a good strategy to enhance the stability and the lithium-ion storage capability of graphene.

Acknowledgements

[1] K. S. Novoselov, A. K. Geim, S. V Morozov, D. Jiang, Y. Zhang, S. V Dubonos, I. V Grigorieva, A. A. Firsov, *Science* **2004**, *306*, 666.

[2] E. Gerstner, *Nat. Phys.* **2010**, *6*, 836.

[3] K. S. Novoselov, V. I. Fal'ko, L. Colombo, P. R. Gellert, M. G. Schwab, K. Kim, *Nature* **2012**, *490*, 192.

[4] L. Grande, V. T. Chundi, D. Wei, C. Bower, P. Andrew, T. Ryhänen, *Particuology* **2012**, *10*, 1.

[5] A. C. Ferrari, F. Bonaccorso, V. Falko, K. S. Novoselov, S. Roche, P. Bøggild, S. Borini, F. Koppens, V. Palermo, N. Pugno, J. a. Garrido, R. Sordan, A. Bianco, L. Ballerini, M. Prato, E. Lidorikis, J. Kivioja, C. Marinelli, T. Ryhänen, A. Morpurgo, J. N. Coleman, V. Nicolosi, L. Colombo, A. Fert, M. Garcia-Hernandez, A. Bachtold, G. F. Schneider, F. Guinea, C. Dekker, M. Barbone, C. Galiotis, A. Grigorenko, G. Konstantatos, A. Kis, M. Katsnelson, C. W. J. Beenakker, L. Vandersypen, A. Loiseau, V. Morandi, D. Neumaier, E. Treossi, V. Pellegrini, M. Polini, A. Tredicucci, G. M. Williams, B. H. Hong, J. H. Ahn, J. M. Kim, H. Zirath, B. J. van Wees, H. van der Zant, L. Occhipinti, A. Di Matteo, I. a. Kinloch, T. Seyller, E. Quesnel, X. Feng, K. Teo, N. Rupesinghe, P. Hakonen, S. R. T. Neil, Q. Tannock, T. Löfwander, J. Kinaret, *Nanoscale* **2015**, *7*, 4598.

[6] M. Peplow, *Nature* **2015**, *522*, 268.

[7] M. F. El-Kady, Y. Shao, R. B. Kaner, *Nat. Rev. Mater.* **2016**, 16033.

[8] F. Bonaccorso, V. Pellegrini, *Mater. Matters* **2016**, *11*, 15.

[9] Z.-S. Wu, G. Zhou, L.-C. Yin, W. Ren, F. Li, H.-M. Cheng, *Nano Energy* **2012**, *1*, 107.

[10] A. Bianco, H.-M. Cheng, T. Enoki, Y. Gogotsi, R. H. Hurt, N. Koratkar, T. Kyotani, M. Monthioux, C. R. Park, J. M. D. Tascon, J. Zhang, *Carbon* **2013**, *65*, 1.

[11] R. Raccichini, A. Varzi, S. Passerini, B. Scrosati, *Nat. Mater.* **2015**, *14*, 271.

[12] J. W. Choi, D. Aurbach, *Nat. Rev. Mater.* **2016**, *1*, 16013.

[13] K. S. Sivudu, Y. R. Mahajan, *Nanotech Insights* **2012**, *3*, 6.

[14] D. Wei, M. R. Astley, N. Harris, R. White, T. Ryhänen, J. Kivioja, *Nanoscale* **2014**, *6*, 9536.

[15] D. Wei, J. Kivioja, *Nanoscale* **2013**, *5*, 10108.

[16] L. Grande, V. T. Chundi, D. Wei, in *Carbon Nanomaterials for Advanced Energy Systems: Advances in Materials Synthesis and Device Applications* (Eds.: W. Lu, J.-B. Baek, L. Dai), John Wiley & Sons, Hoboken, NJ, USA **2015**, p. 472.

[17] M. V. Reddy, G. V. Subba Rao, B. V. R. Chowdari, *Chem. Rev.* **2013**, *113*, 5364.

[18] N. Nitta, G. Yushin, *Part. Part. Syst. Charact.* **2014**, *31*, 317.

[19] M. N. Obrovac, V. L. Chevrier, *Chem. Rev.* **2014**, *114*, 11444.

[20] B. Scrosati, J. Garche, *J. Power Sources* **2010**, *195*, 2419.

[21] J. Cabana, L. Monconduit, D. Larcher, M. R. Palacín, *Adv. Mater.* **2010**, *22*, 170.

[22] M. N. Obrovac, L. Christensen, *Electrochem. Solid-State Lett.* **2004**, *7*, A93.

[23] D. Linden, T. B. Reddy, *Handbook of Batteries*, McGraw-Hill, **2002**.

[24] R. Fong, H. Al-Janby, J. R. Dahn, *US 5028500*, **1991**.

[25] J. Barker, M.-Y. Saidi, J. L. Swoyer, F. Gao, *US 5759715*, **1998**.

[26] J. R. Dahn, T. Zheng, Y. Liu, J. S. Xue, *Science* **1995**, *270*, 590.

[27] K. Sato, M. Noguchi, A. Demachi, N. Oki, M. Endo, *Science* **1994**, *264*, 556.

[28] E. Yoo, J. Kim, E. Hosono, H.-S. Zhou, T. Kudo, I. Honma, *Nano Lett.* **2008**, *8*, 2277.

[29] D. R. Dreyer, S. Park, C. W. Bielawski, R. S. Ruoff, *Chem. Soc. Rev.* **2010**, *39*, 228.

[30] M. Winter, J. O. Besenhard, M. E. Spahr, P. Novák, *Adv. Mater.* **1998**, *10*, 725.

[31] Y. Liu, J. S. Xue, T. Zheng, J. R. Dahn, *Carbon* **1996**, *34*, 193.

[32] S. M. Paek, E. Yoo, I. Honma, *Nano Lett.* **2009**, *9*, 72.

[33] G. Wang, X. Shen, J. Yao, J. Park, *Carbon* **2009**, *47*, 2049.

[34] D. Pan, S. Wang, B. Zhao, M. Wu, H. Zhang, Y. Wang, Z. Jiao, *Chem. Mater.* **2009**, *21*, 3136.

[35] C. Wang, D. Li, C. O. Too, G. G. Wallace, *Chem. Mater.* **2009**, *21*, 2604.

[36] P. Guo, H. Song, X. Chen, *Electrochem. Commun.* **2009**, *11*, 1320.

[37] D. Wang, R. Kou, D. Choi, Z. Yang, Z. Nie, J. Li, L. V. Saraf, D. Hu, J. Zhang, G. L. Graff, J. Liu, M. A. Pope, I. A. Aksay, *ACS Nano* **2010**, *4*, 1587.

[38] J.-Z. Wang, C. Zhong, S.-L. Chou, H.-K. Liu, *Electrochem. Commun.* **2010**, *12*, 1467.

[39] A. Abouimrane, O. C. Compton, K. Amine, S. T. Nguyen, *J. Phys. Chem. C* **2010**, *114*, 12800.

[40] A. L. M. Reddy, A. Srivastava, S. R. Gowda, H. Gullapalli, M. Dubey, P. M. Ajayan, *ACS Nano* **2010**, *4*, 6337.

[41] J. K. Lee, K. B. Smith, C. M. Hayner, H. H. Kung, *Chem. Commun.* **2010**, *46*, 2025.

[42] F. Ji, Y.-L. Li, J.-M. Feng, D. Su, Y.-Y. Wen, Y. Feng, F. Hou, *J. Mater. Chem.* **2009**, *19*, 9063.

[43] P. Guo, H. Song, X. Chen, *J. Mater. Chem.* **2010**, *20*, 4867.

[44] Y.-S. He, D.-W. Bai, X. Yang, J. Chen, X.-Z. Liao, Z.-F. Ma, *Electrochem. Commun.* **2010**, *12*, 570.

[45] S. Yang, G. Cui, S. Pang, Q. Cao, U. Kolb, X. Feng, J. Maier, K. Müllen, *ChemSusChem* **2010**, *3*, 236.

[46] S. Q. Chen, Y. Wang, *J. Mater. Chem.* **2010**, *20*, 9735.

[47] Z. Wu, W. Ren, L. Wen, L. Gao, J. Zhao, Z. Chen, G. Zhou, F. Li, H. Cheng, *ACS Nano* **2010**, *4*, 3187.

[48] P. Lian, X. Zhu, S. Liang, Z. Li, W. Yang, H. Wang, *Electrochim. Acta* **2010**, *55*, 3909.

[49] L.-S. Zhang, L.-Y. Jiang, H.-J. Yan, W. D. Wang, W. Wang, W.-G. Song, Y.-G. Guo, L.-J. Wan, *J. Mater. Chem.* **2010**, *20*, 5462.

[50] Z. Du, X. Yin, M. Zhang, Q. Hao, Y. Wang, T. Wang, *Mater. Lett.* **2010**, *64*, 2076.

[51] T. Bhardwaj, A. Antic, B. Pavan, V. Barone, B. D. Fahlman, *J. Am. Chem. Soc.* **2010**, *132*, 12556.

[52] S.-L. Chou, J.-Z. Wang, M. Choucair, H.-K. Liu, J. A. Stride, S.-X. Dou, *Electrochem. Commun.* **2010**, *12*, 303.

[53] E. Pollak, B. Geng, K. J. Jeon, I. T. Lucas, T. J. Richardson, F. Wang, R. Kostecki, *Nano Lett.* **2010**, *10*, 3386.

[54] A. Ferre-Vilaplana, *J. Phys. Chem. C* **2008**, *112*, 3998.

[55] C. Ataca, E. Aktürk, S. Ciraci, H. Ustunel, *Appl. Phys. Lett.* **2008**, *93*, 132.

[56] Y. Liu, V. I. Artyukhov, M. Liu, A. R. Harutyunyan, B. I. Yakobson, *J. Phys. Chem. Lett.* **2013**, *4*, 1737.

[57] Z.-S. Wu, W. Ren, L. Xu, F. Li, H.-M. Cheng, *ACS Nano* **2011**, *5*, 5463.

[58] H. Wang, C. Zhang, Z. Liu, L. Wang, P. Han, H. Xu, K. Zhang, S. Dong, J. Yao, G. Cui, *J. Mater. Chem.* **2011**, *21*, 5430.

[59] S. Yin, Y. Zhang, J. Kong, C. Zou, C. M. Li, X. Lu, J. Ma, F. Y. C. Boey, X. Chen, *ACS Nano* **2011**, *5*, 3831.

[60] X. Zhao, C. M. Hayner, M. C. Kung, H. H. Kung, *ACS Nano* **2011**, *5*, 8739.

[61] X. Li, D. Geng, Y. Zhang, X. Meng, R. Li, X. Sun, *Electrochem. Commun.* **2011**, *13*, 822.

[62] S. Li, Y. Luo, W. Lv, W. Yu, S. Wu, P. Hou, Q. Yang, Q. Meng, C. Liu, H. M. Cheng, *Adv. Energy Mater.* **2011**, *1*, 486.

[63] Z.-J. Fan, J. Yan, T. Wei, G.-Q. Ning, L.-J. Zhi, J.-C. Liu, D.-X. Cao, G.-L. Wang, F. Wei, *ACS Nano* **2011**, *5*, 2787.

[64] O. C. Compton, B. Jain, D. a. Dikin, A. Abouimrane, K. Amine, S. T. Nguyen, *ACS Nano* **2011**, *5*, 4380.

[65] A. M. Shanmugharaj, W. S. Choi, C. W. Lee, S. H. Ryu, *J. Power Sources* **2011**, *196*, 10249.

[66] J.-H. Jang, D. Rangappa, Y.-U. Kwon, I. Honma, *J. Mater. Chem.* **2011**, *21*, 3462.

[67] P. Guo, H. Song, X. Chen, L. Ma, G. Wang, F. Wang, *Anal. Chim. Acta* **2011**, *688*, 146.

[68] X. L. Li, K. Du, H. Wang, H. F. Song, H. D. Liu, H. Y. Li, Y. X. Zhang, J. M. Huang, *Int. J. Electrochem. Sci.* **2011**, *6*, 4411.

[69] S. M. Yoon, W. M. Choi, H. Baik, H. J. Shin, I. Song, M. S. Kwon, J. J. Bae, H. Kim, Y. H. Lee, J. Y. Choi, *ACS Nano* **2012**, *6*, 6803.

[70] Y.-R. Kang, Y.-L. Li, F. Hou, Y.-Y. Wen, D. Su, *Nanoscale* **2012**, *4*, 3248.

[71] F. Liu, S. Song, D. Xue, H. Zhang, *Adv. Mater.* **2012**, *24*, 1089.

[72] B. P. Vinayan, R. Nagar, V. Raman, N. Rajalakshmi, K. S. Dhathathreyan, S. Ramaprabhu, *J. Mater. Chem.* **2012**, *22*, 9949.

[73] Y. Yan, Y.-X. Yin, S. Xin, Y.-G. Guo, L.-J. Wan, *Chem. Commun.* **2012**, *48*, 10663.

[74] M. Galinski, I. Acznik, *J. Power Sources* **2012**, *216*, 5.

[75] F. Yao, F. Güneş, H. Q. Ta, S. M. Lee, S. J. Chae, K. Y. Sheem, C. S. Cojocaru, S. S. Xie, Y. H. Lee, *J. Am. Chem. Soc.* **2012**, *134*, 8646.

[76] F. Kokai, R. Sorin, H. Chigusa, K. Hanai, A. Koshio, M. Ishihara, Y. Koga, M. Hasegawa, N. Imanishi, Y. Takeda, *Diam. Relat. Mater.* **2012**, *29*, 63.

[77] R. Mukherjee, A. V. Thomas, A. Krishnamurthy, N. Koratkar, *ACS Nano* **2012**, *6*, 7867.

[78] H. F. Xiang, Z. D. Li, K. Xie, J. Z. Jiang, J. J. Chen, P. C. Lian, J. S. Wu, Y. Yu, H. H. Wang, *RSC Adv.* **2012**, *2*, 6792.

[79] C.-M. Chen, Q. Zhang, J.-Q. Huang, W. Zhang, X.-C. Zhao, C.-H. Huang, F. Wei, Y.-G. Yang, M.-Z. Wang, D. S. Su, *J. Mater. Chem.* **2012**, *22*, 13947.

[80] O. A. Vargas C, Á. Caballero, J. Morales, *Nanoscale* **2012**, *4*, 2083.

[81] H. Liu, C. Miao, Z. Tang, X. Zheng, X. Qin, X. Zhang, *Mater. Lett.* **2012**, *83*, 62.

[82] S. H. Lee, S. D. Seo, K. S. Park, H. W. Shim, D. W. Kim, *Mater. Chem. Phys.* **2012**, *135*, 309.

[83] C. Zhang, N. Mahmood, H. Yin, F. Liu, Y. Hou, *Adv. Mater.* **2013**, *25*, 4932.

[84] Z. L. Wang, D. Xu, H. G. Wang, Z. Wu, X. B. Zhang, *ACS Nano* **2013**, *7*, 2422.

[85] Y. Fang, Y. Lv, R. Che, H. Wu, X. Zhang, D. Gu, G. Zheng, D. Zhao, *J. Am. Chem. Soc.* **2013**, *135*, 1524.

[86] Y. Yang, X. Ji, X. Yang, C. Wang, W. Song, Q. Chen, C. E. Banks, *RSC Adv.* **2013**, *3*, 16130.

[87] Z. Jiang, B. Pei, A. Manthiram, *J. Mater. Chem. A* **2013**, *1*, 7775.

[88] G. Ning, C. Xu, Y. Cao, X. Zhu, Z. Jiang, Z. Fan, W. Qian, F. Wei, J. Gao, *J. Mater. Chem. A* **2013**, *1*, 408.

[89] W. Ai, L. Xie, Z. Du, Z. Zeng, J. Liu, H. Zhang, Y. Huang, W. Huang, T. Yu, *Sci. Rep.* **2013**, *3*, 2341.

[90] X. Geng, Y. Guo, D. Li, W. Li, C. Zhu, X. Wei, M. Chen, S. Gao, S. Qiu, Y. Gong, L. Wu, M. Long, M. Sun, G. Pan, L. Liu, *Sci. Rep.* **2013**, *3*, 1134.

[91] X. Ma, G. Ning, Y. Sun, Y. Pu, J. Gao, *Carbon* **2014**, *79*, 310.

[92] L. David, G. Singh, *J. Phys. Chem. C* **2014**, *118*, 28401.

[93] J. Xu, I. Y. Jeon, J. M. Seo, S. Dou, L. Dai, J. B. Baek, *Adv. Mater.* **2014**, *26*, 7317.

[94] C. Hu, L. Lv, J. Xue, M. Ye, L. Wang, L. Qu, *Chem. Mater.* **2015**, *27*, 5253.

[95] H. G. Wang, Y. Wang, Y. Li, Y. Wan, Q. Duan, *Carbon* **2015**, *82*, 116.

[96] L. Ren, K. N. Hui, K. S. Hui, Y. Liu, X. Qi, J. Zhong, Y. Du, J. Yang, *Sci. Rep.* **2015**, *5*, 14229.

[97] X. Liu, Y. Wu, Z. Yang, F. Pan, X. Zhong, J. Wang, L. Gu, Y. Yu, *J. Power Sources* **2015**, *293*, 799.

[98] Y. Yang, F. Zheng, G. Xia, Z. Lun, Q. Chen, *J. Mater. Chem. A* **2015**, *3*, 18657.

[99] Y. Zhou, Y. Zeng, D. Xu, P. Li, H. G. Wang, X. Li, Y. Li, Y. Wang, *Electrochim. Acta* **2015**, *184*, 24.

[100] S. Huang, Y. Li, Y. Feng, H. An, P. Long, C. Qin, W. Feng, *J. Mater. Chem. A* **2015**, *3*, 23095.

[101] J. Sun, L. Wang, R. Song, S. Yang, *RSC Adv.* **2015**, *5*, 91114.

[102] D. Zhao, L. Wang, P. Yu, L. Zhao, C. Tian, W. Zhou, L. Zhang, *Nano Res.* **2015**, *8*, 2998.

[103] R. Raccichini, A. Varzi, V. S. K. Chakravadhanula, C. Kübel, A. Balducci, S. Passerini, *J. Power Sources* **2015**, *281*, 318.

[104] S.-H. Park, H.-K. Kim, S.-B. Yoon, C.-W. Lee, D. Ahn, S.-I. Lee, K. C. Roh, K.-B. Kim, *Chem. Mater.* **2015**, *27*, 457.

[105] J. Ji, J. Liu, L. Lai, X. Zhao, Y. Zhen, J. Lin, Y. Zhu, H. Ji, L. L. Zhang, R. S. Ruoff, *ACS Nano* **2015**, *9*, 8609.

[106] Y. Xu, Z. Lin, X. Zhong, B. Papandrea, Y. Huang, X. Duan, *Angew. Chem., Int. Ed.* **2015**, *54*, 5345.

[107] P. Verma, P. Maire, P. Novák, *Electrochim. Acta* **2010**, *55*, 6332.

[108] J. Yao, X. Shen, B. Wang, H. Liu, G. Wang, *Electrochem. Commun.* **2009**, *11*, 1849.

[109] G. Wang, B. Wang, X. Wang, J. Park, S. Dou, H. Ahn, K. Kim, *J. Mater. Chem.* **2009**, *19*, 8378.

[110] C. Xu, X. Wang, L. Yang, Y. Wu, *J. Solid State Chem.* **2009**, *182*, 2486.

[111] D. Wang, D. Choi, J. Li, Z. Yang, Z. Nie, R. Kou, D. Hu, C. Wang, L. V Saraf, J. Zhang, I. A. Aksay, J. Liu, *ACS Nano* **2009**, *3*, 907.

[112] K. M. S. Yang, X. Feng, S. Ivanovici, *Angew. Chem., Int. Ed.* **2010**, *49*, 8408.

[113] G. Zhou, D. W. Wang, F. Li, L. Zhang, N. Li, Z. S. Wu, L. Wen, G. Q. Lu, H. M. Cheng, *Chem. Mater.* **2010**, *22*, 5306.

[114] P. Lian, X. Zhu, H. Xiang, Z. Li, W. Yang, H. Wang, *Electrochim. Acta* **2010**, *56*, 834.

[115] M. Zhang, D. Lei, X. Yin, L. Chen, Q. Li, Y. Wang, T. Wang, *J. Mater. Chem.* **2010**, *20*, 5538.

[116] H. Wang, L.-F. Cui, Y. Yang, H. Sanchez Casalongue, J. T. Robinson, Y. Liang, Y. Cui, H. Dai, *J. Am. Chem. Soc.* **2010**, *132*, 13978.

[117] B. Wang, X.-L. Wu, C.-Y. Shu, Y.-G. Guo, C.-R. Wang, *J. Mater. Chem.* **2010**, *20*, 10661.

[118] X.-L. Wang, W.-Q. Han, *ACS Appl. Mater. Interfaces* **2010**, *2*, 3709.

[119] N. Zhu, W. Liu, M. Xue, Z. Xie, D. Zhao, M. Zhang, J. Chen, T. Cao, *Electrochim. Acta* **2010**, *55*, 5813.

[120] Y. Qiu, K. Yan, S. Yang, L. Jin, H. Deng, W. Li, *ACS Nano* **2010**, *4*, 6515.

[121] H. Kim, S.-W. Kim, Y.-U. Park, H. Gwon, D.-H. Seo, Y. Kim, K. Kang, *Nano Res.* **2010**, *3*, 813.

[122] Y. Li, X. Lv, J. Lu, J. Li, *J. Phys. Chem. C* **2010**, *114*, 21770.

[123] Z. Wang, H. Zhang, N. Li, Z. Shi, Z. Gu, G. Cao, *Nano Res.* **2010**, *3*, 748.

[124] S. Chen, P. Chen, M. Wu, D. Pan, Y. Wang, *Electrochem. Commun.* **2010**, *12*, 1302.

[125] X. Zhu, Y. Zhu, S. Murali, M. D. Stoller, R. S. Ruoff, *ACS Nano* **2011**, *5*, 3333.

[126] J. Zhu, T. Zhu, X. Zhou, Y. Zhang, X. W. Lou, X. Chen, H. Zhang, H. H. Hng, Q. Yan, *Nanoscale* **2011**, *3*, 1084.

[127] W. Zhou, J. Zhu, C. Cheng, J. Liu, H. Yang, C. Cong, C. Guan, X. Jia, H. J. Fan, Q. Yan, C. M. Li, T. Yu, *Energy Environ. Sci.* **2011**, *4*, 4954.

[128] X. Huang, Z. Zeng, H. Zhang, *Chem. Soc. Rev.* **2013**, *42*, 1934.

[129] K. Chang, W. Chen, *Chem. Commun.* **2011**, *47*, 4252.

[130] K. Chang, W. Chen, *J. Mater. Chem.* **2011**, *21*, 17175.

[131] K. Chang, W. Chen, *ACS Nano* **2011**, *5*, 4720.

[132] J. Xiao, X. Wang, X. Q. Yang, S. Xun, G. Liu, P. K. Koech, J. Liu, J. P. Lemmon, *Adv. Funct. Mater.* **2011**, *21*, 2840.

[133] L.-H. Tao, Y. Cai, Z.-J. Li, G.-X. Ren, J.-K. Liu, *Wuji Cailiao Xuebao/J. Inorg. Mater.* **2011**, *26*, 912.

[134] Y. Zou, Y. Wang, *Nanoscale* **2011**, *3*, 2615.

[135] Y. Sun, X. Hu, W. Luo, Y. Huang, *ACS Nano* **2011**, *5*, 7100.

[136] Y. Sun, X. Hu, W. Luo, Y. Huang, *J. Mater. Chem.* **2011**, *21*, 17229.

[137] A. Yu, H. W. Park, A. Davies, D. C. Higgins, Z. Chen, X. Xiao, *J. Phys. Chem. Lett.* **2011**, *2*, 1855.

[138] C. X. Guo, M. Wang, T. Chen, X. W. Lou, C. M. Li, *Adv. Energy Mater.* **2011**, *1*, 736.

[139] L. Xing, C. Cui, C. Ma, X. Xue, *Mater. Lett.* **2011**, *65*, 2104.

[140] K. Zhang, H. Wang, X. He, Z. Liu, L. Wang, L. Gu, H. Xu, P. Han, S. Dong, C. Zhang, J. Yao, G. Cui, L. Chen, *J. Mater. Chem.* **2011**, *21*, 11916.

[141] G. Wang, J. Bai, Y. Wang, Z. Ren, J. Bai, *Scr. Mater.* **2011**, *65*, 339.

[142] J. Choi, J. Jin, I. G. Jung, J. M. Kim, H. J. Kim, S. U. Son, *Chem. Commun.* **2011**, *47*, 5241.

[143] J. Xie, Y. X. Zheng, R. J. Pan, S. Y. Liu, W. T. Song, G. S. Cao, T. J. Zhu, X. B. Zhao, *Int. J. Electrochem. Sci.* **2011**, *6*, 4811.

[144] L. Ji, Z. Tan, T. Kuykendall, E. J. An, Y. Fu, V. Battaglia, Y. Zhang, *Energy Environ. Sci.* **2011**, *4*, 3611.

[145] S. Ding, D. Luan, F. Y. C. Boey, J. S. Chen, X. W. D. Lou, *Chem. Commun.* **2011**, *47*, 7155.

[146] X. Wang, X. Zhou, K. Yao, J. Zhang, Z. Liu, *Carbon* **2011**, *49*, 133.

[147] P. Lian, X. Zhu, S. Liang, Z. Li, W. Yang, H. Wang, *Electrochim. Acta* **2011**, *56*, 4532.

[148] M. Zhang, D. Lei, Z. Du, X. Yin, L. Chen, Q. Li, Y. Wang, T. Wang, *J. Mater. Chem.* **2011**, *21*, 1673.

[149] C. Zhong, J. Wang, Z. Chen, H. Liu, *J. Phys. Chem. C* **2011**, *115*, 25115.

[150] X. Zhao, C. M. Hayner, M. C. Kung, H. H. Kung, *Adv. Energy Mater.* **2011**, *1*, 1079.

[151] K. Evanoff, A. Magasinski, J. Yang, G. Yushin, *Adv. Energy Mater.* **2011**, *1*, 495.

[152] H. Xiang, K. Zhang, G. Ji, J. Y. Lee, C. Zou, X. Chen, J. Wu, *Carbon* **2011**, *49*, 1787.

[153] H.-C. Tao, L.-Z. Fan, Y. Mei, X. Qu, *Electrochem. Commun.* **2011**, *13*, 1332.

[154] W. Chen, S. Li, C. Chen, L. Yan, *Adv. Mater.* **2011**, *23*, 5679.

[155] J. Su, M. Cao, L. Ren, C. Hu, *J. Phys. Chem. C* **2011**, *115*, 14469.

[156] B. Li, H. Cao, J. Shao, M. Qu, J. H. Warner, *J. Mater. Chem.* **2011**, *21*, 5069.

[157] J. Zhou, H. Song, L. Ma, X. Chen, *RSC Adv.* **2011**, *1*, 782.

[158] B. Li, H. Cao, J. Shao, G. Li, M. Qu, G. Yin, *Inorg. Chem.* **2011**, *50*, 1628.

[159] J. Zhu, Y. K. Sharma, Z. Zeng, X. Zhang, M. Srinivasan, S. Mhaisalkar, H. Zhang, H. H. Hng, Q. Yan, *J. Phys. Chem. C* **2011**, *115*, 8400.

[160] B. Wang, Y. Wang, J. Park, H. Ahn, G. Wang, *J. Alloys Compd.* **2011**, *509*, 7778.

[161] G. Wang, J. Liu, S. Tang, H. Li, D. Cao, *J. Solid State Electrochem.* **2011**, *15*, 2587.

[162] Y. J. Mai, X. L. Wang, J. Y. Xiang, Y. Q. Qiao, D. Zhang, C. D. Gu, J. P. Tu, *Electrochim. Acta* **2011**, *56*, 2306.

[163] L. Q. Lu, Y. Wang, *J. Mater. Chem.* **2011**, *21*, 17916.

[164] J. Zhou, L. Ma, H. Song, B. Wu, X. Chen, *Electrochem. Commun.* **2011**, *13*, 1357.

[165] N. Li, G. Liu, C. Zhen, F. Li, L. Zhang, H. M. Cheng, *Adv. Funct. Mater.* **2011**, *21*, 1717.

[166] S. Yang, X. Feng, K. Müllen, *Adv. Mater.* **2011**, *23*, 3575.

[167] S. Ding, J. S. Chen, D. Luan, F. Y. C. Boey, S. Madhavi, X. W. D. Lou, *Chem. Commun.* **2011**, *47*, 5780.

[168] J. S. Chen, Z. Wang, X. C. Dong, P. Chen, X. W. D. Lou, *Nanoscale* **2011**, *3*, 2158.

[169] Y. Shi, L. Wen, F. Li, H.-M. Cheng, *J. Power Sources* **2011**, *196*, 8610.

[170] L. Shen, C. Yuan, H. Luo, X. Zhang, S. Yang, X. Lu, *Nanoscale* **2011**, *3*, 572.

[171] H. Xiang, B. Tian, P. Lian, Z. Li, H. Wang, *J. Alloys Compd.* **2011**, *509*, 7205.

[172] P. Lian, S. Liang, X. Zhu, W. Yang, H. Wang, *Electrochim. Acta* **2011**, *58*, 81.

[173] Y. Zou, Y. Wang, *ACS Nano* **2011**, *5*, 8108.

[174] X. Li, X. Huang, D. Liu, X. Wang, S. Song, L. Zhou, H. Zhang, *J. Phys. Chem. C* **2011**, *115*, 21567.

[175] J. Z. Wang, C. Zhong, D. Wexler, N. H. Idris, Z. X. Wang, L. Q. Chen, H. K. Liu, *Chemistry (Easton)* **2011**, *17*, 661.

[176] D. Chen, G. Ji, Y. Ma, J. Y. Lee, J. Lu, *ACS Appl. Mater. Interfaces* **2011**, *3*, 3078.

[177] Y. J. Cho, H. S. Kim, H. Im, Y. Myung, G. B. Jung, C. W. Lee, J. Park, M.-H. Park, J. Cho, H. S. Kang, *J. Phys. Chem. C* **2011**, *115*, 9451.

[178] Y. Zhao, J. Li, Y. Ding, L. Guan, *J. Mater. Chem.* **2011**, *21*, 19101.

[179] H. Kim, S.-W. Kim, J. Hong, Y.-U. Park, K. Kang, *J. Mater. Res.* **2011**, *26*, 2665.

[180] X.-W. Yang, Y.-S. He, X.-Z. Liao, Z.-F. Ma, *Wuli Huaxue Xuebao/Acta Phys. - Chim. Sin.* **2011**, *27*, 13.

[181] D.-J. Xue, S. Xin, Y. Yan, K.-C. Jiang, Y.-X. Yin, Y.-G. Guo, L.-J. Wan, *J. Am. Chem. Soc.* **2012**, *134*, 2512.

[182] C. H. Kim, H. S. Im, Y. J. Cho, C. S. Jung, D. M. Jang, Y. Myung, H. S. Kim, S. H. Back, Y. R. Lim, C. W. Lee, J. Park, M. S. Song, W. Il Cho, *J. Phys. Chem. C* **2012**, *116*, 26190.

[183] J. Cheng, J. Du, *Crystallogr. Eng. Commun.* **2012**, *14*, 397.

[184] A. M. Chockla, M. G. Panthani, V. C. Holmberg, C. M. Hessel, D. K. Reid, T. D. Bogart, J. T. Harris, C. B. Mullins, B. A. Korgel, *J. Phys. Chem. C* **2012**, *116*, 11917.

[185] H. Xia, D. Zhu, Y. Fu, X. Wang, *Electrochim. Acta* **2012**, *83*, 166.

[186] Y. Fu, Y. Wan, H. Xia, X. Wang, *J. Power Sources* **2012**, *213*, 338.

[187] Y. Fu, Q. Chen, M. He, Y. Wan, X. Sun, H. Xia, X. Wang, *Ind. Eng. Chem. Res.* **2012**, *51*, 11700.

[188] W. Song, J. Xie, S. Liu, G. Cao, T. Zhu, X. Zhao, *New J. Chem.* **2012**, *36*, 2236.

[189] B. Luo, Y. Fang, B. Wang, J. Zhou, H. Song, L. Zhi, *Energy Environ. Sci.* **2012**, *5*, 5226.

[190] K. Chang, Z. Wang, G. Huang, H. Li, W. Chen, J. Y. Lee, *J. Power Sources* **2012**, *201*, 259.

[191] M. Sathish, S. Mitani, T. Tomai, I. Honma, *J. Phys. Chem. C* **2012**, *116*, 12475.

[192] P. V. Prikhodchenko, J. Gun, S. Sladkevich, A. a. Mikhaylov, O. Lev, Y. Y. Tay, S. K. Batabyal, D. Y. W. Yu, *Chem. Mater.* **2012**, *24*, 4750.

[193] F. Ye, G. Du, Z. Jiang, Y. Zhong, X. Wang, Q. Cao, J. Z. Jiang, *Nanoscale* **2012**, *4*, 7354.

[194] Z. Chen, M. Zhou, Y. Cao, X. Ai, H. Yang, J. Liu, *Adv. Energy Mater.* **2012**, *2*, 95.

[195] J. Xu, K. Jang, J. Choi, J. Jin, J. H. Park, H. J. Kim, D.-H. Oh, J. R. Ahn, S. U. Son, *Chem. Commun.* **2012**, *48*, 6244.

[196] B. Feng, J. Xie, G.-S. Cao, T.-J. Zhu, X.-B. Zhao, *Int. J. Electrochem. Sci.* **2012**, *7*, 5195.

[197] J. Xie, Y.-X. Zheng, S.-Y. Liu, W.-T. Song, Y.-G. Zhu, G.-S. Cao, T.-J. Zhu, X.-B. Zhao, *Int. J. Electrochem. Sci.* **2012**, *7*, 1319.

[198] F. Tu, J. Xie, G.-S. Cao, X.-B. Zhao, *Materials (Basel).* **2012**, *5*, 1275.

[199] W.-T. Song, J. Xie, S.-Y. Liu, Y.-X. Zheng, G.-S. Cao, T.-J. Zhu, X.-B. Zhao, *Int. J. Electrochem. Sci.* **2012**, *7*, 2164.

[200] Y. Lu, X. Wang, Y. Mai, J. Xiang, H. Zhang, L. Li, C. Gu, J. Tu, S. X. Mao, *J. Phys. Chem. C* **2012**, *116*, 22217.

[201] A. K. Rai, J. Gim, J. Song, V. Mathew, L. T. Anh, J. Kim, *Electrochim. Acta* **2012**, *75*, 247.

[202] W. Yue, Z. Lin, S. Jiang, X. Yang, *J. Mater. Chem.* **2012**, *22*, 16318.

[203] Y. Dai, S. Cai, W. Yang, L. Gao, W. Tang, J. Xie, J. Zhi, X. Ju, *Carbon* **2012**, *50*, 4648.

[204] C. Guo, D. Wang, Q. Wang, B. Wang, T. Liu, *Int. J. Electrochem* **2012**, *7*, 8745.

[205] Z.-S. Wu, L. Xue, W. Ren, F. Li, L. Wen, H.-M. Cheng, *Adv. Funct. Mater.* **2012**, *22*, 3290.

[206] X. Zhou, Y.-X. Yin, L.-J. Wan, Y.-G. Guo, *Chem. Commun.* **2012**, *48*, 2198.

[207] J. Luo, X. Zhao, J. Wu, H. D. Jang, H. H. Kung, J. Huang, *J. Phys. Chem. Lett.* **2012**, *3*, 1824.

[208] X. Xin, X. Zhou, F. Wang, X. Yao, X. Xu, Y. Zhu, Z. Liu, *J. Mater. Chem.* **2012**, *22*, 7724.

[209] X. Zhou, A.-M. Cao, L.-J. Wan, Y.-G. Guo, *Nano Res.* **2012**, *5*, 845.

[210] B. Luo, B. Wang, X. Li, Y. Jia, M. Liang, L. Zhi, *Adv. Mater.* **2012**, *24*, 3538.

[211] B. Luo, B. Wang, M. Liang, J. Ning, X. Li, L. Zhi, *Adv. Mater.* **2012**, *24*, 1405.

[212] Z. Wen, S. Cui, H. Kim, S. Mao, K. Yu, G. Lu, H. Pu, O. Mao, J. Chen, *J. Mater. Chem.* **2012**, *22*, 3300.

[213] S. Chen, Y. Wang, H. Ahn, G. Wang, *J. Power Sources* **2012**, *216*, 22.

[214] G. Zhou, D. W. Wang, L. C. Yin, N. Li, F. Li, H. M. Cheng, *ACS Nano* **2012**, *6*, 3214.

[215] Y. Huang, X. Huang, J. Lian, D. Xu, L. Wang, X. Zhang, *J. Mater. Chem.* **2012**, *22*, 2844.

[216] Y. J. Mai, S. J. Shi, D. Zhang, Y. Lu, C. D. Gu, J. P. Tu, *J. Power Sources* **2012**, *204*, 155.

[217] X. Wang, X. Cao, L. Bourgeois, H. Guan, S. Chen, Y. Zhong, D.-M. Tang, H. Li, T. Zhai, L. Li, Y. Bando, D. Golberg, *Adv. Funct. Mater.* **2012**, *22*, 2682.

[218] X. Li, X. Meng, J. Liu, D. Geng, Y. Zhang, M. N. Banis, Y. Li, J. Yang, R. Li, X. Sun, M. Cai, M. W. Verbrugge, *Adv. Funct. Mater.* **2012**, *22*, 1647.

[219] Y. Su, S. Li, D. Wu, F. Zhang, H. Liang, P. Gao, C. Cheng, X. Feng, *ACS Nano* **2012**, *6*, 8349.

[220] S. Mao, Z. Wen, H. Kim, G. Lu, P. Hurley, J. Chen, *ACS Nano* **2012**, *6*, 7505.

[221] M. Sathish, T. Tomai, I. Honma, *J. Power Sources* **2012**, *217*, 85.

[222] M. Zhang, M. Jia, Y. Jin, *Appl. Surf. Sci.* **2012**, *261*, 298.

[223] M. Zhang, B. Qu, D. Lei, Y. Chen, X. Yu, L. Chen, Q. Li, Y. Wang, T. Wang, *J. Mater. Chem.* **2012**, *22*, 3868.

[224] J. Qiu, P. Zhang, M. Ling, S. Li, P. Liu, H. Zhao, S. Zhang, *ACS Appl. Mater. Interfaces* **2012**, *4*, 3636.

[225] L. Tao, J. Zai, K. Wang, H. Zhang, M. Xu, J. Shen, Y. Su, X. Qian, *J. Power Sources* **2012**, *202*, 230.

[226] B. G. Choi, S.-J. Chang, Y. B. Lee, J. S. Bae, H. J. Kim, Y. S. Huh, *Nanoscale* **2012**, *4*, 5924.

[227] C. Peng, B. Chen, Y. Qin, S. Yang, C. Li, Y. Zuo, S. Liu, J. Yang, *ACS Nano* **2012**, *6*, 1074.

[228] Y. Sun, X. Hu, W. Luo, Y. Huang, *J. Phys. Chem. C* **2012**, *116*, 20794.

[229] N. Mahmood, C. Zhang, Y. Hou, *Small* **2013**, *9*, 1321.

[230] D. Chen, G. Ji, B. Ding, Y. Ma, B. Qu, W. Chen, J. Y. Lee, *Nanoscale* **2013**, *5*, 7890.

[231] Y. Gu, Y. Xu, Y. Wang, *ACS Appl. Mater. Interfaces* **2013**, *5*, 801.

[232] N. Mahmood, C. Zhang, J. Jiang, F. Liu, Y. Hou, *Chem. – Eur. J.* **2013**, *19*, 5183.

[233] K. Shiva, H. S. S. Ramakrishna Matte, H. B. Rajendra, A. J. Bhattacharyya, C. N. R. Rao, *Nano Energy* **2013**, *2*, 787.

[234] L. Fei, Q. Lin, B. Yuan, G. Chen, P. Xie, Y. Li, Y. Xu, S. Deng, S. Smirnov, H. Luo, *ACS Appl. Mater. Interfaces* **2013**, *5*, 5330.

[235] Q. Pan, J. Xie, S. Liu, G. Cao, T. Zhu, X. Zhao, *RSC Adv.* **2013**, *3*, 3899.

[236] Z. Zhang, C. Zhou, L. Huang, X. Wang, Y. Qu, Y. Lai, J. Li, *Electrochim. Acta* **2013**, *114*, 88.

[237] N. Mahmood, C. Zhang, F. Liu, J. Zhu, Y. Hou, *ACS Nano* **2013**, *7*, 10307.

[238] J. Chen, L. Yang, S. Fang, Z. Zhang, S. I. Hirano, *Electrochim. Acta* **2013**, *105*, 629.

[239] P. Chen, L. Guo, Y. Wang, *J. Power Sources* **2013**, *222*, 526.

[240] W. Song, J. Xie, W. Hu, S. Liu, G. Cao, T. Zhu, X. Zhao, *J. Power Sources* **2013**, *229*, 6.

[241] Y. Zhao, Y. Huang, Q. Wang, X. Wang, M. Zong, *Ceram. Int.* **2013**, *39*, 1741.

[242] F. Zou, X. Hu, Y. Sun, W. Luo, F. Xia, L. Qie, Y. Jiang, Y. Huang, *Chem. – Eur. J.* **2013**, *19*, 6027.

[243] Z. Chen, Y. Yan, S. Xin, W. Li, J. Qu, Y. G. Guo, W. G. Song, *J. Mater. Chem. A* **2013**, *1*, 11404.

[244] L. Zhang, Z. Wang, L. Wang, Y. Xing, Y. Zhang, *Mater. Lett.* **2013**, *108*, 9.

[245] R. Huang, H. Ge, X. Lin, Y. Guo, R. Yuan, X. Fu, Z. Li, *RSC Adv.* **2013**, *3*, 1235.

[246] M. Yu, H. Sun, X. Sun, F. Lu, T. Hu, G. Wang, H. Qiu, J. Lian, *Mater. Lett.* **2013**, *108*, 29.

[247] Y. Shi, S. L. Chou, J. Z. Wang, H. Z. Li, H. K. Liu, Y. P. Wu, *J. Power Sources* **2013**, *244*, 684.

[248] S. Jin, N. Li, H. Cui, C. Wang, *Nano Energy* **2013**, *2*, 1128.

[249] Y. Shi, J. Wang, S. Chou, D. Wexler, H. Li, K. Ozawa, H. Liu, Y. Wu, J. Accepted, *Nano Lett.* **2013**, *13*, 4715.

[250] Y. Xiao, J. Zai, L. Tao, B. Li, Q. Han, C. Yu, X. Qian, *Phys. Chem. Chem. Phys.* **2013**, *15*, 3939.

[251] L. Su, Z. Zhou, X. Qin, Q. Tang, D. Wu, P. Shen, *Nano Energy* **2013**, *2*, 276.

[252] X. Zhou, L.-J. Wan, Y.-G. Guo, *Adv. Mater.* **2013**, *25*, 2152.

[253] Y. Huang, D. Wu, S. Han, S. Li, L. Xiao, F. Zhang, X. Feng, *ChemSusChem* **2013**, *6*, 1510.

[254] L. Wang, D. Wang, Z. Dong, F. Zhang, J. Jin, *Nano Lett.* **2013**, *13*, 1711.

[255] W. Wei, S. Yang, H. Zhou, I. Lieberwirth, X. Feng, K. Müllen, *Adv. Mater.* **2013**, *25*, 2909.

[256] J. Luo, J. Liu, Z. Zeng, C. F. Ng, L. Ma, H. Zhang, J. Lin, Z. Shen, H. J. Fan, *Nano Lett.* **2013**, *13*, 6136.

[257] X. Cao, Y. Shi, W. Shi, X. Rui, Q. Yan, J. Kong, H. Zhang, *Small* **2013**, *9*, 3433.

[258] Y. Gong, S. Yang, Z. Liu, L. Ma, R. Vajtai, P. M. Ajayan, *Adv. Mater.* **2013**, *25*, 3979.

[259] X. Jiang, X. Yang, Y. Zhu, J. Shen, K. Fan, C. Li, *J. Power Sources* **2013**, *237*, 178.

[260] Y. Sun, X. Hu, W. Luo, F. Xia, Y. Huang, *Adv. Funct. Mater.* **2013**, *23*, 2436.

[261] W. Li, F. Wang, S. Feng, J. Wang, Z. Sun, B. Li, Y. Li, J. Yang, A. a. Elzatahry, Y. Xia, D. Zhao, *J. Am. Chem. Soc.* **2013**, *135*, 18300.

[262] B. Wang, X. Li, X. Zhang, B. Luo, M. Jin, M. Liang, S. a. Dayeh, S. T. Picraux, L. Zhi, *ACS Nano* **2013**, *7*, 1437.

[263] Y. Tang, D. Wu, S. Chen, F. Zhang, J. Jia, X. Feng, *Energy Environ. Sci.* **2013**, *6*, 2447.

[264] Y. Luo, J. Luo, W. Zhou, X. Qi, H. Zhang, D. Y. W. Yu, C. M. Li, H. J. Fan, T. Yu, *J. Mater. Chem. A* **2013**, 273.

[265] G. Xia, N. Li, D. Li, R. Liu, C. Wang, X. Lu, J. Spendelow, J. Zhang, G. Wu, *ACS Appl. Mater. interfaces* **2013**, 5, 8607.

[266] X. L. Huang, R. Z. Wang, D. Xu, Z. L. Wang, H. G. Wang, J. J. Xu, Z. Wu, Q. C. Liu, Y. Zhang, X. B. Zhang, *Adv. Funct. Mater.* **2013**, 23, 4345.

[267] F.-H. Du, K.-X. Wang, W. Fu, P.-F. Gao, J.-F. Wang, J. Yang, J.-S. Chen, *J. Mater. Chem. A* **2013**, 1, 13648.

[268] J. Ji, H. Ji, L. L. Zhang, X. Zhao, X. Bai, X. Fan, F. Zhang, R. S. Ruoff, *Adv. Mater.* **2013**, 25, 4673.

[269] B. Wang, X. Li, T. Qiu, B. Luo, J. Ning, J. Li, X. Zhang, M. Liang, L. Zhi, *Nano Lett.* **2013**, 13, 5578.

[270] B. Qiu, M. Xing, J. Zhang, *J. Am. Chem. Soc.* **2014**, 136, 5852.

[271] J. Qin, C. He, N. Zhao, Z. Wang, C. Shi, E. Z. Liu, J. Li, *ACS Nano* **2014**, 8, 1728.

[272] J. Chang, X. Huang, G. Zhou, S. Cui, P. B. Hallac, J. Jiang, P. T. Hurley, J. Chen, *Adv. Mater.* **2014**, 26, 758.

[273] Y. Gong, S. Yang, L. Zhan, L. Ma, R. Vajtai, P. M. Ajayan, *Adv. Funct. Mater.* **2014**, 24, 125.

[274] X. Cao, B. Zheng, X. Rui, W. Shi, Q. Yan, H. Zhang, *Angew. Chem., Int. Ed.* **2014**, 53, 1404.

[275] Y. Zhao, J. Feng, X. Liu, F. Wang, L. Wang, C. Shi, L. Huang, X. Feng, X. Chen, L. Xu, M. Yan, Q. Zhang, X. Bai, H. Wu, L. Mai, *Nat. Commun.* **2014**, 5, 4565.

[276] Y. Yang, X. Fan, G. Casillas, Z. Peng, G. Ruan, G. Wang, M. J. Yacaman, J. M. Tour, *ACS Nano* **2014**, 8, 3939.

[277] Y. Wang, B. Liu, Q. Li, S. Cartmell, S. Ferrara, Z. D. Deng, J. Xiao, *J. Power Sources* **2015**, 286, 330.

[278] J.-H. Choi, W.-H. Ryu, K. Park, J.-D. Jo, S.-M. Jo, D.-S. Lim, I.-D. Kim, *Sci. Rep.* **2014**, 4, 7334.

[279] H. Song, H. Cui, C. Wang, *ACS Appl. Mater. Interfaces* **2014**, 6, 13765.

[280] R. Purbia, S. Paria, *Nanoscale* **2015**, 19789.

[281] M. B. Gawande, A. Goswami, T. Asefa, H. Guo, A. V Biradar, D. Peng, R. Zboril, R. S. Varma, *Chem. Soc. Rev.* **2015**, 44, 7540.

[282] S. Bhuvaneswari, P. M. Pratheeksha, S. Anandan, D. Rangappa, R. Gopalan, T. N. Rao, *Phys. Chem. Chem. Phys.* **2014**, 16, 5284.

[283] A. Birrozzi, R. Raccichini, F. Nobili, M. Marinaro, R. Tossici, R. Marassi, *Electrochim. Acta* **2014**, 137, 228.

[284] Q. Zhou, Z. Zhao, Z. Wang, Y. Dong, X. Wang, Y. Gogotsi, J. Qiu, *Nanoscale* **2014**, 6, 2286.

[285] L. Li, G. Zhou, X. Y. Shan, S. Pei, F. Li, H. M. Cheng, *J. Power Sources* **2014**, 255, 52.

[286] Y. Miroshnikov, G. Grinbom, G. Gershinsky, G. D. Nessim, D. Zitoun, *Faraday Discuss.* **2014**, 173, 391.

[287] F. Maroni, R. Raccichini, A. Birrozzi, G. Carbonari, R. Tossici, F. Croce, R. Marassi, F. Nobili, *J. Power Sources* **2014**, 269, 873.

[288] H. Mi, Y. Li, P. Zhu, X. Chai, L. Sun, H. Zhuo, Q. Zhang, C. He, J. Liu, *J. Mater. Chem. A* **2014**, 2, 11254.

[289] X. Zhong, J. Wang, W. Li, X. Liu, Z. Yang, L. Gu, Y. Yu, *RSC Adv.* **2014**, 4, 58184.

[290] K. H. Park, D. Lee, J. Kim, J. Song, Y. M. Lee, H.-T. Kim, J.-K. Park, *Nano Lett.* **2014**, 14, 4306.

[291] Y. Chen, J. Zhu, B. Qu, B. Lu, Z. Xu, *Nano Energy* **2014**, 3, 88.

[292] W. Kang, Y. Tang, W. Li, Z. Li, X. Yang, J. Xu, C.-S. Lee, *Nanoscale* **2014**, 6, 6551.

[293] A. K. Rai, T. V. Thi, B. J. Paul, J. Kim, *Electrochim. Acta* **2014**, 146, 577.

[294] L. Zhou, X. Kong, M. Gao, F. Lian, B. Li, Z. Zhou, H. Cao, *Inorg. Chem.* **2014**, 53, 9228.

[295] B. Yao, Z. Ding, X. Feng, L. Yin, Q. Shen, Y. Shi, J. Zhang, *Electrochim. Acta* **2014**, 148, 283.

[296] Y. Ren, H. Wei, B. Yang, J. Wang, J. Ding, *Electrochim. Acta* **2014**, 145, 193.

[297] D. Chen, H. Quan, X. Luo, S. Luo, *Scr. Mater.* **2014**, 76, 1.

[298] Y. Fu, J. Zhu, C. Hu, X. Wu, X. Wang, *Nanoscale* **2014**, 6, 12555.

[299] L. Lai, J. Zhu, B. Li, Y. Zhen, Z. Shen, Q. Yan, J. Lin, *Electrochim. Acta* **2014**, 134, 28.

[300] B. Zhang, G. Cui, K. Zhang, L. Zhang, P. Han, S. Dong, *Electrochim. Acta* **2014**, 150, 15.

[301] R. C. de Guzman, J. Yang, M. Ming-Cheng Cheng, S. O. Salley, K. Y. S. Ng, *J. Mater. Chem. A* **2014**, 2, 14577.

[302] Q. An, F. Lv, Q. Liu, C. Han, K. Zhao, J. Sheng, Q. Wei, M. Yan, L. Mai, *Nano Lett.* **2014**, 14, 6250.

[303] W. Wang, L. Hu, J. Ge, Z. Hu, H. Sun, H. Sun, H. Zhang, H. Zhu, S. Jiao, *Chem. Mater.* **2014**, 26, 3721.

[304] P. Xiong, B. Liu, V. Teran, Y. Zhao, L. Peng, X. Wang, G. Yu, M. Science, E. Program, M. Engineering, U. States, S. Chemistry, F. Materials, C. Engineering, *ACS Nano* **2014**, 8, 8610.

[305] Y. Cao, L. Zhang, D. Tao, D. Huo, K. Su, *Electrochim. Acta* **2014**, 132, 483.

[306] J. Yao, Y. Gong, S. Yang, P. Xiao, Y. Zhang, K. Keyshar, G. Ye, S. Ozden, R. Vajtai, P. M. Ajayan, *ACS Appl. Mater. Interfaces* **2014**, 6, 20414.

[307] Y. Dong, C. Cao, Y.-S. Chui, J. A. Zapien, *Chem. Commun.* **2014**, 50, 10151.

[308] A. K. Rai, T. V. Thi, J. Gim, J. Kim, *Mater. Charact.* **2014**, 95, 259.

[309] K. Wu, J. Shu, X. Lin, L. Shao, M. Lao, M. Shui, P. Li, N. Long, D. Wang, *J. Power Sources* **2014**, 272, 283.

[310] Y. Zhang, J. Xie, T. Zhu, G. Cao, X. Zhao, S. Zhang, *J. Power Sources* **2014**, 247, 204.

[311] H. Yang, L. Li, *J. Alloys Compd.* **2014**, 584, 76.

[312] L. Zhao, W. Yue, Y. Ren, *Electrochim. Acta* **2014**, 116, 31.

[313] J. J. Ma, T. Yuan, Y. S. He, J. L. Wang, W. M. Zhang, D. Z. Yang, X. Z. Liao, Z. F. Ma, *J. Mater. Chem. A* **2014**, 2, 16925.

[314] J. Wang, X. Li, Z. Wang, B. Huang, Z. Wang, H. Guo, *J. Power Sources* **2014**, 251, 325.

[315] Y. Zhang, A. Pan, S. Liang, T. Chen, Y. Tang, X. Tan, *Mater. Lett.* **2014**, 137, 174.

[316] X. Sun, C. Zhou, M. Xie, T. Hu, H. Sun, G. Xin, G. Wang, S. M. George, J. Lian, *Chem. Commun.* **2014**, 50, 10703.

[317] R. S. R. M. D. Stoller, S. Park, Y. Zhu, J. An, *Nano Lett.* **2008**, 8, 3498.

[318] H. Wang, Y. Yang, Y. Liang, J. T. Robinson, Y. Li, A. Jackson, Y. Cui, H. Dai, *Nano Lett.* **2011**, 11, 2644.

[319] A. Vizintin, M. Lozinsek, R. K. Chellappan, D. Foix, A. Krajnc, G. Mali, G. Drazic, B. Genorio, R. Dedryvere, R. Dominko, *Chem. Mater.* **2015**, 27, 7070.

[320] J. Xiao, D. Mei, X. Li, W. Xu, D. Wang, G. L. Graff, W. D. Bennett, Z. Nie, L. V Saraf, I. A. Aksay, J. Liu, J.-G. Zhang, *Nano Lett.* **2011**, 11, 5071.

[321] A. Zhamu, G. Chen, C. Liu, D. Neff, Q. Fang, Z. Yu, W. Xiong, Y. Wang, X. Wang, B. Z. Jang, *Energy Environ. Sci.* **2012**, 5, 5701.

[322] J. K. G. Kucinskis, G. Bajars, *J. Power Sources* **2013**, 240, 66.

[323] J. H. Lee, W. H. Shin, M.-H. Ryou, J. K. Jin, J. Kim, J. W. Choi, *ChemSusChem* **2012**, 5, 2328.

[324] D. Su, H.-J. Ahn, G. Wang, *Chem. Commun.* **2013**, 49, 3131.

[325] D. K. Y. H. Jung, C. H. Lim, *J. Mater. Chem. A* **2013**, 1, 11350.

[326] Y. Li, H. Yadegari, X. Li, M. N. Banis, R. Li, X. Sun, *Chem. c* **2013**, 49, 11731.

[327] J. W. Jung, W. H. Ryu, J. Shin, K. Park, I. D. Kim, *ACS Nano* **2015**, 9, 6717.

[328] L. Ma, X. Zhou, L. Xu, X. Xu, L. Zhang, W. Chen, *J. Power Sources* **2015**, 285, 274.

[329] Y. Wang, B. Qian, H. Li, L. Liu, L. Chen, H. Jiang, *Mater. Lett.* **2015**, 141, 35.

[330] Z. Zhang, Y. Fu, X. Yang, Y. Qu, Q. Li, *Electrochim. Acta* **2015**, *168*, 285.

[331] S. M. Oh, E. Lee, K. Adpakpang, S. B. Patil, M. J. Park, Y. S. Lim, K. H. Lee, J. Y. Kim, S. J. Hwang, *Electrochim. Acta* **2015**, *170*, 48.

[332] Z. Li, H. Xue, J. Wang, Y. Tang, C.-S. Lee, S. Yang, *ChemElectroChem* **2015**, *2*, 1682.

[333] R. Jin, Y. Yang, Y. Li, X. Liu, Y. Xing, S. Song, Z. Shi, *Chem. – Eur. J.* **2015**, *21*, 9014.

[334] X. Wei, C. Tang, X. Wang, L. Zhou, Q. Wei, M. Yan, J. Sheng, P. Hu, B. Wang, L. Mai, *ACS Appl. Mater. Interfaces* **2015**, *7*, 26572.

[335] B. Wang, S. Li, X. Wu, W. Tian, J. Liu, M. Yu, *J. Mater. Chem. A* **2015**, *3*, 13691.

[336] S. Petnikota, S. K. Marka, V. V. S. S. Srikanth, M. V. Reddy, B. V. R. Chowdari, *Electrochim. Acta* **2015**, *178*, 699.

[337] L. Guo, Y. Wang, *J. Mater. Chem. A* **2015**, *3*, 15030.

[338] S. Petnikota, N. K. Rotte, M. V. Reddy, V. V. S. S. Srikanth, B. V. R. Chowdari, *ACS Appl. Mater. Interfaces* **2015**, *7*, 2301.

[339] P. Arunkumar, A. G. Ashish, B. Babu, S. Sarang, A. Suresh, C. H. Sharma, M. Thalakulam, M. M. Shaijumon, *RSC Adv.* **2015**, *5*, 59997.

[340] S. B. Patil, I. Y. Kim, J. L. Gunjakar, S. M. Oh, T. Eom, H. Kim, S. J. Hwang, *ACS Appl. Mater. Interfaces* **2015**, *7*, 18679.

[341] W. Li, D. Chen, G. Shen, *J. Mater. Chem. A* **2015**, *3*, 20673.

[342] F.-X. Xin, H.-J. Tian, X.-L. Wang, W. Xu, W.-G. Zheng, W.-Q. Han, *ACS Appl. Mater. Interfaces* **2015**, *7*, 7912.

[343] C. Zhang, F. Chai, L. Fu, P. Hu, S. Pang, G. Cui, *J. Mater. Chem. A* **2015**, *3*, 22552.

[344] Q. Zhang, H. Chen, X. Han, J. Cai, Y. Yang, M. Liu, K. Zhang, *ChemSusChem* **2016**, *9*, 186.

[345] L. Zhang, Q. Bai, K. Jin, L. Wang, Y. Zhang, S. Yanhua, *Mater. Lett.* **2015**, *141*, 88.

[346] F. Feng, W. Kang, F. Yu, H. Zhang, Q. Shen, *J. Power Sources* **2015**, *282*, 109.

[347] S. B. Kale, R. S. Kalubarme, M. A. Mahadadalkar, H. S. Jadhav, A. P. Bhirud, J. D. Ambekar, C.-J. Park, B. B. Kale, *Phys. Chem. Chem. Phys.* **2015**, *17*, 31850.

[348] H. Li, R. Y. Tay, S. H. Tsang, W. Liu, E. H. T. Teo, *Electrochim. Acta* **2015**, *166*, 197.

[349] B. Wang, G. Wang, H. Wang, *J. Mater. Chem. A* **2015**, *3*, 17403.

[350] A. L. Lu, X. Q. Zhang, Y. Z. Chen, Q. S. Xie, Q. Q. Qi, Y. T. Ma, D. L. Peng, *J. Power Sources* **2015**, *295*, 329.

[351] Z. Jian, M. Zheng, Y. Liang, X. Zhang, S. Gheytani, Y. Lan, Y. Shi, Y. Yao, *Chem. Commun.* **2015**, *51*, 229.

[352] J. Liu, P. J. Lu, S. Liang, J. Liu, W. Wang, M. Lei, S. Tang, Q. Yang, *Nano Energy* **2015**, *12*, 709.

[353] Q. Li, Q. Wei, Q. Wang, W. Luo, Q. An, Y. Xu, C. Niu, C. Tang, L. Mai, *J. Mater. Chem. A* **2015**, *3*, 18839.

[354] W. Li, F. Wang, Y. Liu, J. Wang, J. Yang, L. Zhang, A. A. Elzatahry, D. Al-Dahyan, Y. Xia, D. Zhao, *Nano Lett.* **2015**, *15*, 2186.

[355] G. F. Gu, J. L. Cheng, X. D. Li, W. Ni, Q. Guan, G. X. Qu, B. Wang, *J. Mater. Chem. A* **2015**, *3*, 6642.

[356] C. Chen, Y. Huang, H. Zhang, X. Wang, G. Li, Y. Wang, L. Jiao, H. Yuan, *J. Power Sources* **2015**, *278*, 693.

[357] G. Zeng, N. Shi, M. Hess, X. Chen, W. Cheng, T. Fan, M. Niederberger, *ACS Nano* **2015**, *9*, 4227.

[358] J. Xu, J. Wu, L. Luo, X. Chen, H. Qin, V. Dravid, S. Mi, C. Jia, *J. Power Sources* **2015**, *274*, 816.

[359] H. Xue, D. Y. W. Yu, J. Qing, X. Yang, J. Xu, Z. Li, M. Sun, W. Kang, Y. Tang, C.-S. Lee, *J. Mater. Chem. A* **2015**, *3*, 7945.

[360] X. Liu, J. Zhang, W. Si, L. Xi, B. Eichler, C. Yan, O. G. Schmidt, *ACS Nano* **2015**, *9*, 1198.

[361] W. Li, D. Yoon, J. Hwang, W. Chang, J. Kim, *J. Power Sources* **2015**, *293*, 1024.

[362] H. S. Oh, H. M. Jeong, J. H. Park, I.-W. Ock, J. K. Kang, *J. Mater. Chem. A* **2015**, *3*, 10238.

[363] H.-P. Cong, S. Xin, S.-H. Yu, *Nano Energy* **2015**, *13*, 482.

[364] L. Pan, X. D. Zhu, X. M. Xie, Y. T. Liu, *Adv. Funct. Mater.* **2015**, *25*, 3341.

[365] S. Han, Y. Zhao, Y. Tang, F. Tan, Y. Huang, X. Feng, D. Wu, *Carbon* **2015**, *81*, 203.

[366] L. Zhang, W. Fan, T. Liu, *RSC Adv.* **2015**, *5*, 43130.

[367] F. Pan, J. Wang, Z. Yang, L. Gu, Y. Yu, *RSC Adv.* **2015**, *5*, 77518.

[368] X. Tang, F. Yan, Y. Wei, M. Zhang, T. Wang, T. Zhang, *ACS Appl. Mater. Interfaces* **2015**, *7*, 21890.

[369] A. Birrozzi, F. Maroni, R. Raccichini, R. Tossici, R. Marassi, F. Nobili, *J. Power Sources* **2015**, *294*, 248.

[370] J. Guo, H. Zhu, Y. Sun, X. Zhang, *J. Mater. Chem. A* **2015**, *3*, 19384.

[371] X. Y. Lu, R. H. Wang, Y. Bai, J. J. Chen, J. Sun, *J. Mater. Chem. A* **2015**, *3*, 12031.

[372] D.-H. Liu, H.-Y. Lü, X.-L. Wu, B.-H. Hou, F. Wan, S.-D. Bao, Q. Yan, H.-M. Xie, R.-S. Wang, *J. Mater. Chem. A* **2015**, *3*, 19738.

[373] M. Zhou, X. Li, B. Wang, Y. Zhang, J. Ning, Z. Xiao, X. Zhang, Y. Chang, L. Zhi, *Nano Lett.* **2015**, *15*, 6222.

[374] J. Kim, C. Oh, C. Chae, D.-H. Yeom, J. Choi, N. Kim, E.-S. Oh, J. K. Lee, *J. Mater. Chem. A* **2015**, *3*, 18684.

[375] D. Choi, D. Wang, V. V. Viswanathan, I.-T. Bae, W. Wang, Z. Nie, J.-G. Zhang, G. L. Graff, J. Liu, Z. Yang, T. Duong, *Electrochem. Commun.* **2010**, *12*, 378.

[376] L. Ji, Z. Tan, T. R. Kuykendall, S. Aloni, S. Xun, E. Lin, V. Battaglia, Y. Zhang, *Phys. Chem. Chem. Phys.* **2011**, *13*, 7170.

[377] H. Gwon, H.-S. Kim, K. U. Lee, D.-H. Seo, Y. C. Park, Y.-S. Lee, B. T. Ahn, K. Kang, *Energy Environ. Sci.* **2011**, *4*, 1277.

[378] N. Li, Z. Chen, W. Ren, F. Li, H.-M. Cheng, *Proc. Natl. Acad. Sci.* **2012**, *109*, 17360.

[379] X. Xin, X. Zhou, J. Wu, X. Yao, Z. Liu, *ACS Nano* **2012**, *6*, 11035.

[380] L. Ji, H. Zheng, A. Ismach, Z. Tan, S. Xun, E. Lin, V. Battaglia, V. Srinivasan, Y. Zhang, *Nano Energy* **2012**, *1*, 164.

[381] J.-G. Ren, Q.-H. Wu, G. Hong, W.-J. Zhang, H. Wu, K. Amine, J. Yang, S.-T. Lee, *Energy Technol.* **2013**, *1*, 77.

[382] M. Zheng, D. Qiu, B. Zhao, L. Ma, X. Wang, Z. Lin, L. Pan, Y. Zheng, Y. Shi, *RSC Adv.* **2013**, *3*, 699.

[383] D. Xie, Q. Su, W. Yuan, Z. Dong, J. Zhang, G. Du, *J. Phys. Chem. C* **2013**, *117*, 24121.

[384] M. Arif, I. Shuvo, A. R. Khan, H. Karim, P. Morton, T. Wilson, Y. Lin, *ACS Appl. Mater. Interfaces* **2013**, *5*, 7881.

[385] O. Vargas, Á. Caballero, J. Morales, G. A. Elia, B. Scrosati, J. Hassoun, *Phys. Chem. Chem. Phys.* **2013**, *15*, 20444.

[386] J. Hassoun, F. Bonaccorso, M. Agostini, M. Angelucci, M. G. Betti, R. Cingolani, M. Gemmi, C. Mariani, S. Panero, V. Pellegrini, B. Scrosati, *Nano Lett.* **2014**, *14*, 4901.

[387] Ó. Vargas, Á. Caballero, J. Morales, E. Rodríguez-Castellón, *ACS Appl. Mater. Interfaces* **2014**, *6*, 3290.

[388] H. Kim, K.-Y. Park, J. Hong, K. Kang, *Sci. Rep.* **2014**, *4*, 5278.

[389] J. B. Goodenough, *Energy Environ. Sci.* **2014**, *7*, 14.

[390] M. Ko, S. Chae, S. Jeong, P. Oh, J. Cho, *ACS Nano* **2014**, *8*, 8591.

[391] K. Eom, T. Joshi, A. Bordes, I. Do, T. F. Fuller, *J. Power Sources* **2014**, *249*, 118.

[392] A. Bordes, K. Eom, T. F. Fuller, *J. Power Sources* **2014**, *257*, 163.

[393] C. Chae, H. J. Noh, J. K. Lee, B. Scrosati, Y. K. Sun, *Adv. Funct. Mater.* **2014**, *24*, 3036.

[394] W. Sun, R. Hu, H. Liu, M. Zeng, L. Yang, H. Wang, M. Zhu, *J. Power Sources* **2014**, *268*, 610.

[395] R. Hu, W. Sun, Y. Chen, M. Zeng, M. Zhu, *J. Mater. Chem. A* **2014**, *2*, 9118.

[396] F.-W. Yuan, H.-Y. Tuan, *Chem. Mater.* **2014**, *26*, 2172.

[397] D. Lv, M. L. Gordin, R. Yi, T. Xu, J. Song, Y. B. Jiang, D. Choi, D. Wang, *Adv. Funct. Mater.* **2014**, *24*, 1059.

**ADVANCED
SCIENCE NEWS**

www.advancedsciencenews.com

**ADVANCED
MATERIALS**

www.advmat.de

PROGRESS REPORT

[398] O. Vargas, Á. Caballero, J. Morales, *Electrochim. Acta* **2014**, *130*, 551.

[399] J. Xie, W. Song, G. Cao, T. Zhu, X. Zhao, S. Zhang, *RSC Adv.* **2014**, *4*, 7703.

[400] X. Xu, S. Jeong, C. S. Rout, P. Oh, M. Ko, H. Kim, M. G. Kim, R. Cao, H. S. Shin, J. Cho, *J. Mater. Chem. A* **2014**, *2*, 10847.

[401] Y. Yang, B. Qiao, X. Yang, L. Fang, C. Pan, W. Song, H. Hou, X. Ji, *Adv. Funct. Mater.* **2014**, *24*, 4349.

[402] A. P. Cohn, L. Oakes, R. Carter, S. Chatterjee, A. S. Westover, K. Share, C. L. Pint, *Nanoscale* **2014**, *6*, 4669.

[403] N. Li, H. Sonsg, H. Cui, C. Wang, *Electrochim. Acta* **2014**, *130*, 670.

[404] Z. J. Jiang, Z. Jiang, *ACS Appl. Mater. Interfaces* **2014**, *6*, 19082.

[405] Ó. Vargas, Á. Caballero, J. Morales, *Electrochim. Acta* **2015**, *165*, 365.

[406] K. Rana, S. D. Kim, J.-H. Ahn, *Nanoscale* **2015**, *7*, 7065.

[407] J. R. Nair, G. Rius, P. Jagadale, M. Destro, M. Tortello, M. Yoshimura, A. Tagliaferro, C. Gerbaldi, *Electrochim. Acta* **2015**, *182*, 500.

[408] M. Agostini, L. G. Rizzi, G. Cesareo, V. Russo, J. Hassoun, *Adv. Mater. Interfaces* **2015**, *2*, 1500085.

[409] P. Xiong, L. Peng, D. Chen, Y. Zhao, X. Wang, G. Yu, *Nano Energy* **2015**, *12*, 816.

[410] Y. Shi, L. Wen, G. Zhou, J. Chen, S. Pei, K. Huang, H.-M. Cheng, F. Li, *2D Mater.* **2015**, *2*, 024004.

[411] J. Ma, Y. S. He, W. Zhang, J. Wang, X. Yang, X. Z. Liao, Z. F. Ma, *Nano Energy* **2015**, *16*, 235.

[412] F. Lin, H. Wang, *J. Mater. Res.* **2015**, *30*, 2736.

[413] C. Gao, L. Li, A.-R. O. Raji, A. Kovalchuk, Z. Peng, H. Fei, Y. He, N. D. Kim, Q. Zhong, E. Xie, J. M. Tour, *ACS Appl. Mater. Interfaces* **2015**, *7*, 26549.

[414] B. Wang, G. Wang, Z. Lv, H. Wang, *Phys. Chem. Chem. Phys.* **2015**, *17*, 27109.

[415] X. Fan, S. Li, H. Zhou, L. Lu, *Electrochim. Acta* **2015**, *180*, 1041.

[416] A. G. Ashish, P. Arunkumar, B. Babu, P. Manikandan, S. Sarang, M. M. Shaijumon, *Electrochim. Acta* **2015**, *176*, 285.

[417] Y. S. Kim, G. Shoorideh, Y. Zhmayev, J. Lee, Z. Li, B. Patel, S. Chakrapani, J. H. Park, S. Lee, Y. L. Joo, *Nano Energy* **2015**, *16*, 446.

[418] P. P. Prosini, M. Carewska, G. Tarquini, F. Maroni, A. Birrozzi, F. Nobili, *Ionics (Kiel)* **2015**, *22*, 515.

[419] P. P. Prosini, M. Carewska, F. Maroni, R. Tossici, F. Nobili, *Solid State Ionics* **2015**, *283*, 145.

[420] I. H. Son, J. Hwan Park, S. Kwon, S. Park, M. H. Rümmeli, A. Bachmatiuk, H. J. Song, J. Ku, J. W. Choi, J. Choi, S.-G. Doo, H. Chang, *Nat. Commun.* **2015**, *6*, 7393.

[421] M. Kim, D. Y. Kim, Y. Kang, O. O. Park, *RSC Adv.* **2015**, *5*, 3299.

[422] T. Mori, C. J. Chen, T. F. Hung, S. G. Mohamed, Y. Q. Lin, H. Z. Lin, J. C. Sung, S. F. Hu, R. S. Liu, *Electrochim. Acta* **2015**, *165*, 166.

[423] A. S. Westover, D. Freudiger, Z. S. Gani, K. Share, L. Oakes, R. E. Carter, C. L. Pint, *Nanoscale* **2015**, *7*, 98.

[424] Y. Jiang, Z.-J. Jiang, L. Yang, S. Cheng, M. Liu, *J. Mater. Chem. A* **2015**, *3*, 11847.

[425] X. Yan, Y. J. Li, M. L. Li, Y. C. Jin, F. Du, G. Chen, Y. J. Wei, *J. Mater. Chem. A* **2015**, *3*, 4180.

[426] S. R. Sivakkumar, A. G. Pandolfo, *Electrochim. Acta* **2012**, *65*, 280.